To the Graduate Council :

I am submitting herewith a dissertation written by Jin Whan Kim entitled " On a Taylor Weak Statement for Finite Element Computations in Gas Dynamics ". I have examined the final copy of this dissertation for form and content and recommend that it be accepted in partial fulfillment of the requirement for the degree of Doctor of Philosophy, with a major in Engineering Science.

Allen J. Baker, Major Professor

We have read this dissertation
and recommend its acceptance :

Accepted for the Council :

Vice Provost
and Dean of The Graduate School

On a Taylor Weak Statement

for

Finite Element Computations in

Gas Dynamics

A Dissertation

Presented for the

Doctor of Philosophy

Degree

The University of Tennessee, Knoxville

Jin Whan Kim

December 1988

ACKNOWLEDGMENTS

In the course of this research, my thanks go to Professor A. J. Baker who taught me the Taylor series restatement of the conservation laws. I am also indebted to Professor E. Wachspress for his concern and advice. I also wish to thank Professors J. E. Stoneking, R. V. Arimilli and M. O. Soliman for their help and encouragement. I would also like to thank Dean W. T. Snyder for his consideration of me as the first recipient of the Lyon's scholarship award.

Finally, I thank my parents and wife, Pil-Soo, and son, Hoyean, for their endurance and support.

ABSTRACT

The Taylor Weak Statement has been developed as a potential unified approach for approximate computation of fluid flows. It is verified to contain a variety of numerical dissipative methods developed for advection problems by specific identification of its expansion parameters. Generalized Fourier modal analysis has been completed in one space dimension for both semi- and fully-discrete approximations, from which the flux limiter method is herein developed and evaluated for finite element computations. Its application to 1- and 2-dimensional scalar models is investigated for continuous and discontinuous initial value problems, and its use for the Euler equation system of gas dynamics in 1- and 2-dimensional cases is demonstrated.

TABLE OF CONTENTS

CHAPTER PAGE

1. INTRODUCTION 1

2. THE TAYLOR WEAK STATEMENT 6

   1. Formulation of the TWS

   2. Finite Element Approximation

   3. Transonic Full Potential Equation

3. ANALYSIS OF THE TWS IN ONE DIMENSION 17

   1. Recovery of Various Algorithms

   2. Fourier Modal Analysis

   3. Escape from Godunov

   4. Finite Element Implementation

4. LINEAR AND NONLINEAR MODEL PROBLEMS 42

   1. Computational Form of the TWS for Model Problems

   2. Numerical Experiments

5. THE EULER SYSTEM 58

   1. Governing Equations

   2. Taylor Weak Statement for the Euler System

   3. Numerical Boundary Treatment

   4. Numerical Experiments with the Euler System

6. SUMMARY AND CONCLUSIONS 83

LIST OF REFERENCES 86

APPENDICES

A. SEMI-DISCRETE FOURIER MODAL ANALYSIS OF THE LINEAR ADVECTION EQUATION IN 1-D 92

B. FULLY-DISCRETE FOURIER MODAL ANALYSIS OF THE ADVECTION EQUATION IN 1-D 98

C. A PARABOLIC EQUATION IN 1-D 103

D. SOME ASPECTS ON THE BOUNDARY 105

E. FIGURES 108

VITA 145

LIST OF TABLES

TABLE PAGE

3.1 Taylor Weak Statement Parameters 27

3.2 Damping coefficient (D) and Numerical speed (a^*) due to spatial discretization 29

3.3 Dissipation Error ($\omega \Delta t D$) and Dispersion Error ($\omega \Delta t(a-a^*)$) 30

LIST OF FIGURES

FIGURE PAGE

A-1. Coefficients p_k and q_k in A_1 and A_2 of eq.(A.2) 93

D-1. Definition of x_1-boundary and x_2-boundary 106

1. Region of TVD (shaded area) selected by Sweby (1984) 108

2. Discontinuity of flux gradient in C^0 finite element method 108

3. Initial data (dashed line) and exact solution (solid line) at $t - t_0 = 0.375$ sec for linear step problem 109

4. Initial data (dashed line) and exact solution (solid line) at $t - t_0 = 0.5$ sec for nonlinear Burgers step problem 109

5. TWS Nodal Solutions for Linear Step problem 110

6. TWS Nodal Solutions for Linear Step problem using Flux-limited Galerkin ($\alpha = 0 = \beta$) 111

7. TWS Nodal Solutions for Linear Step problem using Flux-limited Raymond-Garder ($\alpha = (15)^{-1/2} = \beta$), $\theta = 0.5$ 112

8. TWS Nodal Solutions for Linear step problem using Flux-limited Dissipative Galerkin ($\alpha = 0.1 = \beta$), $\theta = 0.5$ 113

9. TWS Nodal Solutions for Linear Step problem 114

10. TWS Nodal Solutions for Burgers Step problem 115

11. TWS Nodal Solutions for Burgers step problem using first-order dissipative Galerkin algorithm with $\varepsilon = 0.0$ 116

12. TWS Nodal Solutions for Burgers Step using Bubnov-Galerkin ($\alpha = 0 = \beta$, $\theta = 0.5$) 117

13. TWS Nodal Solutions for Burgers Step using Raymond-Garder ($\alpha = (15)^{-1/2} = \beta$, $\theta = 0.5$) 118

14. TWS Nodal Solutions for Burgers Step using Dissipative Galerkin ($\alpha = 0.1 = \beta$, $\theta = 0.5$) 119

15. Initial data for discontinuity aligned with grid 120

16. Initial data for the discontinuity skewed to the grid by 45 degrees 120

17. TWS Field Solutions for Two-dimensional linear case
(discontinuity aligned with grid), $C_x = 0.096$, $C_y = 0.032$ 121

18. TWS Field Solutions for Two-dimensional linear case
(45 degree skewed with grid), $C_x = 0.064 = C_y$ 122

19. TWS Field Solutions for Two-dimensional Burgers case
(discontinuity aligned with grid) 123

20. TWS Field Solutions for Two-dimensional Burgers case
(45 degree skewed with grid) 124

21. Local Coordinate axes rotated by angle θ 125

22. Tangential (x_1') and Normal (x_2') axes at a surface 125

23. Exact solution for One-dimensional Riemann shock tube problem 126

24. Riemann shock tube solution by Donor-cell ($\theta = 0.0$) 127

25. Riemann shock tube solution by Raymond-Garder ($\theta = 0.5$) 127

26. Riemann shock tube solution by Euler Taylor-Galerkin 128

27. Riemann shock tube solution by dissipative Galerkin ($\alpha = 0.1 = \beta$) 128

28. Riemann shock tube solution by diss. Galerkin ($\alpha = 0.1 = \beta$)
with $\varepsilon = 0.1$ for non-linear fields only 129

29. Riemann shock tube solution by Bubnov-Galerkin
with $\varepsilon = 0.1$ for non-linear fields only 129

30. Domain and Initial data for two-dimensional shock interaction problem . . . 130

31. ETG solution for two-dimensional shock interaction problem
on a rectangular grid 131

32. Bubnov-Galerkin solution for two-dimensional shock interaction problem
on a rectangular grid with $\varepsilon = 1/6$ for nonlinear field only 132

33. ETG solution for two-dimensional shock interaction problem
on a nonrectangular grid 133

34. Bubnov-Galerkin solution for two-dimensional shock interaction problem on a nonrectangular grid with $\varepsilon = 1/6$ for non-linear field only 134

35. Exact solution for Mach number for Quasi one-dimensional deLaval nozzle problem 135

36. Mach number for Q1D deLaval nozzle problem by Donor-cell and Raymond-Garder methods for $M_S = 1.3$ 136

37. Mach number for Q1D Laval nozzle problem by Bubnov-Galerkin and Raymond-Garder methods with $\varepsilon = 1.0$ for all field ($M_S = 1.3$) 137

38. Mach number for Q1D deLaval nozzle problem by Bubnov-Galerkin and Raymond-Garder methods with ε=1.0 for nonlinear fields only (M_S=1.3) . 138

39. Mach number for Q1D deLaval nozzle problem by Donor-cell and Raymond-Garder methods for $M_S = 1.8$ 139

40. Mach number for Q1D deLaval nozzle problem by Bubnov-Galerkin and Raymond-Garder methods with $\varepsilon = 1.0$ for all field ($M_S = 1.8$) 140

41. Mach number for Q1D deLaval nozzle problem by Bubnov-Galerkin and Raymond-Garder methods with ε=1.0 for nonlinear fields only (M_S=1.8) . 141

42. Wedge flow problem statement 142

43. Shock reflection problem statement 142

44. Density solution for Wedge flow problem 143

45. Density solution for Shock reflection problem 144

CHAPTER 1

INTRODUCTION

In high speed flows such as transonic or supersonic aerodynamics, the most interesting and difficult to understand phenomena occurs, namely shock waves. Across the shock wave surface, there are sudden changes in the flow properties like density and pressure. In the application to aerodynamics, it is important to know at the design stage the shock position if it is present, and its strength, since the shock wave significantly alters flow properties hence pressure distributions around a body.

Since the solution to the system of partial differential equation being solved is not analytic at the shock surface, its approximation is sought as a weak solution of the system of differential equations. Since the weak form of the governing partial differential equation is expressed in an integral form, solutions with discontinuities can be a part of weak solutions. Moreover, when conservative variables are chosen, the weak form of the integral relation reduces to the conservation laws, a feature of which contains the shock jump relations, the so-called Rankine-Hugoniot conditions, as the only relation at the shock to be satisfied. The mathematical description of such flows can be found in the hyperbolic system of conservation laws. According to Lax (1973), weak solutions from the integral relation of the conservation laws are called generalized solutions, and with the same initial data, only one of which has physical significance. A criterion for selecting the right one is termed an entropy condition.

Consequently, there exist difficulties in the numerical solution of first order hyperbolic systems of conservation laws. Finite element theory provides conveniences to the construction of discrete and/or semi-discrete approximations of variational boundary

value problems in mechanics including reduced forms of the Navier-Stokes equations. However, it is now well recognized that the traditional error orthogonalization weak statement is not fully adequate at large Mach and Reynold numbers in computational fluid dynamics (CFD). Research on finite element analysis over the last decade has focused on the derivation and definition of suitable weak statements for the Navier-Stokes equations for high speed flows. Under the assumption of infinite Reynolds number, the Navier-Stokes equations reduce to the inviscid hyperbolic system of conservation laws termed the Euler equations.

Of importance to the current development and its formulational structure, Donea (1984) developed the Taylor- Galerkin finite element algorithm, a numerical procedure for the advection-diffusion equation wherein the weak statement was formed on a Taylor series expansion of the unsteady equation, with higher order derivatives reexpressed in terms of derivatives of the flux vector of the first order hyperbolic conservation law. Baker (1985) noted the richness of the interchanging of weak statement and Taylor series and derived a finite element CFD algorithm for problem classes ranging from transonic potential flow to high speed Navier-Stokes. The major frame of this formulational procedure has been expanded by Baker and Kim (1986) to derive and evaluate a generalized family of finite element functional forms, known as the Taylor Weak Statement (TWS), using the classical Galerkin test space constraint applied to a Taylor series restatement of the governing first order hyperbolic equation. The TWS algorithm is verified to contain as special cases over a dozen independently derived dissipative finite difference and finite element algorithms.

This research is extended toward development and evaluation of a suitable method from the Taylor Weak Statement for the computation of shocked inviscid flow problems. To establish a sharp and monotone shock capturing Galerkin-type scheme, we followed

some precepts of finite difference flux methodology with a different perspective. The widely used technique in recent finite difference methods is a controlling mechanism of the second order correction term of flux functions, known as flux limiters.

The development of flux limiters in finite difference methodology has emerged from van Leer's experiment (1974) on the Fromm's scheme and the diffusion / anti-diffusion step proposed by Boris and Book (1973). The Fromm scheme, being the 3rd order accurate four point scheme, needed to be modified to a three point scheme, as was noted by Roe (1982). In pursuit of a monotone and sharp shock capturing scheme, Roe chose two different schemes, Lax-Wendroff (1960) and Warming-Beam (1975), from which he devised a minmod b-function, i.e,

$$b(x,y) = \text{minimum modulus of } (x,y)$$

$$= \begin{cases} x & \text{if } |x| \le |y| \\ y & \text{if } |x| > |y| \end{cases}$$

to direct the anti-diffusion flux to a proper target. This idea of mixing the central and the upwind differencing was also mentioned by Leonard (1979).

Harten (1983) proposed a sufficient condition, under which monotonicity can be preserved for a second order three point scheme, which is known as the Total Variation Diminishing (TVD) condition. The TVD condition requires that

$$TV(u^{n+1}) \le TV(u^n)$$

for $TV(u) \equiv \sum |u_{j+1} - u_j|$

where the superscripts n+1 and n denote the $n+1^{st}$ and n^{th} time station respectively and the subscripts j+1 and j denote the $j+1^{st}$ and j^{th} spatial positions respectively. Specifically, the TVD condition implies that if a 3-point or a 5-point scheme can be written in the form

$$u_j^{n+1} = u_j^n + C_{j+1/2}\,\delta_+ u_j^n - C_{j-1/2}\,\delta_- u_j^n$$

where $C_{j+1/2} = C(u_{j-1}, u_j, u_{j+1}, u_{j+2})$

and $C_{j-1/2} = C\,(\,u_{j-2}, u_{j-1}, u_j, u_{j+1}\,)$,

then, sufficient conditions for the scheme to be TVD are

$$C_{j+1/2} \geq 0\,,\ C_{j-1/2} \leq 0\,,\ C_{j+1/2} + C_{j-1/2} \leq 1$$

Harten also developed a one parameter family of such schemes from a modified flux function approach.

The development of these schemes preserving sharpness, and at the same time showing a smoothness, required a significant insight into the numerical behavior since they are intrinsically nonlinear schemes, and hence their analysis has not progressed as expected. However, it can be found that some explanation on numerical behavior is possible from the completion of the Fourier modal analysis on the Taylor Weak Statement in one space dimension, and from the analysis, a simple way to incorporate a flux limiting procedure into the standard and dissipative Galerkin methods is developed. Due to its simplicity, the multi-dimensional extension is also straightforward.

In Chapter 2, the Taylor Weak Statement is derived, and its utility is illustrated for the transonic full potential description in multi-dimensional space.

In Chapter 3, a Fourier modal analysis is documented for characterization of the Taylor Weak Statement expansion coefficients. Also a reformulation of the Taylor Weak Statement is shown to establish a flux limiter type switching coefficient.

In Chapter 4, Numerical verifications on the one- and two-dimensional discontinuous initial value problems for both linear and nonlinear cases are documented.

In Chapter 5, the Taylor Weak Statement is applied to the Euler equation system and its numerical boundary treatment is described. Numerical results are presented for the one-dimensional Riemann shock tube problem, a quasi one-dimensional deLaval nozzle problem, a two-dimensional shock interaction problem and a two-dimensional steady state oblique shock problem.

In Chapter 6, a summary and future research directions for this work are stated.

In Appendix A, a generalized formula of the semi-discrete error estimate is derived for the linear advection equation in one space dimension.

In Appendix B, a generalized formula for dissipation and dispersion error estimates is derived for the linear advection equation in one space dimension.

In Appendix C, the generalized formula for the dissipation and dispersion error estimates is extended to a parabolic case.

In Appendix D, based on the papers by Chakravarthy (1983) and Thompson (1987), a new approach for the treatment on the boundary in connection with a first order hyperbolic system is shown.

CHAPTER 2

THE TAYLOR WEAK STATEMENT

(2.1) Formulation of the TWS

We seek to formulate a numerically amenable restatement of conservation laws by means of a Taylor series expansion in time. Consider the following scalar equation in conservation law form.

$$\frac{\partial u}{\partial t} + \frac{\partial f_i}{\partial x_i} = \frac{\partial u}{\partial t} + a_i \frac{\partial u}{\partial x_i} = 0 \tag{2.1}$$

where $a_i \equiv df_i / du$ is termed the Jacobian of the flux vector f_i. The Taylor series expansion in time for u (x,t) is written as

$$\frac{u^{n+1} - u^n}{\Delta t} = \frac{\partial u^n}{\partial t} + \left(\frac{\Delta t}{2}\right) \frac{\partial^2 u^n}{\partial t^2} + \left(\frac{\Delta t^2}{6}\right) \frac{\partial^3 u^n}{\partial t^3} + \ldots \tag{2.2}$$

where the superscript n and n+1 denote the nth and $n+1^{st}$ time level and $\Delta t \equiv t^{n+1} - t^n$.

To restate the conservation law by use of eq.(2.2), the time derivatives are replaced in terms of the spatial derivatives expressed in eq. (2.1). Specifically,

$$\frac{\partial u}{\partial t} = - \frac{\partial f_i}{\partial x_i} \tag{2.3}$$

$$\frac{\partial^2 u}{\partial t^2} = - \frac{\partial}{\partial t}\left(\frac{\partial f_i}{\partial x_i}\right) = - \frac{\partial}{\partial x_i}\left(\frac{\partial f_i}{\partial t}\right) \tag{2.4}$$

Since $\frac{\partial f_i}{\partial t} = \frac{\partial f_i}{\partial u}\frac{\partial u}{\partial t} = a_i \frac{\partial u}{\partial t} = - a_i \frac{\partial f_j}{\partial x_j}$, the second derivative term can be written as a linear combination of $\partial u / \partial t$ and $\partial f_j / \partial x_j$. Hence,

$$\frac{\partial^2 u}{\partial t^2} = \frac{\partial}{\partial x_i}\left\{ a_i \left(\alpha \frac{\partial u}{\partial t} + \beta \frac{\partial f_j}{\partial x_j} \right) \right\} \tag{2.5}$$

where $-\alpha + \beta = 1$ yields the 2nd order time accurate expression for the above process. The third time derivative term can be similarly expressed as

$$\frac{\partial^3 u}{\partial t^3} = \frac{\partial}{\partial t}\left\{ \frac{\partial}{\partial x_i}\left(a_i \frac{\partial f_j}{\partial x_j} \right) \right\} \tag{2.6}$$

$$= \frac{\partial}{\partial x_i}\left\{ \frac{\partial}{\partial t}\left(a_i \frac{\partial f_j}{\partial x_j} \right) \right\}$$

$$\approx \frac{\partial}{\partial x_i}\left\{ a_i \frac{\partial}{\partial x_j}\left(\frac{\partial f_j}{\partial u}\frac{\partial u}{\partial t} \right) \right\} \qquad , \text{for } \frac{\partial a_i}{\partial t} \equiv 0$$

$$= \frac{\partial}{\partial x_i}\left\{ a_i \frac{\partial}{\partial x_j}\left(a_j \frac{\partial u}{\partial t} \right) \right\}$$

$$= -\frac{\partial}{\partial x_i}\left\{ a_i \frac{\partial}{\partial x_j}\left(a_j \frac{\partial f_k}{\partial x_k} \right) \right\}$$

From the linear combination of the last two terms, the third order time derivative expression can be written in conservative law form as

$$\frac{\partial^3 u}{\partial t^3} = \frac{\partial}{\partial x_i}\left\{ a_i \frac{\partial}{\partial x_j} a_j \left(\gamma \frac{\partial u}{\partial t} + \mu \frac{\partial f_k}{\partial x_k} \right) \right\} \tag{2.7}$$

where $\gamma + \mu = 1$ retains third order accuracy in time.

Hence, substitution of the eqs. (2.3),(2.5) and (2.7) into eq. (2.2) yields the following expression :

$$\frac{u^{n+1} - u^n}{\Delta t} = \frac{\partial}{\partial x_i} a_i \left\{ \alpha \left(\frac{\Delta t}{2}\right) \frac{\partial u}{\partial t} + \frac{\partial}{\partial x_j} \gamma \left(\frac{\Delta t^2}{6}\right) a_j \frac{\partial u}{\partial t} \right\}^n \tag{2.8}$$

$$- \left(\frac{\partial f_i}{\partial x_i}\right)^n + \frac{\partial}{\partial x_i} a_i \left\{ \beta \left(\frac{\Delta t}{2}\right) \frac{\partial f_j}{\partial x_j} + \frac{\partial}{\partial x_j} \mu \left(\frac{\Delta t^2}{6}\right) a_j \frac{\partial f_k}{\partial x_k} \right\}^n + \ldots$$

The LHS of the eq.(2.8) is a time discrete forward approximation of $\partial u/\partial t$ on the interval $\Delta t = t^{n+1} - t^n$. The RHS contains continuous expressions evaluated at t^n. To establish the desired modified conservation statement, we accept the following continuous expression obtained from eq. (2.8) in the limit $\Delta t \rightarrow \varepsilon \geq 0$,

$$L(u) \equiv \frac{\partial u}{\partial t} - \frac{\partial}{\partial x_i} a_i \left\{ \alpha \left(\frac{\Delta t}{2}\right) \frac{\partial u}{\partial t} + \frac{\partial}{\partial x_j} \gamma \left(\frac{\Delta t^2}{6}\right) a_j \frac{\partial u}{\partial t} \right\} \tag{2.9}$$

$$+ \left(\frac{\partial f_i}{\partial x_i}\right) - \frac{\partial}{\partial x_i} a_i \left\{ \beta \left(\frac{\Delta t}{2}\right) \frac{\partial f_j}{\partial x_j} + \frac{\partial}{\partial x_j} \mu \left(\frac{\Delta t^2}{6}\right) a_j \frac{\partial f_k}{\partial x_k} \right\} + \ldots$$

Introducing a set of weighting functions $v(\underline{x})$, and forcing the integral inner product between $v(\underline{x})$ and $L(u)$ to vanish on the region $\Omega \subset R^n$, one arrives at the weak statement or weighted residual formulation for $L(u)$, which we term the Taylor Weak Statement TWS (u), as

$$\text{TWS (u)} \equiv \int_\Omega v(\underline{x}) L(u) \, d\underline{x} \equiv 0 \qquad \text{, for all } v(\underline{x}) \in H^m \tag{2.10}$$

(2.2) Finite Element Approximation

Given a finite N-dimensional subspace $S^h \subset H^m$, where H^m denotes an admissible trial function space and $m \geq 1$, an approximation to $u(x,t)$ can be written as

$$u(\underline{x},t) \approx u^N(\underline{x},t) = \sum_{j=1}^{N} \psi_j(\underline{x}) U_j(t), \qquad \text{for } \psi_j(\underline{x}) \in S^h \tag{2.11}$$

where $\psi_j(\underline{x})$, $1 \leq j \leq N$ is the set of trial functions upon which the approximation is supported.

Due to the modified conservation law statement, eq.(2.9), we choose the weighting function approximation from the same space as the trial function space, the so-called Galerkin criteria, i.e.,

$$v(\underline{x}) \approx v^N(\underline{x}) = \sum_{j=1}^{N} \psi_j(\underline{x})\, V_j, \qquad \text{for all } V_j,\ j=1,\ldots,N \tag{2.12}$$

Hence, the substitution of eqs. (2.11) and (2.12) into (2.10) results in the finite element approximate form

$$\int_\Omega \sum_j \psi_j(\underline{x}) V_j \; L(u^N)\, d\underline{x} \equiv 0, \qquad \text{for all } V_j,\ j=1,\ldots,N \tag{2.13}$$

Seeking the null point of the Weak Statement, eq. (2.13), w.r.t. V_j, i.e., $\partial / \partial V_j = 0$ for all j, the Taylor Weak Statement on a finite dimensional subspace S^h becomes

$$\text{TWS}(u^N) = \int_\Omega \psi_j(\underline{x})\; L(u^N)\, d\underline{x} \equiv 0, \qquad 0 \le j \le N \tag{2.14}$$

The essence of a finite element computational method is to define a discretization Ω^h of Ω as a union of subdomains Ω_e, and to define the basis function set $\{N_k(\zeta)\}$ on Ω_e that contains all components of $\psi_j(\underline{x})$ on Ω_e. Hence,

$$\Omega \approx \Omega^h \equiv \bigcup \Omega_e$$

and the approximation of $u(\underline{x},t)$

$$u(\underline{x},t) \approx u^N(\underline{x},t) = \sum_j^N \psi_j(\underline{x})\; U_j(t)$$

is replaced by a union of element approximations

$$u^h(\underline{x},t) = \bigcup_e \{N(\zeta)\}^T \{U(t)\}_e$$

where $\{\cdot\}$ denotes a column matrix of element properties, $\{\cdot\}^T$ is the transpose, $\{N_k(\zeta)\}$ is the kth degree cardinal basis for $\psi_j(\underline{x})$ on the element Ω_e, and $\{U(t)\}_e$ contains the nodal values of $u^h(\underline{x},t)$ on the element Ω_e at time t.

For these restrictions, the Taylor Weak Statement eq.(2.14) takes the specific form

$$TWS\,(u^h) = S_e\left(\,TWS_e(u^h)\,\right) \qquad (2.15)$$

$$= S_e \int_{\Omega_e} \{N_k\}\; L(u^h)\, d\underline{x}$$

where S_e denotes assembly over elements Ω_e of Ω^h, which is a rowwise matrix summation process, cf. Baker (1983, Ch.2).

Let

$$\underline{\alpha}\, h_i \equiv \alpha\ (\Delta t/2)\ a_i$$

$$\underline{\beta}\, h_i \equiv \beta\ (\Delta t/2)\ a_i$$

$$\underline{\gamma}\, h_i h_j \equiv \gamma\ (\Delta t^2/6)\ a_i\ a_j$$

$$\underline{\mu}\, h_i h_j \equiv \mu\ (\Delta t^2/6)\ a_i\ a_j$$

Then, the corresponding modification to eq.(2.9) is

$$L(u) \equiv \frac{\partial u}{\partial t} - \frac{\partial}{\partial x_i}\left\{ \underline{\alpha}\, h_i \frac{\partial u}{\partial t} + \frac{\partial}{\partial x_j} \underline{\gamma}\, h_i h_j \frac{\partial u}{\partial t} \right\} \qquad (2.16)$$

$$+ \left(\frac{\partial f_i}{\partial x_i}\right) - \frac{\partial}{\partial x_i}\left\{ \underline{\beta}\, h_i \frac{\partial f_j}{\partial x_j} + \frac{\partial}{\partial x_j}\, \underline{\mu}\, h_i h_j \frac{\partial f_k}{\partial x_k} \right\}$$

In the definition of the new set of parameters $\underline{\alpha}$, ...,$\underline{\mu}$, the nondimensional Courant number C_i for the ith direction can be introduced as

$$C_i \equiv a_i\, \Delta t / h_i\,, \quad \text{i not summed}$$

where h_i is a measure of the mesh corresponding to an element span in the ith direction.

With some loss of generality, by neglect of the boundary integral terms for the non-physical terms in eq.(2.16), the $TWS_e\,(u^h)$ can be reexpressed as

$$TWS_e(u^h) = \int_{\Omega_e} \{N_k\} \left(1 - \frac{\partial}{\partial x_i}\left(\underline{\alpha}\, h_i + \frac{\partial}{\partial x_j} \underline{\gamma}\, h_i h_j \right) \right) \frac{\partial u^h}{\partial t}\, d\Omega \qquad (2.17)$$

$$- \int_{\Omega_e} \frac{\partial \{N_k\}}{\partial x_i} \left[f_i^h - \left\{ \underline{\beta}\, h_i \frac{\partial f_m^h}{\partial x_m} + \frac{\partial}{\partial x_j} \underline{\mu}\, h_i h_j \frac{\partial f_k^h}{\partial x_k} \right\} \right] d\Omega$$

$$+ \oint_{\partial\Omega \cap \partial\Omega_e} \{N_k\}\, f_i^h \cdot \hat{n}_i \, d\Gamma$$

The traditional dissipative Galerkin procedure, cf., Dendy (1974), Raymond, et al. (1976), requires the weighting function $v(\underline{x})$ to be a perturbation of the trial space basis function $\psi(\underline{x})$ in such a way that

$$v(x) = \psi(x) + \vec{p} \cdot \nabla\psi(x)$$

where $\vec{p}$ is a perturbation parameter to be determined. In the present formulation, and for a scalar equation, this leads to the condition

$$\underline{\alpha} = \underline{\beta}$$
$$\underline{\gamma} = 0 = \underline{\mu}$$

Remark : The second time derivative term in eq. (2.2) of the Taylor series expansion constitutes a damping term. For both the $\underline{\alpha}$ -term and the $\underline{\beta}$ -term to yield a damping,

$$\underline{\alpha} \le 0, \ \underline{\beta} > 0 \quad \text{for } a > 0$$

and $$\underline{\alpha} \ge 0, \ \underline{\beta} < 0 \quad \text{for } a < 0.$$

This formulation leads to a first order accurate scheme in space (see Sec.3.2). In a dissipative Galerkin method, then, the $\underline{\alpha}$ -term is used as an anti-damping term to yield at least second order accuracy in space. Thus, the sign of the coefficient $\underline{\alpha}$ in the methods of Dendy or Raymond and Garder is different from that of the Taylor series expansion.

In Dendy's second method (1974), the test function v(x) is chosen to be

$$v(x) = \psi(x) + \upsilon\, S(a)\, \partial\psi/\partial x$$

where S(a) is the sign of a, the convection velocity, and υ is a constant chosen so that

$$\mathrm{Re}\,[\,\psi,\ \upsilon\, S(a)\, \partial\psi/\partial x\,] \le C_1 \|\psi\|^2, \qquad C_1 < 1$$

This formulation leads to a spatial second-order accuracy, i.e., $\underline{\alpha} = \underline{\beta}$, with a damping at the fourth order.

In Raymond and Garder (1974), $\underline{\alpha} = \underline{\beta}$ and the parameter υ is chosen as $(15)^{-1/2}$. This yields a fourth-order damping, with coefficient equal to $1/\,12\sqrt{15}$, and the numerical speed is accurate to fifth-order in the sense of semi-discrete Fourier modal analysis. It was suggested for use on a variable measure grid to minimize reflections or noise produced at the interface of different grid sizes.

In Baker and Soliman (1983), a penalty-Galerkin method is developed by introducing test functions for the time derivative term different from those for the spatial derivative term. The penalty-Galerkin method can be considered as an extension of the Raymond-Garder method for an equation system, since the coefficient υ of the Raymond-Garder is adjusted for improved solutions for a nonlinear system. The test function thus has two forms, which corresponds to $\underline{\alpha} \ge 0$ and $\underline{\alpha} \ne \underline{\beta}$, hence unique values for the time derivative term and the spatial derivative term. Specifically, the test function is written for the time derivative term as,

$$v(x) = \psi(x) + S(a)\, \upsilon_i\, \partial\psi/\partial x, \qquad \upsilon_i = c_1\,(15^{-1/2}),\quad 0 \le c_1 \le 2 \text{ for the Euler system}$$

and for the spatial derivative term as,

$$v(x) = \psi(x) + S(a)\, \upsilon_d\, \partial\psi/\partial x, \qquad \upsilon_d = c_2\,(15^{-1/2}),\quad 0 < c_2 \le 2 \text{ for the Euler system}$$

(2.3) Transonic Full Potential Equation

In this section, I show that the artificial density method, cf. Hafez,et al. (1979), a theoretical unification for finite difference/finite volume CFD methods for transonic full

potential computations, can be generalized to tensor invariant form using the Taylor series approach in Sec (2.1). The major requirement of the artificial density method is to introduce a dissipation mechanism, accomplished via modification of the density definition in the continuity equation, which yields a modified elliptic-like character for the potential assumption within the range of appropriate transonic Mach number.

The artificial density governing equation, Hafez, et al. (1979), is defined as

$$\nabla \cdot \tilde{\rho} \nabla \phi \equiv 0 \tag{2.18}$$

where

$$\tilde{\rho} \equiv \rho - \mu \frac{\partial \rho}{\partial s} \Delta s$$

The thermodynamic isentropic density ρ is

$$\rho = (M_\infty c)^{\frac{2}{\gamma - 1}} = \left\{ 1 - \left(\frac{\gamma - 1}{2} \right) M_\infty^2 \left(q^2 - 1 \right) \right\}^{\frac{1}{\gamma - 1}}$$

where

$$q^2 = \nabla \phi \, . \, \nabla \phi$$

$$\nabla \phi = u\hat{i} + v\hat{j}$$

c is the speed of sound, where for isentropic flows, $c^2 = dp/d\rho$.

The modification to the true density involves a switch

$$\mu = \max (0, 1 - M_x^{-2})$$

where x is parallel to the freestream, and a discrete statement of density increment along a streamline is

$$\frac{\partial \rho}{\partial s} \Delta s = \frac{u}{q} \frac{\partial \rho}{\partial x} \Delta x + \frac{v}{q} \frac{\partial \rho}{\partial y} \Delta y$$

Osher, et.al.(1984) show that this type of density biasing scheme satisfies the entropy condition through analysis of the hyperbolic system for unsteady isentropic flow.

The continuity equation of the Euler equation set is

$$\frac{\partial \rho}{\partial t} + \nabla \cdot \rho \vec{u} = 0 = \frac{\partial \rho}{\partial t} + \frac{\partial f_j}{\partial x_j}$$

The flux vector $\vec{f}$, with scalar components f_j, and its jacobian $\bar{a}$ can be written as

$$\vec{f} = \rho \vec{u} \tag{2.19-1}$$

$$\bar{a} \equiv d\vec{f} / d\rho = \vec{u} + \rho \, \partial \vec{u} / \partial \rho \tag{2.19-2}$$

From the steady momentum equations in 2-D,

$$\rho \left(u \frac{\partial u}{\partial x} + v \frac{\partial u}{\partial y} \right) + \frac{\partial p}{\partial x} = 0 \tag{2.20-1}$$

$$\rho \left(u \frac{\partial v}{\partial x} + v \frac{\partial v}{\partial y} \right) + \frac{\partial p}{\partial y} = 0 \tag{2.20-2}$$

and from the isentropic relation between p and ρ,

$$dp = c^2 \, d\rho \tag{2.21}$$

one can find expressions for $\partial\rho/\partial x$ and $\partial\rho/\partial y$ such as

$$\frac{\partial \rho}{\partial x} = \frac{-\rho}{c^2} \left(u \frac{\partial u}{\partial x} + v \frac{\partial u}{\partial y} \right) \tag{2.22-1}$$

$$\frac{\partial \rho}{\partial y} = \frac{-\rho}{c^2} \left(u \frac{\partial v}{\partial x} + v \frac{\partial v}{\partial y} \right) \tag{2.22-2}$$

With the irrotational condition,

$$\frac{\partial u}{\partial y} = \frac{\partial v}{\partial x} \tag{2.23}$$

$\partial\rho/\partial x$ and $\partial\rho/\partial y$ can be reexpressed as

$$\frac{\partial \rho}{\partial x} = \frac{-\rho}{c^2} \left(u \frac{\partial u}{\partial x} + v \frac{\partial v}{\partial x} \right) = \frac{-\rho}{c^2} \frac{\partial}{\partial x} \left(\frac{q^2}{2} \right) \tag{2.24-1}$$

$$\frac{\partial \rho}{\partial y} = \frac{-\rho}{c^2} \left(u \frac{\partial u}{\partial y} + v \frac{\partial v}{\partial y} \right) = \frac{-\rho}{c^2} \frac{\partial}{\partial y} \left(\frac{q^2}{2} \right) \tag{2.24-2}$$

Then from eq. (2.24),

$$d\rho = \frac{\partial \rho}{\partial x} dx + \frac{\partial \rho}{\partial y} dy = \frac{-\rho q}{c^2} dq \tag{2.25}$$

where $q = q(\rho)$ only. Hence,

$$\frac{\partial \vec{u}}{\partial \rho} = \frac{\partial u}{\partial \rho} \hat{i} + \frac{\partial v}{\partial \rho} \hat{j} \tag{2.26}$$

$$= \frac{\partial q}{\partial \rho} (\cos\theta)\, \hat{i} + \frac{\partial q}{\partial \rho} (\sin\theta)\, \hat{j}$$

$$= \frac{-c^2}{\rho q} \frac{\vec{u}}{q}$$

Substituting eqs. (2.26) into (2.19-2) verifies that the jacobian of the flux vector is

$$\vec{a} = \vec{u} + \rho \frac{\partial \vec{u}}{\partial \rho} = \left(1 - M^{-2}\right) \vec{u} \tag{2.27}$$

Therefore, the modified flux $\vec{f}^m$ for the TWS, eq.(2.8), can be written as follows:

$$\vec{f}^m = \vec{f} - \beta (\Delta t / 2)\, \vec{a}\, (\nabla \cdot \vec{f}) \tag{2.28}$$

$$= \vec{f} - \beta (\Delta t / 2)\, \vec{a}\, (\vec{a} \cdot \nabla \rho)$$

$$= \rho \vec{u} - \beta (\Delta t / 2)\, \vec{a}\, (1 - M^{-2})\, \vec{u} \cdot \nabla \rho$$

Let the streamline have an angle θ with a local x-coordinate. Then, from

$u = q \cos\theta$

$v = q \sin\theta$

$\Delta x = \Delta s \cos\theta$

$\Delta y = \Delta s \sin\theta$,

the jacobian $\vec{a}$ of the flux vector $\vec{f}$ can be written for 2-D as

$$\vec{a}\, \Delta t = (a_1 \Delta t / \Delta x)\, \Delta s \cos\theta\, \hat{i} + (a_2 \Delta t / \Delta y)\, \Delta s \sin\theta\, \hat{j} \tag{2.29}$$

$$= \frac{\Delta s}{q} \left(C_1 u \hat{i} + C_2 v \hat{j} \right)$$

where $C_1 \equiv$ non-dimensional Courant number in the x-direction, and

$C_2 \equiv$ non-dimensional Courant number in the y-direction.

Substitution of eq.(2.29) into (2.28) results in

$$\vec{f}^m = \left\{ \rho - \left(\frac{\beta}{2}\right) C_1 (1 - M^{-2}) \Delta s \left(\frac{u}{q} \frac{\partial \rho}{\partial x} + \frac{v}{q} \frac{\partial \rho}{\partial y} \right) \right\} u \hat{i} \qquad (2.30)$$

$$+ \left\{ \rho - \left(\frac{\beta}{2}\right) C_2 (1 - M^{-2}) \Delta s \left(\frac{u}{q} \frac{\partial \rho}{\partial x} + \frac{v}{q} \frac{\partial \rho}{\partial y} \right) \right\} v \hat{j}$$

$$= \left\{ \rho - \left(\frac{\beta}{2}\right) C_1 (1 - M^{-2}) \frac{\partial \rho}{\partial s} \Delta s \right\} u\hat{i} + \left\{ \rho - \left(\frac{\beta}{2}\right) C_2 (1 - M^{-2}) \frac{\partial \rho}{\partial s} \Delta s \right\} v\hat{j}$$

By introducing an artificial density $\bar{\rho}$, the modified flux $\vec{f}^m$ may be written conveniently as

$$\vec{f}^m = \bar{\rho} \nabla \phi \qquad (2.31)$$

where

$$\bar{\rho} = \rho - \underline{\beta}_i (1 - M^{-2}) \frac{\partial \rho}{\partial s} \Delta s$$

$$\underline{\beta}_i \equiv \beta C_i / 2$$

and $\underline{\beta}_i$ is the controlling factor of the artificial viscosity term in the ith direction.

Hence, it is verified that the Taylor series expression of the original conservative form, eq.(2.8), can generate a proper damping mechanism for this type of flow.

CHAPTER 3

ANALYSIS OF THE TWS IN ONE DIMENSION

(3.1) Recovery of Various Algorithms

The finite element discretization of the TWS' in the one dimensional case is developed for the linear advection equation

$$\frac{\partial u}{\partial t} + \frac{\partial f(u)}{\partial x} = \frac{\partial u}{\partial t} + a\frac{\partial u}{\partial x} = 0 \tag{3.1}$$

where $a = df / du \equiv$ constant. By definition, eq. (2.17) written for eq.(3.1) is

$$\begin{aligned} \text{TWS}(u^h) = S_e\Bigg[& \int_{\Omega_e} \{N\}\frac{\partial u^h}{\partial t}dx + \int_{\Omega_e} \frac{\partial \{N\}}{\partial x}\left(\underline{\alpha}\, h_e \frac{\partial u^h}{\partial t} + \frac{\partial}{\partial x}\underline{\gamma}\, h_e^2 \frac{\partial u^h}{\partial t}\right) dx \\ & - \int_{\Omega_e} \frac{\partial \{N\}}{\partial x}\vec{f}^h dx + \int_{\Omega_e} \frac{\partial \{N\}}{\partial x}\left(\underline{\beta}\, h_e \frac{\partial \vec{f}^h}{\partial x} + \frac{\partial}{\partial x}\underline{\mu} h_e^2 \frac{\partial \vec{f}^h}{\partial x}\right) dx \\ & + \oint_{\partial\Omega_e} \{N\}\vec{f}^h \cdot \hat{n}\, dx \Bigg] \end{aligned} \tag{3.2}$$

where h_e is the element mesh measure. For the linear basis,

$$\{N_{k=1}\} \equiv \{N\} = \begin{Bmatrix} 1 - \bar{x}/h_e \\ \bar{x}/h_e \end{Bmatrix}$$

and $\bar{x}$ is a local cartesian coordinate with origin at the left end of Ω_e.

Note that the linear basis function cannot support the third derivative term with coefficient $\underline{\mu}$ in eq. (3.2). For convenience, the following definitions are employed.

$$\frac{\partial f_j}{\partial x} \cong \begin{cases} \dfrac{\delta_- f_j}{h_e} \equiv \dfrac{f_j - f_{j-1}}{h_e} & \text{, for } a > 0 \\ \dfrac{-\delta_+ f_j}{h_e} \equiv \dfrac{f_j - f_{j+1}}{h_e} & \text{, for } a < 0 \end{cases} \tag{3.3}$$

The assembly of element matrices for the linear basis function on a uniform mesh then corresponds to familiar finite difference formulae as follows:

$$S_e \int_{\Omega_e} \{N\}\{N\}^T dx = S_e \frac{h_e}{6} \begin{bmatrix} 2 & 1 \\ 1 & 2 \end{bmatrix} \Rightarrow h\left(1 + \frac{\delta_+ \delta_-}{6}\right) \tag{3.4}$$

$$S_e \int_{\Omega_e} \frac{\partial\{N\}}{\partial x}\{N\}^T dx = S_e \frac{1}{2} \begin{bmatrix} -1 & 1 \\ -1 & 1 \end{bmatrix} \Rightarrow h(\delta_+ + \delta_-) \tag{3.5}$$

$$S_e \int_{\Omega_e} \frac{\partial\{N\}}{\partial x}\frac{\partial\{N\}}{\partial x}^T dx = S_e \frac{1}{h_e} \begin{bmatrix} 1 & -1 \\ -1 & 1 \end{bmatrix} \Rightarrow \frac{-1}{h} \delta_+ \delta_- \tag{3.6}$$

The assembly over neighboring elements of a uniform mesh sharing node X_j yields the corresponding TWS nodal finite difference form $L(U_j)$,

$$L(U_j) \equiv A_1 \frac{dU_j}{dt} + A_2\left(\frac{f_j}{h}\right) = 0 \tag{3.7}$$

where

$$A_1 = 1 - \frac{\alpha}{2}(\delta_+ + \delta_-) + \left(\frac{1}{6} - \gamma\right)(\delta_+ - \delta_-)$$

$$A_2 = \begin{cases} \delta_- + \dfrac{(1-2\beta)}{2}(\delta_+ - \delta_-) + \mu(\delta_-\delta_- - \delta_+\delta_-) & \text{, for } a > 0 \\ \delta_+ - \dfrac{(1+2\beta)}{2}(\delta_+ - \delta_-) + \mu(\delta_+\delta_+ - \delta_+\delta_-) & \text{, for } a < 0 \end{cases}$$

To compute an approximation solution, eq.(3.2) or (3.7) are employed to evaluate derivatives in the θ-time integration method, i.e.,

$$u^{n+1} = u^n + \Delta t \left\{ (1-\theta) \frac{\partial u}{\partial t}^n + \theta \frac{\partial u}{\partial t}^{n+1} \right\} + \ldots \tag{3.8}$$

$$= u^n - \Delta t \left\{ (1-\theta) \frac{\partial f}{\partial x}^n + \theta \frac{\partial f}{\partial x}^{n+1} \right\} + \ldots$$

A linearization of the flux f^{n+1} at the new time from the flux f^n at the old time yields

$$f^{n+1} \equiv f^n + \frac{\partial f}{\partial u}^n (u^{n+1} - u^n) \tag{3.9}$$

Substitution of eq.(3.9) into (3.8) shows that,

$$u^{n+1} = u^n - \Delta t \left\{ \frac{\partial f}{\partial x}^n + \theta \frac{\partial}{\partial x} \left(\frac{\partial f}{\partial u}^n (u^{n+1} - u^n) \right) \right\} \tag{3.10-1}$$

or

$$\left(1 + \theta \Delta t \frac{\partial}{\partial x} a^n \right) (u^{n+1} - u^n) + \Delta t \frac{\partial f}{\partial x}^n = 0 \tag{3.10-2}$$

where $a^n = \partial f^n / \partial u$. With a constant coefficient a^n, or a locally frozen coefficient assumption, eq.(3.10-2) can be written as

$$\left(1 + \theta a^n \Delta t \frac{\partial}{\partial x} \right) (u^{n+1} - u^n) + \Delta t \frac{\partial f}{\partial x}^n = 0 \tag{3.11}$$

To recover various algorithms from the TWS expansion parameters, a review on some methods in comparison to eq.(3.7) is pertinent :

The Donor-cell method was proposed by Courant, et al. (1952) and is also known as the upstream-differencing method (see Harten, et al. (1983)). For the constant coefficient scalar equation,

$$\frac{\partial u}{\partial t} + a \frac{\partial u}{\partial x} = 0, \quad a \equiv \text{constant},$$

the Donor-cell method is written as

$$u_j^{n+1} = u_j^n - \lambda a \begin{cases} u_j^n - u_{j-1}^n, & \text{for } a > 0 \\ u_{j+1}^n - u_j^n, & \text{for } a < 0 \end{cases} \qquad (3.12)$$

which can be rewritten as

$$u_j^{n+1} = u_j^n - \lambda \left(a^+ \delta_- u_j^n + a^- \delta_+ u_j^n \right) \qquad (3.13)$$

where $a^+ \equiv \max(a,0) = (a + |a|) / 2$

$a^- \equiv \min(a,0) = (a - |a|) / 2$

Hence, by reference to eq.(3.7), the Donor-cell method corresponds to

$\underline{\alpha} = 0 = \underline{\mu}$, $\underline{\gamma} = 1/6$ (a diagonal mass matrix, see eq.(3.4)), and $\underline{\beta} = S(a)/2$.

The Lax-Wendroff (1960) method can be recovered as a one step method from the TWS eq.(2.8) as

$\underline{\alpha} = 0 = \underline{\mu}$, $\underline{\gamma} = 1/6$ (a diagonal mass matrix), and $\underline{\beta} = \lambda/2$

where $\lambda \equiv a\Delta t/\Delta x$ = Courant number.

The Warming and Beam (1975) method is viewed as an upwinding correction to the Lax-Wendroff (L-W) method. From eq.(3.7), the L-W method is written as

$$L(U_j) = \frac{dU_j}{dt} + \left(\delta_- + \frac{1-\lambda}{2} (\delta_+ - \delta_-) \right) \left(\frac{f_j}{h} \right) \qquad \text{,for } a > 0$$

The central differenced diffusion term is corrected by the upwinding ($\underline{\mu}$-) term as

$$L(U_j) = \frac{dU_j}{dt} + \left(\delta_- + \frac{1-\lambda}{2} (\delta_+ - \delta_-) + \frac{1-\lambda}{2} (\delta_- \delta_- - \delta_+ \delta_-) \right) \left(\frac{f_j}{h} \right) \qquad \text{,for } a > 0$$

which is the Warming-Beam method. Hence, for either $a > 0$ or $a < 0$,

$\underline{\alpha} = 0$, $\underline{\beta} = \lambda/2$, $\underline{\gamma} = 1/6$ and $\underline{\mu} = S(a) (1 - |\lambda|) / 2$.

Godunov (1959) made a three point scheme for solution of a Riemann initial value problem by considering piecewise constant data on the interval $(x_{j-1/2}, x_{j+1/2})$. The

Godunov scheme, discussed in van Leer (1984) for a scalar equation and in Holt (1984) for the Euler equation system, approximates solution of eq.(3.1) by the integral

$$0 = \frac{1}{\Delta x}\int_t^{t+\Delta t}\int_{x_{j-1/2}}^{x_{j+1/2}} \left(\frac{\partial u}{\partial t} + \frac{\partial f}{\partial x}\right) dx\, dt \qquad (3.14)$$

This procedure can bewritten in the finite difference operator form as

$$u_j^{n+1} = u_j^n - \frac{\Delta t}{\Delta x}\left(f_j^n - f_{j-1}^n\right) \qquad \text{for } a = df/du > 0$$

$$= u_j^n - \frac{\Delta t}{\Delta x}\left(f_j^n - f_{j+1}^n\right) \qquad \text{for } a = df/du < 0$$

Across a sonic point ($a_{j-1} \le 0 \le a_{j+1}$), the flux f_j at node j is evaluated as

$f_j = f(u_0)$, $u_0 \equiv$ the sonic value of u between u_{j-1} and u_{j+1}.

Across a shock point ($a_j \ge 0 \ge a_{j+1}$), depending on the shock speed $s_{j+1/2}$,

$$s_{j+1/2} = \frac{f(u_{j+1}) - f(u_j)}{u_{j+1} - u_j}$$

the flux at node j is evaluated as

$f_j = f(u_j)$ if $s_{j+1/2} > 0$

$= f(u_{j+1})$ if $s_{j+1/2} < 0$

Therefore, except for the sonic and the shock point special cases, the Godunov scheme is identified by the TWS parameter definitions

$$\alpha = 0 = \mu,\ \beta = S(a)/2,\ \gamma = 1/6.$$

In the MUSCL (Monotonic Upstream-centered Scheme for Conservation Laws) differencing, van Leer (1979) replaced the Godunov piecewise constant function U_j in the interval ($x_{j-1/2}$, $x_{j+1/2}$) by the piecewise linear function v(x,t),

$$v(x,t) = U_j + s_j (x - x_j) \qquad \text{for } x \in (x_{j-1/2}, x_{j+1/2}) \qquad (3.15)$$

where s_j is a slope function monitoring smoothness. The original scheme of van Leer (1979) was applied to the Lagrangian flow equations and it is not possible for the TWS to reproduce it for a scalar equation. However, in Anderson, et al. (1985), a simplified version of the MUSCL scheme is developed for steady state problems in a flux vector splitting algorithm. In flux vector splitting methods, the flux vector is split into a positive flux F^+ and a negative flux F^- according to the eigenvalue signs of the flux vector jacobian matrix A of the Euler equations. Then, the Euler equation system approximate solution in 1D can be written as,

$$\frac{\partial U}{\partial t} + \frac{\partial F^+}{\partial x} + \frac{\partial F^-}{\partial x} = 0$$

where $F^+ \equiv A^+ U$

$F^- \equiv A^- U$

$F = F^+ + F^-$

The spatial differencing of $\partial F^+/\partial x$ at node j for a uniform grid is written as

$$A_2\left(\frac{F_j^h}{h}\right) \equiv \left(F_j^+ - F_{j-1}^+\right) + \frac{\phi_j}{2}\left(F_j^+ - F_{j-1}^+\right) - \frac{\phi_{j-1}}{2}\left(F_{j-1}^+ - F_{j-2}^+\right) \qquad (3.16)$$

$$= \delta_- F_j^+ + \left(\frac{\delta_+ - \delta_-}{2}\right)\phi_j F_j^+ - \left(\frac{\delta_+ - \delta_-}{2}\right)\delta_-\phi_j F_j^+$$

where ϕ_j is a switch controlling the spatial accuracy between first-order and second-order and $0 \le \phi_j \le 1$. Similarly, the spatial differencing of $\partial F^-/\partial x$ at node j is written as

$$A_2\left(\frac{F_j^-}{h}\right) \equiv \delta_+ F_j^- - \left(\frac{\delta_+ - \delta_-}{2}\right)\phi_j F_j^- - \left(\frac{\delta_+ - \delta_-}{2}\right)\delta_-\phi_j F_j^-$$

Then, for a scalar model equation, the flux vector splitting algorithm can be written as

$$L(U_j) = A_1\frac{dU_j}{dt} + A_2\left(\frac{f_j}{h}\right)$$

where

$$A_1 = 1.0$$

$$A_2 = \delta_- + \frac{\phi_j}{2}(\delta_+ - \delta_-) - \frac{\phi_{j-1}}{2}(\delta_+ - \delta_-)\delta_- \qquad \text{, for a positive flux } f^+$$

$$= \delta_+ - \frac{\phi_j}{2}(\delta_+ - \delta_-) - \frac{\phi_{j+1}}{2}(\delta_+ - \delta_-)\delta_+ \qquad \text{, for a negative flux } f^-$$

Hence, $\alpha = 0 = \beta$, $\gamma = 1/6$ and $\mu = \phi_j$ (flux limiter) in the TWS, eq.(3.7).

The Euler Taylor-Galerkin (ETG) method of Donea (1984) is based on an explicit Taylor series expansion as shown in Sec (2.1). From eq.(2.8) and (2.17), thus

$$\alpha = 0 = \mu, \quad \beta = \frac{\lambda}{2}, \quad \gamma = \frac{\lambda^2}{6}, \qquad \lambda = a\,\Delta t / \Delta x \equiv \text{Courant number.}$$

The Crank-Nicolson Taylor-Galerkin (CN-TG) method of Donea (1984) is based on the following Taylor series expansions :

$$u^{n+1} = u^n + \Delta t \frac{\partial u^n}{\partial t} + \frac{\Delta t^2}{2}\frac{\partial^2 u^n}{\partial t^2} + \frac{\Delta t^3}{6}\frac{\partial^3 u^n}{\partial t^3} + \cdots \qquad (3.17\text{-}1)$$

$$u^n = u^{n+1} - \Delta t \frac{\partial u^{n+1}}{\partial t} + \frac{\Delta t^2}{2}\frac{\partial^2 u^{n+1}}{\partial t^2} - \frac{\Delta t^3}{6}\frac{\partial^3 u^{n+1}}{\partial t^3} + \cdots \qquad (3.17\text{-}2)$$

Subtracting eq.(3.17-2) from (3.17-1), one can write

$$\frac{u^{n+1} - u^n}{\Delta t} = \frac{1}{2}\left(\frac{\partial u^n}{\partial t} + \frac{\partial u^{n+1}}{\partial t}\right) + \frac{\Delta t}{4}\left(\frac{\partial^2 u^n}{\partial t^2} - \frac{\partial^2 u^{n+1}}{\partial t^2}\right) + \frac{\Delta t^2}{12}\left(\frac{\partial^3 u^n}{\partial t^3} - \frac{\partial^3 u^{n+1}}{\partial t^3}\right) \qquad (3.18)$$

Replacing the time derivatives with spatial derivatives by means of eqs.(2.3-1) and (2.3-2),

(3.19)

$$\frac{u^{n+1} - u^n}{\Delta t} = -\frac{a}{2}\left(\frac{\partial u^n}{\partial x} + \frac{\partial u^{n+1}}{\partial x}\right) + \frac{a^2\Delta t}{4}\left(\frac{\partial^2 u^n}{\partial x^2} - \frac{\partial^2 u^{n+1}}{\partial x^2}\right) + \frac{a^2\Delta t^2}{12}\frac{\partial^2}{\partial x^2}\left(\frac{\partial u^n}{\partial t} - \frac{\partial u^{n+1}}{\partial t}\right)$$

Posing that,

$$\frac{1}{2}\left(\frac{\partial u^n}{\partial t} + \frac{\partial u^{n+1}}{\partial t}\right) \equiv \frac{u^{n+1} - u^n}{\Delta t} \qquad (3.20)$$

eq.(3.19) takes the form

$$\left(1 - \frac{a^2\Delta t^2}{6}\frac{\partial^2}{\partial x^2}\right)\left(\frac{u^{n+1} - u^n}{\Delta t}\right) \equiv -\frac{a}{2}\left(\frac{\partial u^n}{\partial x} + \frac{\partial u^{n+1}}{\partial x}\right) + \frac{a^2\Delta t}{4}\left(\frac{\partial^2 u^n}{\partial x^2} - \frac{\partial^2 u^{n+1}}{\partial x^2}\right) \tag{3.21}$$

To interpret the above equation within the TWS parameter set $\underline{\alpha},\ldots,\underline{\mu}$, the linearization of the flux at the new time level in eq.(3.9) is taken as

$$a\frac{\partial u^{n+1}}{\partial x} = \frac{\partial f^{n+1}}{\partial x} \approx \frac{\partial}{\partial x}\left(f^n + a\left(u^{n+1} - u^n\right)\right) \tag{3.22-1}$$

$$\equiv \frac{\partial}{\partial x} f^n + \frac{\partial}{\partial x} a\Delta t \frac{\partial u}{\partial t}$$

Simalarly,

$$a^2\frac{\partial^2 u^{n+1}}{\partial x^2} \equiv a^2\frac{\partial^2 u^n}{\partial x^2} + \frac{\partial^2}{\partial x^2} a^2\Delta t \frac{\partial u}{\partial t} \tag{3.22-2}$$

Hence, eq. (3.21) is converted to

$$\left(1 + \frac{\lambda^2}{12} h^2 \frac{\partial^2}{\partial x^2}\right)\frac{\partial u}{\partial t} + \frac{\partial f^n}{\partial x} = 0, \qquad \text{for } \theta = 0.5 \tag{3.23}$$

Then, within the TWS,

$$\underline{\alpha} = 0 = \underline{\beta} = \underline{\mu} \quad \text{and} \quad \underline{\gamma} = \lambda^2/12.$$

The Euler Characteristic-Galerkin (ECG) method of Morton (1985) uses a test function which widens its nodal support as the Courant number λ is increased. This scheme is considered as a Taylor series restatement for $\alpha = 0 = \gamma$, $\beta = 1 = \mu$ in eq.(2.9). If the Courant number is less than 1, the ECG scheme is written as

$$0 = \left(1 + \frac{\delta_+ - \delta_-}{6}\right)\frac{dU_j}{dt} + \left(\delta_- + \left(\frac{1 - \lambda}{2}\right)\left(\delta_+ - \delta_-\right) + \frac{\lambda}{6}\left(\delta_-\delta_- - \delta_+\delta_-\right)\right) U_j^n \tag{3.24}$$

from which $\underline{\alpha} = 0 = \underline{\gamma}$, $\underline{\beta} = \lambda/2$ and $\underline{\mu} = \lambda^2/6$.

The Streamline Upwind Petrov-Galerkin (SUPG) method by Hughes and Brooks (1979) uses a test function for the convection term which is different from the test function

for the diffusion term. Its development is based on the steady-state convection-diffusion equation

$$u\frac{\partial T}{\partial x} - k\frac{\partial^2 T}{\partial x^2} = 0, \qquad 0 \le x \le 1 \tag{3.25}$$

where $u \equiv$ flow velocity,

$k \equiv$ thermal conductivity

$T \equiv$ Temperature.

Specifically, the test function v(x) is written

$$v(x) = \psi(x) + \upsilon\, \partial\psi/\partial x$$

where

$\upsilon = b\, uh/2$ for the convection term

$= 0$ for the conduction term

$b = \coth \alpha - 1/\alpha$

$\alpha = uh/2k \equiv$ cell Peclet number

Hence, as $u >> k$, $b \rightarrow 1$.

In this steady-state case, $\underline{\alpha}$ and $\underline{\gamma}$ are thus undefined, while $\underline{\beta} = \frac{u}{2} + \frac{k}{uh}$ and $\underline{\mu} = 0$.

Another form of a Taylor-Galerkin algorithm, the Swansea-Taylor-Galerkin (STG) method, was developed by the CFD group at Swansea. Originally conceived as a Galerkin algorithm with added (Lapidus) dissipation, cf., Lohner, Morgan and Zienkiewicz (1984), a recent reformulation has identified the underlying Taylor series conservation law statement, cf., Lohner, et al. (1986). The STG finite element algorithm is an explicit two-step procedure, akin to Lax-Wendroff, that constitutes retention of a second-order term in the Taylor series. The STG method is identified by the TWS as a Lax-Wendroff method with a mass matrix. Hence,

$$\underline{\alpha} = 0 = \underline{\gamma} = \underline{\mu} \quad \text{and} \quad \underline{\beta} = \lambda/2.$$

In Table (3.1), these algorithms as well as several well known dissipative discrete methods are illustrated for their corresponding rederivation via TWS parameters.

(3.2) Fourier Modal Analysis

The Fourier series representation of the analytical solution u(x,t) to eq. (3.1) is written as

$$u(x,t) = \sum_{p=-\infty}^{\infty} Q_p \exp [\, i\omega_p (x - at) \,] \tag{3.26}$$

where $i = \sqrt{-1}$

$\omega_p = 2\pi / L_p \equiv$ wave number

L_p = wave length of the pth Fourier mode.

Due to spatial discretization, wave lengths can be resolved only by an integer multiple of mesh length and the minimum wave length L_1 is $2\Delta x$. Hence, any numerical solution $u^h(x,t)$ on Ω^h cannot avoid discretization error. Assuming the numerical solution behaves similarly to the analytical one, its form at node j of Ω^h, i.e., $u^h(x_j,t)$, for a typical mode is written as

$$u^h(x_j,t) = \exp [\, i\omega (jh - \Gamma t) \,] \tag{3.27}$$

where

$\Gamma = a^* + i D$

a^* = numerical wave speed

D = damping coefficient

The damping coefficient D and the numerical speed a^* yield a potential error since the semi-discrete nodal value can be expressed as

$$U_j (t) = \exp[\, i\omega (jh - at) \,] \exp[\, \omega Dt \,] \exp[\, i\omega (a - a^*) t \,] \tag{3.28}$$

Table (3.1)

Taylor Weak Statement Parameters

Method	$\underline{\alpha}$	$\underline{\beta}$	$\underline{\gamma}$	$\underline{\mu}$	comment
Bubnov-Galerkin	0	0	0	0	$0 \le \theta \le 1$
Dissipative Galerkin	υ	υ	0	0	$\underline{\alpha} = \upsilon = \underline{\beta}$, $0 \le \theta \le 1$
Raymond-Garder	$S(a)\upsilon$	$S(a)\upsilon$	0	0	$0 \le \theta \le 1, \upsilon=(15)^{-1/2}$
ETG	0	$\lambda/2$	$\lambda^2/6$	0	$\theta = 0$
CN-TG	0	0	$\lambda^2/12$	0	$\theta = 0.5$
ECG	0	$\lambda/2$	0	$\lambda^2/6$	$0 \le \lambda \le 1$, $\theta = 0$
STG*	0	$\lambda/2$	0	0	$\theta = 0$
Donor-cell	0	$S(a)/2$	1/6	0	$\theta = 0$
Lax-Wendroff	0	$\lambda/2$	1/6	0	$\theta = 0$
Warming-Beam	0	$\lambda/2$	1/6	$S(a)\,(1-\lvert\lambda\rvert)/2$	$\theta = 0$
Flux Vector Splitting	----	0	1/6	ϕ_j	$\phi_j \equiv$ flux limiter, $\theta = 1$
SUPG	----	$S(u)/2 + k/uh$	----	0	$k \equiv$ conductivity

$S(a) \equiv$ Sign of a

$\lambda \equiv$ Courant number

*two-step method

For a scheme to be stable, the damping coefficient D must be non-positive, i.e., $D \leq 0$.

The coefficients of damping and numerical speed can be expressed in terms of the (uniform) mesh measure h as

$$D = a\left(M_2(\omega h) - M_4(\omega h)^3 + \ldots \right) \tag{3.29}$$

$$a^* = a\left(M_1 - M_3(\omega h)^2 + M_5(\omega h)^4 - \ldots \right) \tag{3.30}$$

Algorithm accuracy, as controlled by the TWS parameters $\underline{\alpha}, \ldots, \underline{\mu}$, thus involves the coefficients M_i which are readily determined(see Appendix A) as

$$M_1 = 1 \tag{3.31-1}$$

$$M_2 = \underline{\alpha} - \underline{\beta} \tag{3.31-2}$$

$$M_3 = \underline{\gamma} - S(a)\underline{\mu} + \underline{\alpha} M_2 \tag{3.31-3}$$

$$M_4 = \frac{\underline{\alpha}}{6} - \frac{\underline{\beta}}{12} + \frac{\underline{\mu}}{2} - \left(\frac{1}{6} - \underline{\gamma}\right) M_2 + \underline{\alpha} M_3 \tag{3.31-4}$$

$$M_5 = \frac{-1}{180} - \frac{S(a)\,\underline{\mu}}{4} + \frac{\underline{\gamma}}{12} + \frac{\underline{\alpha} M_2}{6} - \left(\frac{1}{6} - \underline{\gamma}\right) M_3 + \underline{\alpha} M_4 \tag{3.31-5}$$

where $S(a) \equiv$ Sign of a .

In Table (3.2), the damping coefficient D and the numerical speed a^* are evaluated for several well-known methods. From this Table, it may be noted that the Lax-Wendroff and ETG methods have a second-order damping in space while the Galerkin types have a fourth-order damping coefficient. In Table (3.3), the fully discrete error modes(dissipation and dispersion) are shown. It is found that the error modes computed from the formulae in Appendix (A) and Appendix (B) correspond exactly to those reported in the literature using various alternative procedures.

Noting the directional sensitivity within the choice of TWS expansion parameters $\underline{\alpha}, \ldots \underline{\mu}$, eq.(2.16) in Ch. 2 is now rewritten as

Table (3.2)

Damping coefficient (D) and Numerical speed (a^*)
due to spatial discretization

Method	M_2	M_3	M_4	M_5
Bubnov-Galerkin	0	0	0	$-1/180$
Dissipation Galerkin	0	0	$\beta/24$	$-1/180 + \beta^2/48$
Raymond-Garder	0	0	$S(a)/(12\sqrt{15})$	0
ETG	$-\lambda/2$	$\lambda^2/6$	$\lambda(1 - 2\lambda^2)/24$	$(10\lambda^4 - 5\lambda^2 - 2)/360$
Donor-cell	$-S(a)/2$	1/6	----	----
Lax-Wendroff	$-\lambda/2$	1/6	$-\lambda/24$	---
Warming-Beam	$-\lambda/2$	$(3\lambda - 2)/6$	$(-7\lambda + 6\,S(a))/24$	---

$D = a[\, M_2(\omega h) - M_4(\omega h)^3 + \ldots \,]$

$a^* = a[\, 1 - M_3(\omega h)^2 + M_5(\omega h)^4 - \ldots \,]$

$S(a) \equiv$ Sign of a

Table (3.3)

Dissipation Error ($\omega \Delta t D$) and Dispersion Error ($\omega \Delta t (a - a^*)$)

Method	b_2	b_3	b_4	b_5
Bubnov-Galerkin	$\lambda (1/2 - \theta)$	$\lambda^2 (\theta^2 - \theta + 1/3)$	$\lambda^3 (\theta^3 - \theta^2 + \theta/2 - 1/8)$	$-\lambda^4 (\theta^4 - \theta^3 + \theta^2/2 - \theta/6 + 1/36)$
$\theta = 1/2$	0	$\lambda^2/12$	0	$-\lambda^4/144$
Dissipation Galerkin	$\lambda (1/2 - \theta)$	$\lambda^2 (\theta^2 - \theta + 1/3)$	$\lambda^3 (\theta^3 - \theta^2 + \theta/2 - 1/8) - \beta / 24$	-----
$\theta = 1/2$	0	$\lambda^2/12$	$- \beta/24$	-----
ETG	0	0	$- (\lambda/24) (1 - \lambda^2)$	$(1-4\lambda^2)(1-\lambda^2) / 180$
Donor-cell	$(\lambda - S(a)) / 2$	$(1 - 2\lambda)(1 - \lambda) / 6$	-----	-----
Lax-Wendroff	0	$(1 - \lambda^2) / 6$	$- \lambda (1 - \lambda^2) / 8$	-----
Warming-Beam	0	$- (1 - \lambda)(2 - \lambda) / 6$	$-S(a) (1 - \lambda)^2 (2 - \lambda) / 8$	-----

$$\omega \Delta t D = \lambda [b_2 (\omega h)^2 + b_4 (\omega h)^4 + \ldots]$$

$$\omega \Delta t (a - a^*) = \lambda [b_1 (\omega h) + b_3 (\omega h)^3 + b_5 (\omega h)^5 + \ldots]$$

$$L(u) = \left\{ 1 - \frac{\partial}{\partial x}\left(S(a)\,|\underline{\alpha}|\,h + \frac{\partial}{\partial x}\,|\underline{\gamma}|\,h^2 \right) \right\} \frac{\partial u}{\partial t} \qquad (3.32)$$

$$+ \frac{\partial}{\partial x} \left\{ f - \frac{\partial}{\partial x}\left(S(a)\,|\underline{\beta}|\,h\,f + S(a)\,|\underline{\mu}|\,h^2 \frac{\partial f}{\partial x} \right) \right\}$$

From eqs. (3.31-1) through (3.31-5), the coefficients M_i are now reevaluated as

$$M_1 = 1 \qquad (3.33\text{-}1)$$

$$M_2 = S(a)\,\left(|\underline{\alpha}| - |\underline{\beta}|\right) \qquad (3.33\text{-}2)$$

$$M_3 = |\underline{\gamma}| - |\underline{\mu}| + S(a)\,|\underline{\alpha}|\,M_2 \qquad (3.33\text{-}3)$$

$$M_4 = S(a)\left(\frac{|\underline{\alpha}|}{6} - \frac{|\underline{\beta}|}{12} + \frac{|\underline{\mu}|}{2}\right) - \left(\frac{1}{6} - |\underline{\gamma}|\right) M_2 + S(a)\,|\underline{\alpha}|\,M_3 \qquad (3.33\text{-}4)$$

$$M_5 = \frac{-1}{180} - \frac{|\underline{\mu}|}{4} + \frac{|\underline{\gamma}|}{12} + S(a)\,\frac{|\underline{\alpha}|\,M_2}{6} - \left(\frac{1}{6} - |\underline{\gamma}|\right) M_3 + S(a)\,|\underline{\alpha}|\,M_4 \qquad (3.33\text{-}5)$$

From eqs.(3.33-1) to (3.33-5), the following observations are now made :

1. For a scheme to be spatially diffusive,

   $|\underline{\alpha}| < |\underline{\beta}|$

2. For a scheme to be spatially accurate to 2nd order,

   $|\underline{\alpha}| = |\underline{\beta}|$

3. For a scheme to be spatially accurate to 3rd order,

   $|\underline{\alpha}| = |\underline{\beta}|$ and $|\underline{\gamma}| = |\underline{\mu}|$

4. If $|\underline{\alpha}| = |\underline{\beta}| \neq 0$ and $|\underline{\gamma}| \neq |\underline{\mu}|$,

   then the damping coefficient D and the numerical speed a^* are

$$D = a \left\{ -S(a) \left(\frac{|\underline{\beta}|}{12} + \frac{|\underline{\mu}|}{2} + |\underline{\alpha}|\,M_3 \right) (\omega h)^3 + \ldots \right\}$$

$$a^* = a \left\{ 1 - \left(|\underline{\gamma}| - |\underline{\mu}| \right) (\omega h)^2 + \ldots \right\}$$

5. If $|\underline{\alpha}| = 0 = |\underline{\beta}|$ and $|\underline{\gamma}| \neq |\underline{\mu}|$,

$$D = a \left\{ - S(a) \left(\frac{|\underline{\mu}|}{2} \right) (\omega h)^3 + \ldots \right\}$$

$$a^* = a \left\{ 1 - (|\underline{\gamma}| - |\underline{\mu}|) (\omega h)^2 + \ldots \right\}$$

6. If $|\underline{\alpha}| = |\underline{\beta}|$ and $|\underline{\gamma}| = |\underline{\mu}|$,

$$D = a \left\{ - S(a) \left(\frac{|\underline{\beta}|}{12} + \frac{|\underline{\mu}|}{2} \right) (\omega h)^3 + \ldots \right\}$$

$$a^* = a \left\{ 1 - \left(\frac{1 + 30\,|\underline{\mu}|}{180} - |\underline{\beta}| \left(\frac{|\underline{\beta}|}{12} + \frac{|\underline{\mu}|}{2} \right) \right) (\omega h)^4 + \ldots \right\}$$

7. If $|\underline{\alpha}| = |\underline{\beta}| \neq 0$ and $|\underline{\gamma}| < |\underline{\mu}|$,

then from item number 4, the fourth order damping by the $\underline{\mu}$-term of the TWS may not be effective.

To expose the effect of the upwinding term ($\underline{\mu}$-term) on the dissipation error and the dispersion error, eqs.(B.16) and (B.17) from Appendix B are now rewrittem for θ = 0.0 and for θ = 0.5. For θ = 0.0,

$$\omega \Delta t\, D = \lambda \left\{ \left(\frac{\lambda}{2} + M_2 \right) (\omega h)^2 - \left(\frac{\lambda^3}{8} + \frac{\lambda^2}{2} M_2 + \lambda M_3 + M_4 \right) (\omega h)^4 + \ldots \right\} \qquad (3.34\text{-}1)$$

$$\omega \Delta t\, (a - a^*) = \lambda \left\{ \left(\frac{\lambda^2}{3} + \lambda M_2 + M_3 \right) (\omega h)^3 \right. \qquad (3.34\text{-}2)$$

$$\left. - \left(\frac{\lambda^4}{30} + \frac{\lambda^3}{6} M_2 + \frac{\lambda^2}{2} M_3 + \lambda M_4 + M_5 \right) (\omega h)^5 + \ldots \right\}$$

For θ = 0.5,

$$\omega \Delta t\, D = \lambda \left\{ M_2 (\omega h)^2 - \left(\frac{\lambda^2}{4} M_2 - \frac{\lambda}{2} M_2^2 + M_4 \right) (\omega h)^4 + \dots \right\} \tag{3.34-3}$$

$$\omega \Delta t\, (a - a^*) = \lambda \left\{ \left(\frac{\lambda^2}{12} + M_3 \right) (\omega h)^3 \right. \tag{3.34-4}$$

$$\left. - \left(\frac{\lambda^4}{180} - \frac{\lambda^3}{12} M_2 + \frac{\lambda^2}{4} \left(M_2^2 + M_3 \right) - \lambda M_2 M_3 + M_5 \right) (\omega h)^5 + \dots \right\}$$

Now consider the following three cases for the TWS with γ and μ as variables.

(1). Bubnov-Galerkin ($\theta = 0.5$)

$|\alpha| \equiv 0 \equiv |\beta|$, thus

$M_2 = 0,\ M_3 = |\gamma| - |\mu|,\ M_4 = S(a)\, |\mu| / 2$

$$\omega \Delta t\, D = \lambda \left[- S(a) \frac{|\mu|}{2} (\omega h)^4 + \dots \right] \tag{3.35-1}$$

$$\omega \Delta t\, (a - a^*) = \lambda \left[\left\{ \frac{\lambda^2}{12} + |\gamma| - |\mu| \right\} (\omega h)^3 + \dots \right] \tag{3.35-2}$$

(2). Dissipative-Galerkin ($\theta = 0.5$)

$|\alpha| = |\beta| \neq 0$, thus

$$M_2 = 0, \quad M_3 = |\gamma| - |\mu|, \quad M_4 = S(a) \left(\frac{|\beta|}{12} + \frac{|\mu|}{2} + |\beta| \left(|\gamma| - |\mu| \right) \right)$$

$$\omega \Delta t\, D = \lambda \left[- S(a) \left(\frac{|\beta|}{12} + \frac{|\mu|}{2} + |\beta| \left(|\gamma| - |\mu| \right) \right) (\omega h)^4 + \dots \right] \tag{3.36-1}$$

$$\omega \Delta t\, (a - a^*) = \lambda \left[\left\{ \frac{\lambda^2}{12} + |\gamma| - |\mu| \right\} (\omega h)^3 + \dots \right] \tag{3.36-2}$$

(3). Lax-Wendroff / ETG ($\theta = 0.0$)

$|\alpha| = 0,\ |\beta| = |\lambda| / 2$

$$M_2 = - S(a) |\lambda| / 2, \quad M_3 = |\gamma| - |\mu|, \quad M_4 = S(a) \left(\frac{|\lambda|}{24} - |\gamma| \frac{|\lambda|}{2} + \frac{|\mu|}{2} \right)$$

$$\omega \Delta t D = \lambda [- S(a) \left(\frac{|\lambda|}{24} \left(1 - 3|\lambda|^2 \right) + |\gamma| \frac{|\lambda|}{2} + |\mu| \frac{1 - |\lambda|}{2} \right) (\omega h)^4 + \dots] \quad (3.37\text{-}1)$$

$$\omega \Delta t (a - a^*) = \lambda [\left\{ \frac{- |\lambda|^2}{6} + |\gamma| - |\mu| \right\} (\omega h)^3 + \dots] \quad (3.37\text{-}2)$$

From the first two cases, the Bubnov-Galerkin generalization can experience a more effective damping than a dissipative-Galerkin method when using the upwind term (μ-term). Further, for the Bubnov-Galerkin case, the use of the coefficient $|\gamma|$ can control the phase error without affecting the fourth-order damping if $|\gamma|$ is chosen to be

$$|\gamma| = |\mu| - \lambda^2/12 \geq 0 .$$

This additional forth order damping is independent of time step for the Galerkin family.

These observations are the basis of my finite element flux limiting approach. In the Lax-Wendroff / ETG case, the ETG method can be considered the perturbation of Lax-Wendroff for $|\gamma| = \lambda^2 / 6$ and $|\mu| = 0$. Even though the ETG is accurate to 3rd order, the 4th order damping is not effective since it is dependent on the Courant number λ. However, the Lax-Wendroff / ETG can be modified to preserve 3rd order accuracy and to yield an effective damping at the 4th order for

$$|\gamma| - |\mu| = \frac{|\lambda|^2}{6}$$

and $|\mu|$ need not depend on the Courant number λ.

(3.3) Escape from Godunov

It is stated in Holt (1984) that Godunov (1959) proposed three main requirements as an alternative to the method of characteristics for solution of the compressible Euler equations. One requirement is monotonic behavior of a predicted solution and a qualitative agreement with the analytical solution. On the search for a scheme to satisfy this requirement, Godunov found that no second order scheme with

fixed coefficients can satisfy the monotonic property for a first order linear wave equation using a three point difference scheme.

The literature verifies that much of the recent effort has been devoted to the establishment of a sharper but still monotone solution for a discontinuous initial value problem. Recent techniques for such schemes introduce a controlling mechanism to the second order correction term, which is usually called an anti-diffusion flux term. Since this correction process controls the amount of anti-diffusion flux, depending on the underlying data, schemes developed this way are called non-linear and the coefficients of the second order process are defined by flux limiters.

To expose the backbone of such techniques, consider the known diffusive Donor-cell method.

$$L(U_j) = U_j^{n+1} - U_j^n + \frac{\Delta t}{\Delta x}\left[\frac{a}{2}\left(U_{j+1} - U_{j-1}\right)^n - \frac{|a|}{2}\left(U_{j+1} - 2U_j + U_{j-1}\right)^n\right] \qquad (3.38)$$

From eq. (B.15) in Appendix B, this is a second order accurate approximation to the viscous equation

$$\frac{\partial u}{\partial t} + a\frac{\partial u}{\partial x} = \frac{\partial}{\partial x}\frac{\Delta x}{2}(1 - |\lambda|)\,|a|\frac{\partial u}{\partial x} \qquad (3.39)$$

The RHS of the above equation is known as the artificial viscosity term with viscosity coefficient $(\Delta x/2)(1 - |\lambda|)\,|a|$. To achieve a second order accurate approximation to the original equation, the artificial term must be eliminated. This is known as the anti-diffusion process.

Hence, consider the following :

$$L(U_j) = U_j^{n+1} - U_j^n + \left(\frac{\Delta t}{\Delta x}\right)\left[\frac{a}{2}(U_{j+1} - U_{j-1})^n - \frac{|a|}{2}(U_{j+1} - 2U_j + U_{j-1})^n\right] \qquad (3.40)$$

$$+ \left(\frac{\Delta t}{\Delta x}\right)\frac{\partial}{\partial x}\left[\frac{(1 - |\lambda|)}{2}|a|\frac{\partial u}{\partial x}\right](\Delta x)^2$$

A proper differencing of the last term in eq. (3.40) will result in a second order accurate scheme. Central differencing results in the Lax-Wendroff (1960) method, while upwind differencing results in the Warming-Beam (1975) method, both of which are known to produce oscillatory solutions around discontinuities. However, a specific combination of the central and the upwind procedure can result in a sharp and monotonic solution that still preserves second order accuracy whenever possible. This is the basic reasoning of the flux limiter method proposed by Roe (1982).

It can be verified that this combination can have more damping and less dispersion than the original scheme. To see this, choose the TWS coefficients as

$$\underline{\alpha} = 0,\ \underline{\beta} = \frac{\lambda}{2},\ \underline{\gamma} = \frac{1}{6},\ \underline{\mu} = \frac{\varepsilon}{2}(1-2\underline{\beta}),\quad a > 0 \text{ and } 0 \le \varepsilon \le 1$$

Then,

$$L(U_j) = \frac{dU_j}{dt} + A_2\left(\frac{f_j}{h}\right) \tag{3.41}$$

where

$$A_2 = \delta_- + \frac{(1-\varepsilon)}{2}\left\{(1-2\underline{\beta})\,\delta_+ - (1-2\underline{\beta})\,\delta_-\right\} + \frac{\varepsilon}{2}\left\{(1-2\underline{\beta})\,\delta_- - (1-2\underline{\beta})\,\delta_{-2}\right\}$$

From Appendix (B), the dissipation error $\omega\Delta t\, D$ and the dispersion error $\omega\Delta t\,(a - a^*)$ are

$$\omega\Delta t\, D = \lambda\left\{\frac{-\lambda(1-\lambda^2)}{8} - \frac{\varepsilon(1-\lambda)(1-2\lambda)}{4}\right\}(\omega h)^4 + \ldots \tag{3.42-1}$$

$$\omega\Delta t\,(a - a^*) = \lambda\left\{\frac{1-\lambda^2}{6} - \frac{\varepsilon(1-\lambda)}{2}\right\}(\omega h)^3 + \ldots \tag{3.42-2}$$

Hence, the inclusion of the $\underline{\mu}$-term this way results in more damping and less dispersive error than that of Lax-Wendroff while preserving second order accuracy. However, this property is restricted to a Courant number λ less than 1/2. If one converts this four

point scheme into a three point scheme, one then has a nonlinear scheme where the coefficient of the anti-diffusive flux varies according to the neighboring data.

Sweby (1984) generalized various flux limiters into the following form

$$0 = U_j^{n+1} - U_j^n + \left(\frac{\Delta t}{\Delta x}\right)\left\{ \delta_- f_j + \delta_- \varphi_j \frac{(1 - 2\underline{\beta})}{2} \delta_+ f_j \right\}, \quad a > 0 \qquad (3.43)$$

where φ_j is the flux limiter

$r_j = \delta_- f_j \; / \; \delta_+ f_j$

$\varphi_j = \varphi_j(r_j)$ and $\varphi_j = 0$ if $r_j \leq 0$

$\underline{\beta} = \lambda$ (Courant number) for Lax-Wendroff

and the region of φ_j has been selected to satisfy the TVD condition, see Figure 1.*

Harten (1983) claims that the above three point flux limiter method is second order accurate by showing that the local Taylor series expansion of the flux term in space is identical to that of the Lax-Wendroff scheme to $O(\Delta x^2)$. In this sense, one can achieve a second order accurate monotone solution, hence escape from Godunov's theorem.

(3.4) Finite Element Implementation

In the C^0 finite element method, one must accept at any point the discontinuity of a secondary variable, namely, the gradient of data. Also, one cannot avoid an oscillatory solution when one fails to control the discontinuity of the secondary variable. Flux limiters can be viewed as a controlling device of these unwanted jumps at node points of the mesh. In general, finite element methods based on the standard or a dissipative Galerkin method are spatially high order accurate schemes. The attendant lack of spatial damping would likely cause a stability problem since discontinuities lie in space not in time. Any scheme that could be used for a discontinuous solution should thus have enough

* All figures may be found in Appendix E.

damping in the spatial discretization. Hence, the lack of spatial damping can be compensated by the flux limiting process when the gradients of data are not uniform.

Following the previous analysis, the flux limiting process can be put into the Taylor Weak Statement as follows: let

$$|\underline{\mu}| = \frac{(1 - 2|\underline{\beta}|)\,\varepsilon}{2}, \qquad 0 \le \varepsilon \le 1$$

Then from eq.(3.32),

$$L(u) = \left\{ 1 - \frac{\partial}{\partial x}\left(S(a)\,|\underline{\alpha}|\,h + \frac{\partial}{\partial x}\underline{\gamma}\,h^2 \right) \right\} \frac{\partial u}{\partial t}$$

$$+ \frac{\partial}{\partial x}\left\{ f - \frac{\partial}{\partial x} S(a)\left(|\underline{\beta}|\,h\,f - |\underline{\mu}|\,h^2 \frac{\partial f}{\partial x} \right) \right\}$$

$$= \left\{ 1 - \frac{\partial}{\partial x}\left(S(a)\,|\underline{\alpha}|\,h + \frac{\partial}{\partial x}\underline{\gamma}\,h^2 \right) \right\} \frac{\partial u}{\partial t}$$

$$+ \frac{\partial}{\partial x}\left\{ f - \frac{S(a)}{2} h \frac{\partial f}{\partial x} \right\}$$

$$+ \frac{\partial}{\partial x}\left\{ \frac{S(a)}{2} h\,(1 - 2|\underline{\beta}|)\frac{\partial f}{\partial x} - \frac{S(a)}{2}(1 - 2|\underline{\beta}|)\,\varepsilon\,h^2 \frac{\partial^2 f}{\partial x^2} \right\}$$

$$= \left\{ 1 - \frac{\partial}{\partial x}\left(S(a)\,|\underline{\alpha}|\,h + \frac{\partial}{\partial x}\underline{\gamma}\,h^2 \right) \right\} \frac{\partial u}{\partial t} \qquad (3.44)$$

$$+ \frac{\partial}{\partial x}\left\{ f - \frac{S(a)}{2} h \frac{\partial f}{\partial x} \right\}$$

$$+ \frac{\partial}{\partial x}\left\{ \frac{S(a)}{2} h\,(1 - 2|\underline{\beta}|)\left(\frac{\partial f}{\partial x} - \varepsilon \frac{\partial}{\partial x} h \frac{\partial f}{\partial x} \right) \right\}$$

Since the coefficients $S(a)h(1-2|\underline{\beta}|)/2$ and εh can be considered locally (nodally) constant, the last term in eq. (3.44) is written for a node j coefficient evaluation as

$$\frac{\partial}{\partial x}\left\{\frac{S(a)}{2} h (1 - 2 |\beta|) \left(\frac{\partial f}{\partial x} - \varepsilon \frac{\partial}{\partial x} h \frac{\partial f}{\partial x} \right)\right\} \tag{3.45}$$

$$= \frac{S(a)}{2} h (1-2|\beta|) \left(\frac{\partial^2 f}{\partial x^2} - \frac{\partial}{\partial x} \varepsilon h \frac{\partial^2 f}{\partial x^2} \right)$$

$$\cong \frac{S(a)}{2} h (1-2|\beta|) \left(1 - \frac{\left((\partial/\partial x)\, \varepsilon h \left(\partial^2 f / \partial x^2\right)\right)_j}{\left(\partial^2 f / \partial x^2\right)_j} \right) \frac{\partial^2 f}{\partial x^2}$$

The third derivative term $(\partial/\partial x)\, \varepsilon h\, (\partial^2 f/\partial x^2)_j$ in eq.(3.45) may be expressed in difference form as

$$\left(\frac{\partial}{\partial x} \varepsilon h \frac{\partial^2 f}{\partial x^2} \right)_j \equiv (\partial^2 f / \partial x^2)_j - (\partial^2 f / \partial x^2)_{j-S(a)} \tag{3.46}$$

Then, the last term in eq.(3.44) can be approximated as

$$(\,.\,)_{,} \cong \frac{\partial}{\partial x} \left\{ \frac{S(a)}{2} h (1-2|\beta|) \left(1 - \varepsilon \left(1 - \frac{\left(\partial^2 f / \partial x^2\right)_{j-S(a)}}{\left(\partial^2 f / \partial x^2\right)_j} \right) \right) \frac{\partial f}{\partial x} \right\} \tag{3.47}$$

Remark : Since one wants to establish a nodally appropriate expression, a direct application of a finite element weak statement to the last term of eq. (3.44) at this stage may not lead to the disired result. The derivation of the nodal equation with the differenced form of the coefficient should be completed before the weak statement is formed.

Since the nodal second derivative terms $(\partial^2 f / \partial x^2)_j$ and $(\partial^2 f / \partial x^2)_{j-S(a)}$ are the jumps in flux gradient at nodes "j" and "j-S(a)" respectively, I choose to compare the magnitudes of these jumps between node "j" and its upwind node (j - S(a)). If the

magnitude of the jump at the upwind node is smaller than that at node "j", one concludes that the flux at "j" may need some correction. Hence, define

$$r_j \equiv \frac{\left| \delta_+ f_{j\text{-}S(a)} - \delta_- f_{j\text{-}S(a)} \right|}{\left| \delta_+ f_j - \delta_- f_j \right|} \tag{3.48}$$

With reference to Figure 2, choose r_j as follows :

if $r_j \geq 1$, which signals the jump in the flux gradient at the node "j" is correct, i.e., the jump at node "j" is less than that at the upwind node, then $r_j = 1$ which yields a central differencing.

if $r_j < 1$, the jump in the flux gradient at the node "j" needs correction, i.e., the jump at node "j" is greater than that at the upwind node, then let $r_j = r_j$ which yields upwind differencing.

The upwind flux jump correction is enforced by the parameter ε, $0 \leq \varepsilon \leq 1$, as follows :

for $\varepsilon = 1$, correction is done using only upwind information,

for $\varepsilon = 1/2$, correction is done using half upwind and half central information,

for $\varepsilon = 0$, no correction is done,

for $\varepsilon > 1/2$, correction is done by proportionally more upwind information, and

for $\varepsilon < 1/2$, correction is done by proportionally less upwind information.

Hence, introducing the definition for a limiter φ_j as

$$\varphi_j = 1 - \varepsilon(1 - \tilde{r}_j) \tag{3.49}$$

where $$\tilde{r}_j = \frac{\left(\partial^2 f/\partial x^2\right)_{j\text{-}S(a)}}{\left(\partial^2 f/\partial x^2\right)_j}$$

eq.(3.44) can be written as

$$L(u) = \left\{ 1 - \frac{\partial}{\partial x}\left(S(a)\,|\underline{\alpha}|\,h + \frac{\partial}{\partial x}\,\underline{\gamma}\,h^2 \right) \right\} \frac{\partial u}{\partial t} \qquad (3.50)$$

$$+ \frac{\partial}{\partial x}\left\{ f - \frac{S(a)}{2} h \frac{\partial f}{\partial x} \right\}$$

$$+ \frac{\partial}{\partial x}\left\{ \frac{S(a)}{2} h \,(1 - 2\,|\underline{\beta}|\,)\,\varphi_j \frac{\partial f}{\partial x} \right\}$$

The prime difference between the present approach and others, as shown in Sweby (1984), is use of a different signal to establish the flux limiter function. That is, the present formulation uses the amount of the discontinuity in the flux gradient while the others use the flux gradient only. In the context of C^0 finite element methods, the gradient of flux may not exist at a nodal point, and this fact leads to use of the jump in flux gradient. In this way, only one limiter is needed to write a nodal difference form while others need two, one coming from the left cell and the other from the right cell. Hence, this scheme requires less effort in programming and still leaves room to work on the parameter ε which controls the imposition of the $\underline{\mu}$-term in the Taylor Weak Statement.

CHAPTER 4

LINEAR AND NONLINEAR MODEL PROBLEMS

(4.1) Computational Form of the TWS for Model Problems

In the form of eq.(2.17), the TWS written with properly signed coefficients is,

$$\text{TWS}\,(u^h) = S_e \Bigg[\int_{\Omega_e} \{N\} \left\{ 1 - \frac{\partial}{\partial x_i} \left(S(a_i)\,|\underline{\alpha}|\,h_{\underline{i}} + \frac{\partial}{\partial x_j} S(a_i) S(a_j)\,\gamma\,h_{\underline{i}} h_j \right) \right\} \frac{\partial u^h}{\partial t}\, d\underline{x} \qquad (4.1)$$

$$- \int_{\Omega_e} \frac{\partial \{N\}}{\partial x_i} \left\{ f_i^h - \left(S(a_i)\,|\underline{\beta}|\,h_{\underline{i}} \frac{\partial f_j^h}{\partial x_j} + \frac{\partial}{\partial x_j} S(a_i)\,|\underline{\mu}|\,h_{\underline{i}} h_{\underline{i}} \frac{\partial f_k^h}{\partial x_k} \right) \right\} d\underline{x}$$

$$+ \oint_{\partial\Omega \cap \partial\Omega_e} \{N\}\, f_i^h\, \hat{n}_i\, d\Gamma \Bigg]$$

where the underbar on subscripts i and j denotes indexes not elegible for a summation. However, it is not practical to work with eq.(4.1) directly. Instead, a multi-dimensional version of L(u) from eq.(3.50) is now written as

$$L(u) = \left\{ 1 - \frac{\partial}{\partial x_i} \left(S(a_i)\,|\underline{\alpha}|\,h_{\underline{i}} + \frac{\partial}{\partial x_j} S(a_i)\,S(a_j)\,|\underline{\gamma}|\,h_{\underline{i}} h_{\underline{j}} \right) \right\} \frac{\partial u}{\partial t} \qquad (4.2)$$

$$+ \frac{\partial}{\partial x_i} \left(f_i - S(a_i) \frac{h_{\underline{i}}}{2} \frac{\partial f_j}{\partial x_j} \right)$$

$$+ \frac{\partial}{\partial x_i} \left\{ S(a_i)\,h_{\underline{i}} \left(\frac{1 - 2|\underline{\beta}|}{2} \right) \varphi_{\underline{i}} \frac{\partial f_j}{\partial x_j} \right\}$$

where $|\underline{\mu}| = \{(1-2|\underline{\beta}|)/2\}\,\varepsilon$. The flux limiter $\varphi_{\underline{p}}$ is defined at a node point $\underline{p}$ for an ith-coordinate direction as

$$\varphi_p = 1 - \varepsilon\,(1 - r_p)$$

and the ratio r_p is defined at a pth node in the ith-coordinate direction as

$$r_p = \frac{|\delta_+ f_{p-1} - \delta_- f_{p-1}|}{|\delta_+ f_p - \delta_- f_p|} \qquad \text{for } a_i \text{ at the } p^{th} \text{ node} > 0$$

$$r_p = \frac{|\delta_+ f_{p+1} - \delta_- f_{p+1}|}{|\delta_+ f_p - \delta_- f_p|} \qquad \text{for } a_i \text{ at the } p^{th} \text{ node} < 0$$

Then, the TWS for eq.(4.2) is written as

(4.3)

$$\begin{aligned} TWS\,(u^h) = S_e \Bigg[& \int_{\Omega_e} \{N\} \left\{ 1 - \frac{\partial}{\partial x_i} \left(S(a_i)\,|\underline{\alpha}|\,h_{\underline{i}} + \frac{\partial}{\partial x_j} S(a_i) S(a_j)\,|\underline{\gamma}|\,h_{\underline{i}} h_{\underline{j}} \right) \right\} \frac{\partial u^h}{\partial t}\, d\underline{x} \\ & - \int_{\Omega_e} \frac{\partial \{N\}}{\partial x_i} \left(f_i^h - \frac{S(a_i)\,h_{\underline{i}}}{2} \frac{\partial f_j^h}{\partial x_j} \right) d\underline{x} \\ & - \int_{\Omega_e} \frac{\partial \{N\}}{\partial x_i}\, S(a_i)\,h_{\underline{i}} \left(\frac{1 - 2|\underline{\beta}|}{2} \right) \varphi_{\underline{i}}\, \frac{\partial f_j^h}{\partial x_j}\, d\underline{x} \\ & + \oint_{\partial\Omega \cap \partial\Omega_e} \{N\}\, f_i^h\, \hat{n}_i\, d\Gamma \Bigg] \end{aligned}$$

Define the following element matrices :

$$[M^e] \equiv \int_{\Omega_e} \{N\}\,\{N\}^T d\underline{x} \qquad (4.4\text{-}1)$$

$$[C_i^e] \equiv \int_{\Omega_e} \{N\} \frac{\partial \{N\}^T}{\partial x_i} d\underline{x} \qquad (4.4\text{-}2)$$

$$[C_i^e]^T \equiv \int_{\Omega_e} \frac{\partial \{N\}}{\partial x_i} \{N\}^T d\underline{x} \qquad (4.4\text{-}3)$$

$$[D_{ij}^e] \equiv \int_{\Omega_e} \frac{\partial \{N\}}{\partial x_i} \frac{\partial \{N\}^T}{\partial x_j} d\underline{x} \qquad (4.4\text{-}4)$$

$$\left(\partial C_i^e\right) \equiv \int_{\partial\Omega_e} \{N\}\{N\}^T \hat{n}_i \, d\Gamma \tag{4.4-5}$$

With these definitions, eq. (4.3) can be rewritten as

(4.5)

$$\begin{aligned} TWS(u^h) = S_e \Bigg[& \left\{ \left(M^e\right) + S(a_i)|\alpha| h_i \left(C_i^e\right)^T + S(a_i)S(a_j)|\gamma| h_i h_j \left(D_{ij}^e\right) \right\} \frac{d\{U\}_e}{dt} \\ & + \left\{ -\left(C_i^e\right)^T \delta_{ij} + S(a_i)\frac{h_i}{2}\left(D_{ij}^e\right) \right\} \{f_j\}_e \\ & - \left\{ S(a_i) h_i \left(\frac{1-2|\beta|}{2}\right) \varphi_j \left(D_{ij}^e\right) \right\} \{f_j\}_e \\ & + \left(\partial C_i^e\right) \{f_i\}_e \Bigg] \end{aligned}$$

where $\delta_{ij} = 1$ if $i = j$ and $\delta_{ij} = 0$ if $i \neq j$.

. More sophisticated forms of element matrix construction may be implemented by use of hypermatrices (see Baker, 1983). In this study, a group approximation is employed, wherein flux functions are evaluated nodally before finite element interpolations are used. Also, the following assumptions are imposed.

$$|\gamma| \equiv 0 \qquad \text{if } S(a_i)\, S(a_j) < 0$$

$$\left(D_{ij}^e\right) \equiv 0 \qquad \text{if } i \neq j$$

By introducing the assembly notation,

$$[M] \equiv S_e\left(M^e\right)$$
$$[C_i^T] \equiv S_e\left(C_i^e\right)^T$$
$$[D_{ij}] \equiv S_e\left(D_{ij}^e\right)$$
$$[\partial C_i] \equiv S_e\left(\partial C_i^e\right)$$

then,

$$TWS\,(u^h) = S_e[TWS_e] = [\bar{M}]\frac{d\{U\}}{dt} + [\bar{C}_i]\{f_i\} = \{0\} \tag{4.6}$$

where

$$[\bar{M}] \equiv [M] + S_e\left[S(a_i)\,|\alpha|\,h_i\left(C_i^e\right)^T + |\gamma|\,h_i h_j\left(D_{ij}^e\right)\right]$$

$$[\bar{C}_i] \equiv [\bar{C}_i^d] - [\bar{C}_i^a] + [\partial C_i]$$

$$[\bar{C}_i^d] \equiv S_e\left[-\left(C_i^e\right)^T + S(a_i)\frac{h_i}{2}\left(D_{ij}^e\right)\right]$$

$$[\bar{C}_i^a] \equiv S_e\left[S(a_i)\,h_i\left(\frac{1-2|\beta|}{2}\right)\varphi_i\left(D_{ij}^e\right)\right]$$

Eq.(4.6) is used to evaluate the θ-implicit time integration algorithm. The resultant residual is,

$$\{R\}^{n+1} = [\bar{M}]\left(\{U\}^{n+1} - \{U\}^n\right) + \theta\,\Delta t\,[\bar{C}_i]\{f_i\}^{n+1} + (1-\theta)\,\Delta t\,[\bar{C}_i]\{f_i\}^n \tag{4.7}$$

and the Newton iteration method yields,

$$\frac{\partial\{R\}^{n+(p)}}{\partial\{U\}}\{\Delta U\}^{n+(p)} = -\{R\}^{n+(p)}$$

$$\{U\}^{n+(p)} = \{U\}^n + \{\Delta U\}^{n+(p)}$$

where (p) is the iteration index. The Newton iteration matrix $\partial\{R\}/\partial\{U\}$ is

$$\frac{\partial\{R\}}{\partial\{U\}} = [\bar{M}] + \theta\,\Delta t\,[\bar{C}_i]\frac{\partial\{f_i\}}{\partial\{U\}} \tag{4.8}$$

and the solution $\{U\}^{n+1}$ is obtained when a norm of $\{\Delta U\}$ is less than a specified tolerance. In forming the Newton iteration matrix $\partial\{R\}/\partial\{U\}$, the upwind correction non-linearity in φ_i is ignored to avoid a penta-diagonal matrix structure. For time dependent problems, $\theta = 0.5$ is assumed unless otherwise specified.

To illustrate the construction of the Newton iteration matrix, consider the following residual $\{R^d\}$,

$$\{R^d\} \equiv S_e \left[- \int_{\Omega_e} \frac{\partial\{N\}}{\partial x_i} \left(f_i^h - \frac{S(a_i)}{2} h_i \frac{\partial f_j^h}{\partial x_j} \right) d\underline{x} \right]$$

Then, the Newton matrix contribution from the residual $\{R^d\}$ is,

$$\frac{\partial\{R^d\}}{\partial\{U\}} = S_e \left[- \int_{\Omega_e} \frac{\partial\{N\}}{\partial x_i} \frac{\partial}{\partial u} \left(f_i^h - \frac{S(a_i)}{2} h_i \frac{\partial f_j^h}{\partial x_j} \right) d\underline{x} \right]$$

$$= S_e \left[- \int_{\Omega_e} \frac{\partial\{N\}}{\partial x_i} \left(a_i^h - \frac{S(a_i)}{2} h_i \frac{\partial a_j^h}{\partial x_j} \right) d\underline{x} \right]$$

$$= S_e \left[- \int_{\Omega_e} \frac{\partial\{N\}}{\partial x_i} \left(\{N\}^T - \frac{S(a_i)}{2} h_i \frac{\partial\{N\}^T}{\partial x_j} \right) d\underline{x} \, \lceil a_i \rfloor \right]$$

$$= S_e \left[\left[\left(-\left(C_i^e\right)^T + S(a_i) \frac{h_i}{2} \left(D_{ij}^e\right) \right) \lceil a_i \rfloor \right] \right]$$

$$\equiv [\bar{C}_i^d] \frac{\partial\{f_i\}}{\partial\{U\}}$$

where the nodal values of a_i^h are denoted by a diagonal matrix $\lceil a_i \rfloor$ and are multiplied by the element matrix.

For a two-domensional problem, the Newton iteration matrix is split, i.e., approximately factored, into two one-dimensional matrices as

$$\frac{\partial\{R\}}{\partial\{U\}} \approx \left[[\bar{M}_1] + \theta \Delta t [\bar{C}_1] \frac{\partial\{f_1\}}{\partial\{U\}} \right] \left[[\bar{M}_2] + \theta \Delta t [\bar{C}_2] \frac{\partial\{f_2\}}{\partial\{U\}} \right] \tag{4.9}$$

where

$$[\overline{M}_1] \equiv [M_1] + S_e \left[S(a_1) |\underline{\alpha}| h_1 \left(C_1^e\right)^T + |\underline{\gamma}| (h_1)^2 \left(D_{11}^e\right) \right]$$

$$[\overline{M}_2] \equiv [M_2] + S_e \left[S(a_2) |\underline{\alpha}| h_2 \left(C_2^e\right)^T + |\underline{\gamma}| (h_2)^2 \left(D_{22}^e\right) \right]$$

and subscrtpts 1 and 2 indicate the 1st and the 2nd coordinate directions respectively.

(4.2) Numerical Experiments

To verify the new Galerkin-type flux-limited formulation for the Taylor Weak Statement, one- and two-dimensional step initial data have been chosen for both linear and nonlinear scalar equations. To quantify the anticipated effect of the upwinding($|\mu|$) term in the TWS, the analytical form for the fourth-order spatial damping coefficient is derived for three Galerkin-type finite element methods. Spatially second-order accurate Galerkin-type methods require $|\underline{\alpha}| = |\underline{\beta}|$. From the corresponding Fourier modal analysis in Sec.(3.2),

$$D = a \{ -S(a) D_4 (\omega h)^3 + ... \} \qquad (4.10\text{-}1)$$

$$a^* = a \{ 1 + A_3 (\omega h)^2 + ... \} \qquad (4.10\text{-}2)$$

where $D_4 = |\underline{\beta}|/12 + |\underline{\mu}|/2 + |\underline{\beta}| (|\underline{\gamma}| - |\underline{\mu}|)$ and $A_3 = - (|\underline{\gamma}| - |\underline{\mu}|)$.

For $|\underline{\mu}| = \{(1 - 2|\underline{\beta}|)/2\} \varepsilon$, $0 \le \varepsilon \le 1$, and $|\underline{\gamma}| = 0$, the terms in eq.(4.10) become

$$D_4 = |\underline{\beta}|/12 + \{(1 - 2 |\underline{\beta}|)/2\}^2 \varepsilon \qquad (4.11\text{–}1)$$

$$A_3 = \{(1 - 2 |\underline{\beta}|)/2\} \varepsilon \qquad (4.11\text{–}2)$$

Hence, the fourth order damping coefficient D_4 varies linearly with ε. Specifically, for ε = 0.0, 0.125, 0.25, 0.50, 0.75 and 1.0, the fourth-order damping coefficients D_4 are :

for Bubnov-Galerkin ($|\underline{\beta}| = 0.0$),

D_4 = 0.0, 0.03125, 0.06250, 0.1250, 0.1875 and 0.25,

for a dissipative Galerkin($|\beta| = 0.1$),

D_4 = 0.0, 0.03125, 0.06250, 0.1250, 0.1875 and 0.25,

for a dissipative Galerkin($|\beta| = 0.1$),

D_4 = 0.00833, 0.02833, 0.04833, 0.08833, 0.12833 and 0.16833,

for Raymond-Garder ($|\beta| = (15)^{-1/2} \cong 0.2582$),

D_4 = 0.02152, 0.02883, 0.03614, 0.05076, 0.06537 and 0.07999.

Thus, the Bubnov-Galerkin damping is most affected by varying ε.

1-D linear test case. The linear advection equation

$$\frac{\partial u}{\partial t} + \frac{\partial u}{\partial x} = 0, \quad a \equiv 1.0$$

with step initial data (shown on Figure 3 as dashed line)

$$u = 1.5 \qquad , 0.0 \leq x \leq 0.2$$

$$u = 0.5 \qquad , 0.2 \leq x \leq 1.0$$

is chosen for the one-dimensional test case. The exact solution (shown on Figure 3 as the solid line) at $t = 0.375 = (37.5)10^{-2}$ is

$$u = 1.5 \qquad 0.0 \leq x \leq 0.575$$

$$u = 0.5 \qquad 0.575 \leq x \leq 1.0.$$

For the test case executions, the selected Courant number ($a\Delta t/\Delta x$) is 0.25 as results for $\Delta t = (0.5)10^{-2}$. The solutions at time $t - t_0 = 75\ \Delta t = (37.5)10^{-2}$ sec are shown in Figure 5 for (a) Bubnov-Galerkin (θ=0.5), (b) Raymond-Garder (θ=0.5), (c) Donor-cell finite difference (θ=0.0), and (d) a dissipative Galerkin for $|\underline{\alpha}| = 0.1 = |\underline{\beta}|$, $|\underline{\gamma}| = 0 = |\underline{\mu}|$ (θ=0.5), respectively. None of these represent a satisfactory solution for the test problem.

To remove the oscillations present in Figure 5 (a), (b) and (d), and/or the excessive diffusion in (c), upwind information may be imposed by choosing $\varepsilon > 0$. Figure 6 (a) to (d) shows the numerical results obtained for flux-limited TWS definitions for the Bubnov-

Galerkin method($\underline{\alpha} = 0.0 = \underline{\beta}$) for $\varepsilon = 0.1, 0.3, 0.5$ and 1.0 respectively. Figures 7 and 8 show the results obtained for the flux-limited TWS definition for Raymond-Garder ($\underline{\alpha} = (15)^{-1/2} = \underline{\beta}$) and a dissipative Galerkin form ($\underline{\alpha} = 0.1 = \underline{\beta}$, chosen arbitrarily), each with the additional fourth-order upwind flux correction modulated by choosing values of ε. All results with the upwind correction show monotonic behavior and sharper solutions than the non-flux corrected TWS algorithm, Figure 5. Moreover, as ε is increased, the solutions get smoother as expected, since the fourth-order damping increases with ε, eq.(4.11-1).

When there is no upwind correction, as in Figure 5, the Bubnov-Galerkin method shows the wildest oscillatory solution. Hence, one might expect that the upwind corrected Bubnov-Galerkin solution would be the sharpest. However, the computed results are quite opposite. The Raymond-Garder method, which has a fourth-order damping coefficient of 0.02152, shows the sharpest result. The fourth-order damping coefficients for the Bubnov-Galerkin and the dissipative Galerkin($\underline{\alpha} = 0.1 = \underline{\beta}$) are 0.0 and 0.00833 respectively. From eq.(4.11), one sees that the Bubnov-Galerkin method has the most damping, when treated by the upwind information, hence produces the relatively diffused solution.

An additional experiment was conducted by further reducing the value of ε to 0.01, see Figure 9. The fourth-order damping coefficients in this case are 0.0025, 0.00993, and 0.02381, for Bubnov-Galerkin, dissipative Galerkin and Raymond-Garder respectively. If the foregoing arguments are true, the Bubnov-Galerkin must show the sharpest result. But the solution in Figure 9 (d), which is from flux-limited Raymond-Garder, is again the best. Further, the data in Figure 9 (a), which is a first-order method with $\underline{\alpha} = 0.0 = \underline{\gamma} = \underline{\mu}$ and $\underline{\beta} = 0.125$, shows a slight wiggle near the discontinuity.

Hence, for these data the following conjectures are made :

(1). Nodes with high damping in second-order influence adjacent nodes with a damping in fourth-order, hence make the solution even smoother. Due to the present construction of the flux limiter φ_j, a node between opposite slopes in the flux gradient degenerates to a node with Donor-cell type second-order damping.

(2). The selected dissipative Galerkin ($\alpha = 0.1 = \beta$), with fourth-order damping coefficient 0.00993 for $\varepsilon = 0.01$, already shows smoothing behavior (see Fig.9(b)) when used with the flux limiter. This fact suggests that a scheme with a base fourth-order damping is affected least by nodes with locally second-order damping under the present flux limiter.

Thus, the relatively larger smoothing behavior of the Bubnov-Galerkin form with upwind correction by $\varepsilon = 0.01$ can be explained as the contamination by damping at second-order near the discontinuity. For this test case, the solutions obtained from the flux limited Bubnov-Galerkin, dissipative Galerkin and Raymond-Garder methods with $\varepsilon = 0.1$ are considered acceptable since they all show monotone smoothness with relative sharpness.

1-D nonlinear test case. The nonlinear test case is the inviscid Burgers equation,

$$\frac{\partial u}{\partial t} + \frac{\partial}{\partial x}\left(\frac{u^2}{2}\right) = \frac{\partial u}{\partial t} + u\frac{\partial u}{\partial x} = 0$$

with step initial data (shown in Figure 4 as dashed line) given by

$$u = -0.2 \quad , 0.0 \le x \le 0.2$$

$$u = 1.2 \quad , 0.2 < x \le 1.0$$

The resultant shock speed S is computed as,

$$S \equiv \frac{f_R - f_L}{u_R - u_L}$$

and the average shock speed is 0.5. The exact solution at time $t - t_0 = 0.5$ sec is shown on Figure 4 as the solid line and is

$$u = -0.2 \qquad , 0.0 \le x \le 0.45$$

$$u = 1.2 \qquad , 0.45 < x \le 1.0$$

Figure 10 shows nodal solutions obtained for (a) Bubnov-Galerkin for $\theta = 1.0$, (b) Raymond-Garder ($\underline{\alpha} = (15)^{-1/2} = \underline{\beta}$) for $\theta = 0.5$, (c) Donor-cell for $\theta = 0.0$, and (d) a dissipative Galerkin ($\underline{\alpha} = 0.1 = \underline{\beta}$) for $\theta = 0.5$, for $\Delta t = (0.5)10^{-2}$, hence Courant number = 0.125. Figure 11 shows results for a first-order dissipative Galerkin method for (a) $\underline{\alpha} = 0.0$, $\underline{\beta} = 0.25$ for $\theta = 0.5$, (b) $\underline{\alpha} = 0.0$, $\underline{\beta} = 0.75$ for $\theta = 0.5$, (c) $\underline{\alpha} = 0.0$, $\underline{\beta} = 0.25$ with the lumped mass matrix ($\underline{\gamma} = 1/6$, eq.(3.7)) for $\theta = 0.5$, and (d) $\underline{\alpha} = 0.0$, $\underline{\beta} = 0.375$ with lumped mass matrix for $\theta = 0.5$. Figures 12,13 and 14 show corresponding solutions as obtained using the upwind correction scheme applied to the Bubnov-Galerkin, Raymond-Garder, and dissipative Galerkin formulations, respectively, for (a) $\varepsilon = 0.25$, (b) $\varepsilon = 0.50$ with lumped mass matrix, and (c) $\varepsilon = 0.25$, (d) $\varepsilon = 0.5$ with consistent mass matrix.

The first thing to note is the distinct differences in solutions obtained using the lumped mass matrix ($\underline{\gamma} = 1/6$) and the finite element consistent mass matrix forms. Solutions without use of the lumped mass matrix always exhibit oscillations ahead of a shock, while solutions using the lumped mass matrix exhibit oscillations behind the shock if at all. For this nonlinear case, it is difficult to apply the linear Fourier analysis. However, it is known that wiggles behind a shock, which occur for use of the lumped mass matrix, are associated with a relatively larger lagging phase error (see Baker, 1983,p.226). To verify this, eq. (3.36-2) is invoked, hence

$$\omega\Delta t\,(a - a^*) = \lambda\,[\,\{\,\lambda^2/12 + |\underline{\gamma}| - |\underline{\mu}|\,\}\,(\omega h)^3 + \ldots\,] \qquad (3.36\text{-}2)$$

and $|\underline{\gamma}| = 1/6$ yields the lumped mass matrix while $|\underline{\gamma}| = 0$ corresponds to the finite element mass matrix form. Then,

$$\omega\Delta t\, a^*|_{lump} = \omega\Delta t\, a - \lambda\,[\,(\lambda^2/12 + 1/6 - |\underline{\mu}|)\,(\omega h)^3 + \ldots\,]$$

$$< \omega\Delta t\, a - \lambda\,[\,(\lambda^2/12 - |\underline{\mu}|)\,(\omega h)^3 + \ldots\,] = \omega\Delta t\, a^*|_{FEM}$$

and if $|\underline{\mu}| = 0.0$, then $\omega\Delta t\, a^*|_{lump} < \omega\Delta t\, a^*|_{FEM} < \omega\Delta t\, a$.

Hence, for $\underline{\mu} = 0$, the phase lagging of the lumped matrix form is always greater than that of the finite element mass matrix. But, the better numerical results in general are obtained with use of the lumped matrix, which may be associated with its more diagonally dominant property especially near the region of the shock. Among the solutions obtained using the finite element mass matrix, i.e., Figure 12 (c),(d) by Bubnov-Galerkin with flux limiter, Figure 13 (c),(d) by Raymond-Garder with flux limiter, and Figure 14 (c),(d) by dissipative Galerkin with flux limiter, the solution in Figure 13 (c), which is Raymond-Garder with $\varepsilon = 0.25$, is the best while that in Figure 13 (d) from Raymond-Garder with $\varepsilon = 0.50$ is next best. Since the fourth-order damping in Raymond-Garder with $\varepsilon = 0.25$ is the least among them, this behavior can only be explained by the phase accuracy of a scheme. The Raymond-Garder method is known to be phase accurate to fifth-order from the semi-discrete Fourier analysis. This may suggest that as a nonlinear error control, semi-discrete phase accuracy optimazation may be useful.

The second item to note is that the amount of ε has very little influence on solution behavior for this nonlinear problem. Across the shock, all schemes degenerate to a first-order Donor-cell type, i.e., damping at second-order. Thus, second-order damping seems to override the nearby fourth-order damping. If the initial oscillations are severe, then the fourth-order upwinding also has little influence.

The third feature of note is the danger of central differenced diffusion near the shock, which is likely to cause oscillations due to acceptance of different types of signals. In Figure 13 (a) and (b), the Raymond-Garder solutions show oscillations, and in Figure 14 (a) and (b), the dissipative Galerkin ($\alpha = 0.1 = \beta$) solutions show slight overshoot. These are the consequence of the fourth-order damping by central differenced diffusion. However, in Figure 12 (a) and (b), the Bubnov-Galerkin does not show any wiggles. From eq.(4.11-1), the amount of fourth-order damping in the dissipative Galerkin method is 0.08833 for $\varepsilon = 0.5$, while the fourth-order damping in the Bubnov-Galerkin is 0.0625 for $\varepsilon = 0.25$. This wiggle-free solution for the upwind corrected Bubnov-Galerkin with less damping coefficient might support the foregoing second argument.

In conclusion, these data for the 1-D nonlinear (inviscid Burgers problem) experiment indicate that dispersion error control becomes relatively more important. Use of the lumped mass matrix form (γ=1/6) may be viewed as one TWS option for dispersion error control. Due to existence of a shock wave, the algorithm designer requires selective use of upwind and/or central differencing. Such non-linear schemes are not a priori known. However, solutions obtained using the upwind corrected Bubnov-Galerkin form with lumped mass matrix show overall acceptable results.

2-D linear case. To evaluate the new flux-corrected Galerkin scheme in two dimensions, two discontinuous data definitions are considered for the linear model equation. First, the discontinuities are aligned with grid lines, while the second is skewed to the mesh by 45 degrees. For the first case, the model advection equation is,

$$\frac{\partial u}{\partial t} + 0.3\frac{\partial u}{\partial x} + 0.1\frac{\partial u}{\partial y} = 0$$

and the initial data, depicted in Figure 15, is

$u = 2.0$, $0 \le x \le 0.2,\ 0 \le y \le 0.2$

$u = -1.0$, elsewhere

For the second case, the equation is

$$\frac{\partial u}{\partial t} + 0.2\frac{\partial u}{\partial x} + 0.2\frac{\partial u}{\partial y} = 0$$

and the initial data, depicted in Figure 16, is

$u = 2.0$, $0 \le y \le 0.2 - x$

$u = -1.0$, elsewhere

In both cases, the results were taken at time $t = 150\ \Delta t$, with $\Delta t = 10^{-2}$ (see Fig. 17) and $\Delta x = \Delta y = 1/32$. The resulting Courant numbers are $C_x = 0.096$, $C_y = 0.032$ for the first case, and $C_x = 0.064 = C_y$ for the second case.

For the first case, the flux limited Bubnov-Galerkin solution is compared with the standard Raymond-Garder form in Figures 17 (a) and (b). One can immediately notice the much improved behavior of the new method for this 2-D linear problem. In Figure 17(a), the flux limited Bubnov-Galerkin solution, a slight oscillation behind the discontinuity running along the y-direction is just noticable. The reason could be the rather narrow spatial domain available to damp out wiggles behind the discontinuity running in the y-direction. In the standard Raymond-Garder solution, these wiggles propagate to the boundary while those behind the interaction of discontinuities spread over much of the domain. The fourth-order damping coefficients for the upwind corrected Bubnov-Galerkin and the standard Raymond-Garder forms are 0.04167 and 0.02152 respectively.

For the second test case, shown in Figure 18, most noticable are the wild oscillations present in the standard Raymond-Garder solution (the vertical axis span is zero to 40). From Figure 16, the initial maximum number of elements behind the discontinuity along the direction of propagation is only four. This lack of enough region to damp out

wiggles may be the primary cause of the wild oscillations. Conversely, the flux limited Bubnov-Galerkin solution, which has a larger fourth-order damping coefficient, does not show any sign of wiggles and at the same time preserves a sharpness. The solution from the flux limited Galerkin method is quite acceptable, and also shows the advantage of a flux limiter method.

2-D nonlinear case. Here I also consider two cases. The first has the discontinuities aligned with the grid while the latter is skewed by 45 degrees. The equation used for the first case is,

$$\frac{\partial u}{\partial t} + 0.3u\frac{\partial u}{\partial x} + 0.1u\frac{\partial u}{\partial y} = 0$$

and the initial data shown in Figure 15 is

$$u = 2.0 \qquad , 0 \le x \le 0.2,\ 0 \le y \le 0.2$$

$$u = -1.0 \qquad , \text{elsewhere}$$

The results shown in Figures 19 (a) and (b) are taken from the standard Raymond-Garder and the flux limited Bubnov-Galerkin respectively at time $t = (400)\ \Delta t$ for $\Delta t = 10^{-2}$, which yields a maximum Courant number $C_{max} = 0.15$.

As in the corresponding 1-D test case, a lumped mass matrix is employed for both methods due to the inherent stability problem with use of the finite element consistent mass matrix. Notice that for the Raymond-Garder solution, Figure 19 (a), the region behind the shock interaction is smoother than in the linear case (Figure 17(a)). This is due to use of the lumped mass matrix ($\gamma = 1/6$) for a more diagonally dominant matrix. Also, the solution behind the shock running in the y-direction is contaminated because the region is of limited extent. In the flux limited Bubnov-Galerkin solution (Figure 19(b)), there are some very modest oscillations behind the shock interaction. This indicates that the shock interaction of

the inviscid Burgers problem is of strong nonlinear behavior. However, the flux limited Bubnov-Galerkin solution looks quite acceptable in general.

For the second test case, the equation used is

$$\frac{\partial u}{\partial t} + 0.2u\frac{\partial u}{\partial x} + 0.2u\frac{\partial u}{\partial y} = 0$$

and the initial data, shown in Figure 16, is

$u = 2.0$, $0.0 \leq y \leq -x + 0.2$

$u = -1.0$, elsewhere

The result shown in Figures 20 (a) and (b) are taken from the same situation as in the first case, i.e., at time $t = (400)\Delta t$ for $\Delta t = 10^{-2}$, but the consistent mass matrix is used in this case. The maximum Courant numbers are $C_x = 0.032 = C_y$.

In comparison, the flux limited Bubnov-Galerkin solution is not more crosswind diffusive than is the standard Raymond-Garder solution. The exact solution is propagation of the initial shock along the domain diagonal. Since the initial data along the shock is saw-tooth, and the grid is not aligned with the discontinuity, one may expect the shock to diffuse laterally in this nonlinear problem. In the Raymond-Garder solution (Fig.20(a)), one can notice milder oscillations than those in the linear case (Fig.18(a)). This is also due to the lateral diffusion of flux in this problem. Considering all aspects, the solution from the flux limited Bubnov-Galerkin method is again quiet acceptable.

As a whole, the flux limited Bubnov-Galerkin method shows a robustness for all model test cases. In the linear cases, the smoothness/oscillation character can be traced to be the fourth-order damping coefficient. In the nonlinear case, mass lumping appears an appropriate choice, and can be viewed as a dispersion error control mechanism. For the nonlinear shock, a central differencing for the anti-diffusion flux may cause oscillations

near the shock due to a transfer of inappropriate information. Also, a more sophisticated flux limiter could be helpful to improve solution behavior near a discontinuity.

CHAPTER 5

THE EULER SYSTEM

(5.1) Governing Equations

Let U be a vector of conservative variables satisfying

$$\frac{\partial U}{\partial t} + \frac{\partial F_i}{\partial x_i} + C_i = 0 \qquad (5.1)$$

where F_i is the flux vector and C_i is the non-homogeneous term that does not contain derivatives. Then, for the system definitions,

$$U = [\rho,\ m_1,\ m_2,\ E]^T$$

$$F_i = \begin{bmatrix} u_i \rho \\ u_i m_1 \\ u_i m_2 \\ u_i \rho h \end{bmatrix} + \begin{bmatrix} 0 \\ \delta_{i1} P \\ \delta_{i2} P \\ 0 \end{bmatrix}$$

where,

$m_1 = \rho u_1 \equiv$ momentum in x_1-direction

$m_2 = \rho u_2 \equiv$ momentum in x_2-direction

$h = \dfrac{\gamma P}{(\gamma - 1)\rho} + \dfrac{u_i u_i}{2} = \dfrac{E + P}{\rho} \equiv$ specific enthalpy

$\gamma = c_p / c_v \equiv$ specific heat ratio

$P = (\gamma - 1)\left(E - \dfrac{\rho}{2} u_i u_i \right) = \left(\dfrac{\gamma - 1}{\gamma}\right) \rho \left(h - \dfrac{u_i u_i}{2} \right) \equiv$ static pressure

$E = \rho \left(\varepsilon + \dfrac{u_i u_i}{2} \right) \equiv$ Total energy

$\varepsilon \equiv$ specific internal energy

eq.(5.1) expresses the two-dimensional Euler equations of gas dynamics.

An alternative quasi-linear form of eq.(5.1) is

$$\frac{\partial U}{\partial t} + A_i \frac{\partial U}{\partial x_i} + C_i = 0 \tag{5.2}$$

where $A_i = dF_i/dU$ is the jacobian(matrix) of the flux vector F_i. For the Euler system, it is readily determined that

(5.3)

$$A_i = \begin{bmatrix} 0 & \delta_{i1} & \delta_{i2} & 0 \\ -u_i u_1 + \delta_{i1}\phi^2 & u_i - \delta_{i1}(\gamma-2)u_1 & \delta_{i2}u_1 - \delta_{i1}(\gamma-1)u_2 & \delta_{i1}(\gamma-1) \\ -u_i u_2 + \delta_{i2}\phi^2 & \delta_{i1}u_2 - \delta_{i2}(\gamma-2)u_1 & u_i - \delta_{i2}(\gamma-2)u_2 & \delta_{i2}(\gamma-1) \\ -u_i(h-\phi^2) & \delta_{i1}h - (\gamma-1)u_i u_1 & \delta_{i2}h - (\gamma-1)u_i u_2 & \gamma u_i \end{bmatrix}$$

where

$$\phi^2 = \left(\frac{\gamma-1}{2}\right) u_i u_i = (\gamma-1)h - \frac{\gamma P}{\rho}$$

The eigenvalues of A_i are $u_i - c$, u_i, u_i and $u_i + c$, which are all real, hence the Euler system is hyperbolic. The eigenvalue matrices Λ_i of A_i are

$$\Lambda_i = \text{Diag}\,[\,u_i - c\,,\ u_i\,,\ u_i\,,\ u_i + c\,]\,, \qquad 1 \le i \le 2 \tag{5.4}$$

where

$$c = c(\rho,p) \equiv \text{speed of sound}$$
$$= \sqrt{\frac{\gamma p}{\rho}} \quad \text{for an ideal gas}$$

The right and left eigenvector matrices R_i and L_i, such that $L_{\underline{i}} A_i R_{\underline{i}} = \Lambda_i$, where the underbar denotes a direction indicator (no summation), can be determined using bi-orthogonality between the right and left eigenvector matrices, as

$$R_i = \begin{bmatrix} \alpha & 1 & 0 & \alpha \\ \alpha(u_1 - c\delta_{i1}) & u_1 & \delta_{i2}\rho & \alpha(u_1 + c\delta_{i1}) \\ \alpha(u_2 - c\delta_{i2}) & u_2 & -\delta_{i1}\rho & \alpha(u_2 + c\delta_{i2}) \\ \alpha(h - cu_i) & \frac{u_j u_j}{2} & \rho(u_1\delta_{i2} - u_2\delta_{i1}) & \alpha(h + cu_i) \end{bmatrix} \tag{5.5}$$

$$L_i = \begin{bmatrix} \beta(\phi^2 + cu_i) & -\beta(\delta_{i1}c + \tilde{\gamma}u_1) & -\beta(\delta_{i2}c + \tilde{\gamma}u_2) & \beta\tilde{\gamma} \\ 1 - \phi^2 c^{-2} & \tilde{\gamma}u_1 c^{-2} & \tilde{\gamma}u_2 c^{-2} & -\tilde{\gamma}c^{-2} \\ \frac{-(\delta_{i2}u_1 - \delta_{i1}u_2)}{\rho} & \rho^{-1}\delta_{i2} & -\rho^{-1}\delta_{i1} & 0 \\ \beta(\phi^2 - cu_i) & \beta(\delta_{i1}c - \tilde{\gamma}u_1) & \beta(\delta_{i2}c - \tilde{\gamma}u_2) & \beta\tilde{\gamma} \end{bmatrix} \tag{5.6}$$

where $\alpha = \rho\, c^{-1} / \sqrt{2}$

$\beta = \rho^{-1}\, c^{-1} / \sqrt{2}$

$\tilde{\gamma} = \gamma - 1$

Should one choose a preferred coordinate direction, for example when a discontinuity is not aligned with the mesh, it may be necessary (or desirable) to rotate the coordinate system to resolve the flux vector into normal and tangential components to avoid excessive smoothing. This was first suggested by Davis (1984). The Euler equation system written in the local rotated (x'_i) coordinate system (see Fig. 21) is

$$\frac{\partial U'}{\partial t} + \frac{\partial F'_i}{\partial x'_i} = 0 \tag{5.7}$$

where $U' = [\rho, \rho u'_1, \rho u'_2, E]^T$

$$F'_i = u'_i \begin{bmatrix} \rho \\ \rho u'_1 \\ \rho u'_2 \\ \rho h \end{bmatrix} + \begin{bmatrix} 0 \\ P\delta_{i1} \\ P\delta_{i2} \\ 0 \end{bmatrix} = \begin{bmatrix} \rho u'_i \\ u'_i \rho u'_1 + P\,\delta_{i1} \\ u'_i \rho u'_2 + P\,\delta_{i2} \\ u'_i \rho h \end{bmatrix}$$

$$u'_i = T_{ij}\, u_j$$

$$[T] = T_{ij} = \begin{bmatrix} \cos\theta, & \sin\theta \\ -\sin\theta, & \cos\theta \end{bmatrix} \qquad \text{for 2-D}$$

Define the transformation matrix Q between the primed and the unprimed variables as

$$Q \equiv \frac{\partial U'}{\partial U} = \begin{bmatrix} 1, & 0, & 0, & 0 \\ 0, & \cos\theta, & \sin\theta, & 0 \\ 0, & -\sin\theta, & \cos\theta, & 0 \\ 0, & 0, & 0, & 1 \end{bmatrix}$$

Then, eq.(5.7) written in the rotated coordinate system yields

$$0 = \frac{\partial U}{\partial t} + \frac{\partial (Q^{-1} F_i')}{\partial x_i'} \tag{5.8}$$

$$= \frac{\partial U}{\partial t} + T_{ji} \frac{\partial (Q^{-1} F_j')}{\partial x_i}$$

$$= \frac{\partial U}{\partial t} + Q^{-1} \frac{\partial}{\partial x_1} \left(\cos\theta \; F_1' - \sin\theta \; F_2' \right)$$

$$+ Q^{-1} \frac{\partial}{\partial x_2} \left(\sin\theta \; F_1' + \cos\theta \; F_2' \right)$$

Comparing to eq.(5.2), the fluxes F_1 and F_2 in the x_i coordinate system are

$$F_1 = Q^{-1} \left(\cos\theta \, F_1' - \sin\theta \, F_2' \right) \tag{5.9-1}$$

$$F_2 = Q^{-1} \left(\sin\theta \, F_1' + \cos\theta \, F_2' \right) \tag{5.9-2}$$

Similarly, the jacobians A_1 and A_2 in the x_i coordinate system are

$$A_1 = \frac{\partial F_1}{\partial U} = \frac{\partial F_1}{\partial U'} Q \tag{5.10-1}$$

$$A_2 = \frac{\partial F_2}{\partial U} = \frac{\partial F_2}{\partial U'} Q \tag{5.10-2}$$

Since $A_i' = R_i' \Lambda_i' L_i'$, the corresponding Jacobian matrices A_1 and A_2 can be written in terms of local properties as

$$A_1 = (Q^{-1} R_1')(\cos\theta \; \Lambda_1')(L_1' Q) - (Q^{-1} R_2')(\sin\theta \; \Lambda_2')(L_2' Q) \tag{5.11-2}$$

$$A_2 = (Q^{-1} R_2')(\sin\theta \; \Lambda_1')(L_1' Q) + (Q^{-1} R_2')(\cos\theta \; \Lambda_2')(L_2' Q) \tag{5.11-2}$$

(5.2) Taylor Weak Statement for the Euler System

The Taylor series modified conservation law, recall eq.(2.9), is extended to the multi-dimensional system case by replacing the scalar flux vector jacobian a_i by the matrix flux vector jacobian A_i. Then eq.(2.9) reads as

$$L(U) \equiv \left[1 - \frac{\partial}{\partial x_i} A_i \left\{ \left(\frac{\alpha \Delta t}{2} \right) + \frac{\partial}{\partial x_j} \left(\frac{\gamma \Delta t^2}{6} \right) A_j \right\} \right] \frac{\partial U}{\partial t} \qquad (5.12)$$

$$+ \left[F_i - A_i \left\{ \left(\frac{\beta \Delta t}{2} \right) \frac{\partial F_j}{\partial x_j} + \frac{\partial}{\partial x_j} \left(\frac{\mu \Delta t^2}{6} \right) A_j \frac{\partial F_k}{\partial x_k} \right\} \right]$$

Since $A_i = R_i \Lambda_i L_i$ and $\partial F_j / \partial x_j = A_j \, \partial U / \partial x_j$, where $R_i = L_i^{-1}$, then eq.(5.12) can be rewritten as

$$L(U) \equiv \left[1 - \frac{\partial}{\partial x_i} R_i \Lambda_i \left\{ \left(\frac{\alpha \Delta t}{2} \right) L_i + L_i \frac{\partial}{\partial x_j} R_j \Lambda_j \left(\frac{\gamma \Delta t^2}{6} \right) L_j \right\} \right] \frac{\partial U}{\partial t} \qquad (5.13)$$

$$+ \frac{\partial}{\partial x_i} \left[F_i - R_i \left\{ \Lambda_i \left(\frac{\beta \Delta t}{2} \right) L_i R_j \Lambda_j L_j \frac{\partial U}{\partial x_j} \right.\right.$$

$$\left.\left. + \Lambda_i L_i \frac{\partial}{\partial x_j} R_j \Lambda_j \left(\frac{\mu \Delta t^2}{6} \right) L_j R_k \Lambda_k L_k \frac{\partial U}{\partial x_k} \right\} \right]$$

where underbar denotes the direction indicator (no summation). By using the following assumptions,

(1) a locally frozen coefficient is used to evaluate the γ- and μ-terms, and

(2) The γ- and μ-terms are added only along the ith-direction, then

eq.(5.13) is simplified to the form

$$L(U) \equiv \left[1 - \frac{\partial}{\partial x_i} R_i \left\{ \Lambda_i \left(\frac{\alpha \Delta t}{2} \right) L_i + \delta_{ij} \Lambda_i \Lambda_j \left(\frac{\gamma \Delta t^2}{6} \right) \frac{\partial}{\partial x_j} L_i \right\} \right] \frac{\partial U}{\partial t} \qquad (5.14)$$

$$+ \frac{\partial}{\partial x_j} \left[F_i - R_i \left\{ \delta_{ij} \Lambda_i \Lambda_j \left(\frac{\beta \Delta t}{2} \right) L_i \frac{\partial U}{\partial x_j} \right.\right.$$

$$\left.\left. + \delta_{ij} \delta_{jk} \Lambda_i \Lambda_j \Lambda_k \left(\frac{\mu \Delta t^2}{6} \right) \frac{\partial}{\partial x_j} L_k \frac{\partial U}{\partial x_k} \right\} \right]$$

The one-dimensional homogenous Euler equation system is

$$\frac{\partial U}{\partial t} + R \Lambda L \frac{\partial U}{\partial x} = 0 \qquad (5.15)$$

Defining a new set of variables $W = \{w^{(k)}\}$ by

$$dW \equiv L\, dU \qquad (5.16)$$

eq.(5.15) is then transformed into,

$$\frac{\partial w^{(k)}}{\partial t} + \lambda^{(k)} \frac{\partial w^{(k)}}{\partial x} = 0, \qquad k=1,2,3 \qquad (5.17)$$

where $\lambda^{(1)} = u - c$, $\lambda^{(2)} = u$ and $\lambda^{(3)} = u + c$. Each $\lambda^{(k)}$ is thus the wave velocity of the kth wave equation for the Euler system, and it equals the slope of a curve C_k defined in the (x,t) plane by $dx/dt = \lambda^{(k)}$. The curve C_k is a kth characteristic curve of the wave system of eq.(5.17) along which the amplitude $w^{(k)}$ is constant. Equation (5.17) is called the characteristic equation form of the Euler system. In two dimensions, the Euler equation system may be written as

$$\frac{\partial U}{\partial t} + R_1 \Lambda_1 L_1 \frac{\partial U}{\partial x_1} + R_2 \Lambda_2 L_2 \frac{\partial U}{\partial x_2} = 0 \qquad (5.18)$$

Since the right eigenvector matrices R_1 and R_2 are not identical, the Euler system in 2-D cannot be simultaneously diagonalized.

To express eq.(5.14) in a form similar to eq.(2.16), define a new set of TWS coefficients by

$$S(\Lambda_i)\,[|\underline{\alpha}|]\,h_i \equiv \Lambda_i\,(\alpha\,\Delta t/2) \tag{5.19-1}$$

$$[\underline{\gamma}]\,h_i\,h_j \equiv \Lambda_i\,\Lambda_j\,(\gamma\,\Delta t2/6) \tag{5.19-2}$$

$$S(\Lambda_i)\,[|\underline{\beta}|]\,h_i\,|\Lambda_j| \equiv \Lambda_i\,\Lambda_j\,(\beta\Delta t/2) \tag{5.19-3}$$

$$S(\Lambda_i)\,[|\underline{\mu}|]\,h_i\,h_j\,|\Lambda_k| \equiv \Lambda_i\,\Lambda_j\,\Lambda_k\,(\mu\Delta t^2/6) \tag{5.19-4}$$

where $|\Lambda_i| = \text{Diag}\,[\,\ldots, |\lambda^{(k)}|, \ldots\,]$ for the ith-coordinate direction, the subscript k denotes the kth wave field, and $S(\Lambda_i)$ is the sign of the eigenvalue Λ_i.

The formulation of eq.(5.14), and the definition in eq.(5.19), allow the higher order terms in the Taylor series restatement of conservation laws to be directly added through the characteristic equation form for the Euler system. Hence, the diagonal elements of the TWS coefficient matrices need not be the same for all wave fields, specifically, they may vary depending on the character of each wave equation. Lax(1973) states that the kth characteristic field is genuinely nonlinear if $\underline{r}^{(k)}\cdot\nabla_U\lambda^{(k)} = 1$, and is linear if $\underline{r}^{(k)}\cdot\nabla_U\lambda^{(k)} = 0$, where $\underline{r}^{(k)}$ is the kth right eigenvector and ∇_U is a differentiation with respect to the vector U. Hence, in the Euler system, the wave equations with wave speed $\lambda^{(k)} = u \pm c$ are nonlinear and the wave equation with $\lambda^{(k)} = u$ is linear.

In the two-dimensional case, eq.(5.14) is expanded as

$$\begin{aligned} L(U) = \Bigg[1 - \frac{\partial}{\partial x_1}h_1\Big\{R_1\,S(\Lambda_1)\,[|\underline{\alpha}|]\,L_1 + \frac{\partial}{\partial x_1}h_1\,R_1\,[\underline{\gamma}]\,L_1\Big\} \\ - \frac{\partial}{\partial x_2}h_2\Big\{R_2\,S(\Lambda_2)\,[|\underline{\alpha}|]\,L_2 + \frac{\partial}{\partial x_2}h_2\,R_2\,[\underline{\gamma}]\,L_2\Big\}\Bigg]\frac{\partial U}{\partial t} \\ + \frac{\partial}{\partial x_1}\left\{F_1 - \frac{\partial}{\partial x_1}h_1 R_1\left([|\underline{\beta}|]\,|\Lambda_1|\,L_1\,U + [|\underline{\mu}|]\,|\Lambda_1|\,L_1\,h_1\frac{\partial U}{\partial x_1}\right)\right\} \end{aligned} \tag{5.20}$$

$$+ \frac{\partial}{\partial x_2}\left\{ F_2 - \frac{\partial}{\partial x_2} h_2 R_2 \left([|\underline{\beta}|]\, |\Lambda_2|\, L_2 U + [|\underline{\mu}|]\, |\Lambda_2|\, L_2 h_2 \frac{\partial U}{\partial x_2} \right) \right\}$$

The flux limiter φ_i, recall eq.(4.2), can now be inserted into this modified form of the Euler equations yielding

$$L(U) = \left[1 - \frac{\partial}{\partial x_1} h_1 \left\{ R_1 S(\Lambda_1) [|\underline{\alpha}|] L_1 + \frac{\partial}{\partial x_1} h_1 R_1 [\underline{\gamma}] L_1 \right\} \right. \tag{5.21}$$

$$\left. - \frac{\partial}{\partial x_2} h_2 \left\{ R_2 S(\Lambda_2) [|\underline{\alpha}|] L_2 + \frac{\partial}{\partial x_2} h_2 R_2 [\underline{\gamma}] L_2 \right\} \right] \frac{\partial U}{\partial t}$$

$$+ \frac{\partial}{\partial x_1} \left\{ F_1 - \frac{\partial}{\partial x_1} h_1 R_1 [\tfrac{1}{2}]\, |\Lambda_1|\, L_1 U \right\}$$

$$+ \frac{\partial}{\partial x_1} \varphi_1 \frac{\partial}{\partial x_1} \left(h_1 R_1 \left[\frac{1 - 2|\underline{\beta}|}{2} \right] |\Lambda_1|\, L_1 U \right)$$

$$+ \frac{\partial}{\partial x_2} \left\{ F_2 - \frac{\partial}{\partial x_2} h_2 R_2 [\tfrac{1}{2}]\, |\Lambda_2|\, L_2 U \right\}$$

$$+ \frac{\partial}{\partial x_2} \varphi_2 \frac{\partial}{\partial x_2} \left(h_2 R_2 \left[\frac{1 - 2|\underline{\beta}|}{2} \right] |\Lambda_2|\, L_2 U \right)$$

where $S(\Lambda) \equiv$ Sign of an eigenvalue (diagonal element of Λ), and

$\varphi_i = 1 - \varepsilon\,(1 - r_i) \equiv$ flux limiter

When it is preferred to rotate the local coordinate system, due to the discontinuity not being aligned with the mesh, the modified conservation equation can be written as follows:

$$L(U) = \left[1 - (\cos\theta) \frac{\partial}{\partial x_1} h_1 \left\{ (Q^{-1} R_1') [\underline{\alpha}] (L_1' Q) \right. \right. \tag{5.22}$$

$$\left. \left. + \frac{\partial}{\partial x_1} h_1 (Q^{-1} R_1') [\underline{\gamma}] (L_1' Q) \right\} \right]$$

$$- (\sin\theta)\frac{\partial}{\partial x_2} h_2 \left\{ (Q^{-1}R_2')[\underline{\alpha}](L_2'Q) + \frac{\partial}{\partial x_2} h_2 (Q^{-1}R_2')[\underline{\gamma}](L_2'Q) \right\} \frac{\partial U}{\partial t}$$

$$+ (\cos\theta)\frac{\partial}{\partial x_1}\left\{ Q^{-1}F_1' - \frac{\partial}{\partial x_1} h_1 (Q^{-1}R_1')\left[\frac{1}{2}\right] S(\Lambda_1)(L_1'Q)U \right\}$$

$$- (\sin\theta)\frac{\partial}{\partial x_1}\left(Q^{-1}F_2'\right)$$

$$+ (\cos\theta)\frac{\partial}{\partial x_1}\varphi_1\frac{\partial}{\partial x_1} h_1 \left\{ (Q^{-1}R_1')\left[\frac{1-2|\underline{\beta}|}{2}\right] |\Lambda_1| (L_1'Q)U \right\}$$

$$+ (\sin\theta)\frac{\partial}{\partial x_2}\left\{ Q^{-1}F_1' - \frac{\partial}{\partial x_2} h_2 (Q^{-1}R_1')\left[\frac{1}{2}\right] S(\Lambda_2)(L_1'Q)U \right\}$$

$$+ (\cos\theta)\frac{\partial}{\partial x_2}\left(Q^{-1}F_2'\right)$$

$$+ (\sin\theta)\frac{\partial}{\partial x_2}\varphi_2\frac{\partial}{\partial x_2} h_2 \left\{ (Q^{-1}R_1')\left[\frac{1-2|\underline{\beta}|}{2}\right] |\Lambda_2| (L_2'Q)U \right\}$$

The Taylor Weak Statement for an Euler system is thus

$$\text{TWS}(U^h) = S_e \int_{\Omega_e} \{N\} L(U^h)\, d\underline{x} \tag{5.23}$$

Using the notations of eq.(4.4) for the element matrices, the TWS eq.(5.23) for L(U) in eq.(5.21) can be written as

$$\text{TWS}(U^h) = S_e \left[[\overline{M}]_e \frac{d\{U\}_e}{dt} - \left(C_i^e\right)^T \{F_i\}_e + \left(\partial C_i^e\right)\{F_i\}_e + \delta_{ij}\left(D_{ij}^e\right)\left\{ R_i |\Lambda_i| \left[\frac{1-\varphi(1-|\underline{\beta}|)}{2}\right]_i h_i L_j U \right\}_e \right] \tag{5.24}$$

where

$$[\bar{M}]_e \equiv (M^e) + h_i (C_i^e)^T R_i [\,|\underline{\alpha}|\,] S(\Lambda_i) L_i + \delta_{ij} h_i h_j (D_{ij}^e) R_i [\,\underline{\chi}\,] L_j \qquad (5.25)$$

and $\delta_{ij} = 1$ if $i = j$

$= 0$ if $i \neq j$

The TWS eq.(5.24) is again employed for derivative evaluation in a θ-implicit integration algorithm, recall Sec.(4.1). The RHS residual $\{R\}$ thus becomes

$$\{R\} \equiv [\bar{M}] \left(\{U\}^{n+1} - \{U\}^n \right) + \theta \Delta t \{G\}^{n+1} + (1-\theta) \Delta t \{G\}^n \qquad (5.26)$$

where

$$\{G\} \equiv S_e \left[- (C_i^e)^T \{F_i\}_e + (\partial C_i^e) \{F_i\}_e + \delta_{ij} (D_{ij}^e) \left\{ R_i |\Lambda_i| \left[\frac{1 - \varphi(1 - |\underline{\beta}|)}{2} \right]_i h_i L_i U \right\}_e \right] \qquad (5.27)$$

$$[\bar{M}] = S_e [\bar{M}]_e$$

The Newton iteration matrix $\partial\{R\}/\partial\{U\}^{n+1}$ is computed (in linearized form, recall eq.(4.8)) as

$$\frac{\partial \{R\}}{\partial \{U\}^{n+1}} = [\bar{M}] + \theta \Delta t \frac{\partial \{G\}}{\partial \{U\}^{n+1}} \qquad (5.28)$$

$$= [\bar{M}] + S_e \, \theta \Delta t \left[- (C_i^e)^T A_i + (\partial C_i^e) A_i \right.$$

$$\left. + \delta_{ij} (D_{ij}^e) \left\{ R_i |\Lambda_i| \left[\frac{1 - \varphi(1 - |\underline{\beta}|)}{2} \right]_i h_i L_i \right\}_e \right]^{n+1}$$

Then, the solution $\{U\}^{n+1}$ is obtained as described in Sec.(4.1).

(5.3) Numerical Boundary Treatment

For an approximate factorization scheme, as developed by Beam and Warming (1976), the Newton iteration matrix $\partial\{R\}/\partial\{U\}^{n+1}$ of eq.(5.28) is approximated as,

$$\frac{\partial\{R\}}{\partial\{U\}^{n+1}} \cong \left([\overline{M}_2] + \theta\Delta t \frac{\partial\{G_2\}}{\partial\{U\}^{n+1}}\right)\left([\overline{M}_1] + \theta\Delta t \frac{\partial\{G_1\}}{\partial\{U\}^{n+1}}\right) \tag{5.29}$$

where

$$[\overline{M}_1] = S_e \left[(M^e) + h_1 (C_1^e)^T R_1 [|\underline{\alpha}|] S(\Lambda_1) L_1 \right] \tag{5.30}$$

$$[\overline{M}_2] = S_e \left[(M^e) + h_2 (C_2^e)^T R_2 [|\underline{\alpha}|] S(\Lambda_2) L_2 \right]$$

$$\frac{\partial\{G_1\}}{\partial\{U\}^{n+1}} = S_e \theta\Delta t \left[-(C_1^e)^T A_1 + (\partial C_1^e) A_1 + h_1 (D_{11}^e) R_1 |\Lambda_1| [\frac{1 - \varphi(1 - |\underline{\beta}|)}{2}]_1 L_1 \right]$$

$$\frac{\partial\{G_2\}}{\partial\{U\}^{n+1}} = S_e \theta\Delta t \left[-(C_2^e)^T A_2 + (\partial C_2^e) A_2 + h_2 (D_{22}^e) R_2 |\Lambda_2| [\frac{1 - \varphi(1 - |\underline{\beta}|)}{2}]_2 L_2 \right]$$

Then, the algebraic solution procedure becomes

$$\left([\overline{M}_2] + \theta\Delta t \frac{\partial\{G_2\}}{\partial\{U\}^{n+1}}\right)\{\Delta U^*\} = -\{R\}^{n+(p)} \tag{5.31-1}$$

$$\left([\overline{M}_1] + \theta\Delta t \frac{\partial\{G_1\}}{\partial\{U\}^{n+1}}\right)\{\Delta U\}^{n+(p)} = \{\Delta U^*\} \tag{5.31-2}$$

and

$$\{U\}^{n+1} = \{U\}^n + \{\Delta U\}^{n+(p)} \tag{5.31-3}$$

The computational form of either eq.(5.31-1) or (5.31-2) appears at each interior point as

$$A_i \Delta U_{i-1} + B_i \Delta U_i + C_i \Delta U_{i+1} = D_i \tag{5.32}$$

where A_i , B_i and C_i are 4 x 4 matrices (for 2-D) evaluated with data known at time level n, D_i on the right hand side is a vector of data at node point i and at time level n + (p), and ΔU_i is the (vector) unknown to be found at node i. For a system of equations to be well-posed, a proper number of boundary conditions must be given. In two dimensions, a characteristic analysis verifies that three conditions for subsonic inflow, one condition for subsonic outflow, four conditions for supersonic inflow and none for supersonic outflow are appropriate for the Euler equations.

Subsonic inflow. Suppose ρ, u_1 and u_2 are given, hence E may not be specified. The following extrapolation from the interior can then be used (Liou, et.al., 1988) :

Since

$$E = \frac{P}{\gamma - 1} + \frac{\rho \left(u_1^2 + u_2^2 \right)}{2} ,$$

then ΔE can be written as

$$\Delta E = \frac{\Delta P}{\gamma - 1} - \frac{1}{2} (u_1^2 + u_2^2) \, \Delta \rho + u_1 \Delta (\rho u_1) + u_2 \Delta (\rho u_2) \tag{5.33}$$

and $\Delta \rho = \Delta \rho u_1 = \Delta \rho u_2 = 0$ by definition at node column i = 1. Then, at node column i = 1

$$(\Delta E)_1 = \frac{\Delta P_1}{\gamma - 1}$$

By linear extrapolation of ΔP from the interior

$$(\Delta E)_1 = \frac{\Delta P_2}{\gamma - 1} = (\Delta E)_2 + \frac{u_1^2 + u_2^2}{2} (\Delta \rho)_2 - u_1 (\Delta \rho u_1)_2 - u_2 (\Delta \rho u_2)_2 \tag{5.34}$$

Hence, the constraint statement for ΔU_1 on node column 1 is

$$\Delta U_1 = T \, \Delta U_2 \tag{5.35}$$

where

$$T = \begin{bmatrix} 0 & 0 & 0 & 0 \\ 0 & 0 & 0 & 0 \\ 0 & 0 & 0 & 0 \\ \frac{u_1^2 + u_2^2}{2} & -u_1 & -u_2 & 1 \end{bmatrix}$$

Substituting eq.(5.35) into (5.31-3), the i=1 column disappears and for i = 2,

$$(A_2 T + B_2) \Delta U_2 + C_2 \Delta U_3 = D_2 \tag{5.36}$$

Subsonic outflow. Suppose the static pressure P is given at node column i = I ; hence,

$$\Delta P_I = 0 \tag{5.37}$$

Then, from eq.(5.33), the change in the energy is

$$(\Delta E)_I = \left(\frac{-(u_1^2 + u_2^2)}{2} (\Delta \rho) + u_1 (\Delta \rho u_1) + u_2 (\Delta \rho u_2) \right)_I \tag{5.38}$$

Linear extrapolation of the remaining variables, $\Delta \rho$, $\Delta \rho u_1$ and $\Delta \rho u_2$ from the interior yields

$$(\Delta \rho)_I = (\Delta \rho)_{I-1} \tag{5.39}$$

$$(\Delta \rho u_1)_I = (\Delta \rho u_1)_{I-1} \tag{5.40}$$

$$(\Delta \rho u_2)_I = (\Delta \rho u_2)_{I-1} \tag{5.41}$$

and reduces the equation at node row i = I to

$$A_I \Delta U_{I-1} + B_I \Delta U_I = 0 \tag{5.42}$$

where

$$A_I = \begin{bmatrix} -1, & 0, & 0, & 0 \\ 0, & -1, & 0, & 0 \\ 0, & 0, & -1, & 0 \\ 0, & 0, & 0, & 0 \end{bmatrix}$$

$$B_I = \begin{bmatrix} 1 & , & 0 & , & 0 & , & 0 \\ 0 & , & 1 & , & 0 & , & 0 \\ 0 & , & 0 & , & 1 & , & 0 \\ \frac{u_1^2 + u_2^2}{2}, & & -u_1, & & -u_2, & & 1 \end{bmatrix}$$

Substituting ΔU_I into the interior equation written at node row I- 1 then yields

$$A_{I-1}\Delta U_{I-2} + (B_{I-1} - C_{I-1}B_I^{-1}A_I)\Delta U_{I-1} = D_{I-1} \qquad (5.43)$$

where

$$B_I^{-1} = \begin{bmatrix} 1 & , & 0 & , & 0 & , & 0 \\ 0 & , & 1 & , & 0 & , & 0 \\ 0 & , & 0 & , & 1 & , & 0 \\ -\frac{u_1^2 + u_2^2}{2}, & & u_1, & & u_2, & & 1 \end{bmatrix}$$

$$B_I^{-1} A_I = \begin{bmatrix} -1 & 0 & 0 & 0 \\ 0 & -1 & 0 & 0 \\ 0 & 0 & -1 & 0 \\ \frac{u_1^2 + u_2^2}{2} & -u_1 & -u_2 & 0 \end{bmatrix}$$

Solid wall boundary. Let a solid wall segment have angle θ with respect to the x_1 global coordinate axis, see Fig.22. Define the axis tangent to the wall as x_1' and the wall normal as x_2'. Then, the impervious solid wall boundary condition is $u_2' = 0$. Under the local coordinate rotation, the Euler equation system at the solid wall is

$$0 = \frac{\partial U}{\partial t} + Q^{-1} \frac{\partial}{\partial x_1} \left(\cos\theta F_1' - \sin\theta F_2' \right) + Q^{-1} \frac{\partial}{\partial x_2} \left(\sin\theta F_1' + \cos\theta F_2' \right) \qquad (5.44)$$

where

$$Q^{-1} = \begin{bmatrix} 1, & 0, & 0, & 0 \\ 0, & \cos\theta, & -\sin\theta, & 0 \\ 0, & \sin\theta, & \cos\theta, & 0 \\ 0, & 0, & 0, & 1 \end{bmatrix}$$

$$F_1' = u_1' \begin{pmatrix} \rho \\ \rho u_1' \\ 0 \\ \rho h \end{pmatrix} + \begin{pmatrix} 0 \\ P \\ 0 \\ 0 \end{pmatrix}$$

$$F_2' = \begin{pmatrix} 0 \\ 0 \\ P \\ 0 \end{pmatrix}$$

$$u_i' = T_{ij} u_j$$

$$T = \begin{bmatrix} \cos\theta, & \sin\theta \\ -\sin\theta, & \cos\theta \end{bmatrix}$$

In summary, at the inflow/outflow boundary, the boundary conditions compatible with the characteristic analysis have been applied to the linear algebra procedure. For the solid wall boundary, the boundary condition has been applied to the governing equation. The boundary conditions described in this section are called an implicit extrapolation procedure, and are widely used for steady state problems (see Liou, et al., 1988).

(5.4) Numerical Experiments with the Euler System

To evaluate the accuracy hence utility of the developed flux-limited Galerkin-type TWS algorithm, several test cases have been conducted for the Euler system of gas dynamics. First is the Riemann shock tube problem as defined by Sod(1978). Second is a two-dimensional shock tube interaction problem on a rectangular mesh and on a non-rectangular mesh. Third is the quasi-one dimensional Euler problem of the deLaval nozzle. The fourth definitions involve two-dimensional oblique shock problems.

I again consider several forms for the TWS algorithm as follows :

For the Donor-cell method, the TWS coefficients in eq.(5.20) are assigned as

$[|\underline{\alpha}|] = \text{Diag.}[\ ...,0.0,\ ...] = [|\underline{\mu}|]$, $[|\underline{\beta}|] = \text{Diag.}[...,0.0,...]$ and

$[|\underline{\gamma}|] = \text{Diag.}[...,1/6,...]$.

For the Euler Taylor-Galerkin (ETG) method,

$[|\underline{\alpha}|] = \text{Diag.}[...,0.0,...] = [|\underline{\mu}|]$, $[|\underline{\beta}|] = \text{Diag.}[\ |u-c|/2,\ |u|/2,\ |u|/2,\ |u+c|/2\ ]$ and

$[|\underline{\gamma}|] = \text{Diag.}[\ (u-c)^2/6,\ u^2/6,\ u^2/6,\ (u+c)^2/6\ ]$.

For the Raymond-Garder method,

$[|\underline{\alpha}|] = \text{Diag.}[\ ..., (15)^{-1/2}, ...] = [|\underline{\beta}|]$ and $[|\underline{\gamma}|] = \text{Diag.}[\ ..., 0.0, ...\ ] = [|\underline{\mu}|]$

For a dissipative Galerkin method chosen in this study,

$[|\underline{\alpha}|] = \text{Diag.}[\ ..., 0.1, ...\ ] = [|\underline{\beta}|]$ and $[|\underline{\gamma}|] = \text{Diag.}[\ ..., 0.0, ...\ ] = [|\underline{\mu}|]$

For the flux-limited Bubnov-Galerkin method,

$[|\underline{\alpha}|] = \text{Diag.}[..., 0.0, ...] = [|\underline{\gamma}|]$, and $|\underline{\beta}|$ and $|\underline{\mu}|$ are combined as

$$[|\underline{\beta}|] = \text{Diag.}\left[\frac{\varepsilon^{(1)}}{2}\left(1 - r_j^{(1)}\right), \frac{\varepsilon^{(2)}}{2}\left(1 - r_j^{(2)}\right), \frac{\varepsilon^{(2)}}{2}\left(1 - r_j^{(2)}\right), \frac{\varepsilon^{(3)}}{2}\left(1 - r_j^{(3)}\right)\right]$$

In the last instances, the superscripts denote the corresponding wave fields and r_j is defined in eq.(3.48).

The Euler flux F_i in Sec.(5.1) can be decomposed into each (characteristic) wave component yielding,

$$F_i = F_i^{(1)} + F_i^{(2)} + F_i^{(3)} \tag{5.45}$$

where

$$F_i^{(1)} = (u_i - c)\frac{\rho}{2\gamma}\begin{pmatrix} 1 \\ u_1 - c \\ u_2 - c \\ h - u_i c \end{pmatrix} \qquad F_i^{(2)} = u_i \frac{\gamma - 1}{\gamma}\rho \begin{pmatrix} 1 \\ u_1 \\ u_2 \\ h - \gamma P/((\gamma-1)\rho) \end{pmatrix}$$

$$F_i^{(3)} = (u_i + c)\frac{\rho}{2\gamma}\begin{pmatrix} 1 \\ u_1 + c \\ u_2 + c \\ h + u_i c \end{pmatrix}$$

The use of the flux vector in eq.(5.45) allows one to use the scalar model of the TWS eq.(4.3) for the spatial derivative terms. In the Riemann shock tube problem, and the two-dimensional shock interaction problem, the Euler fluxes as given in eq.(5.45) are used in the computational experiments.

Riemann shock tube problem. The exact solution at $t = 0.1415$ sec. for the Sod problem definition with initial conditions $u = 0$, $P = 1 = \rho$ on $0 \leq x \leq 0.5$, $P = 0.1$, $\rho = 0.125$ on $0.5 < x \leq 1.0$, is shown in Figure 23 (a) for density and (b) for energy. The shock is centered at x=0.75, the contact discontinuity is centered at $x = 0.625$, and the rarefaction wave lies upstream of $x = 0.5$. Four TWS methods were tested and the results are summarized in Figures 24 thru 27. The four selected TWS methods include Donor-cell explicit (Fig.24), Raymond-Garder for $\theta = 0.5$ (Fig.25), Euler Taylor-Galerkin (ETG) for $\theta = 0.0$ (Fig.26), and a dissipative Galerkin method ($|\alpha| = 0.1 = |\beta|$) for $\theta = 0.5$ (Fig.27). Even though the Donor-cell method showed a very good result for the one-dimensional Burgers problem, its excessive smoothness (as also shown in the one-dimensional linear test case) eliminates most of the contact discontinuity, which is a linear wave. The Raymond-Garder method shows a slight improvement over the Donor-cell solution at the contact discontinuity and in resolution of the shock with some undershoot ahead of the shock. Considering that the shock is a nonlinear wave field, this undershoot may be related to the finite element consistent mass matrix. The third order accurate ETG solution shows much improvement for resolution of the contact discontinuity and the rarefaction wave. However, the contact discontinuity still lies over several elements and the shock can not avoid a small undershoot. The dissipative Galerkin solution, with some oscillations across the shock (Fig.27), does not show better results than the ETG at the contact discontinuity and the rarefaction wave fields.

However, the upwind information can be used to improve these results, as shown in Figure 28 for a dissipative Galerkin method, and in Figure 29 for the Bubnov-Galerkin algorithm. Since the upwind information is applied only to the nonlinear wave components, the oscillations present in the dissipative Galerkin (Fig.27) have been removed but the shape of the contact discontinuity (linear wave) has not been significantly

altered. In Figure 29, the flux limited Bubnov-Galerkin solution exhibits the best resolution of the contact discontinuity and the rarefaction wave field among the results shown. Even though there is a slight undershoot at the shock, the overall solution behavior is quite acceptable. The crispness shown in this method seems to stem from both the spatial and the temporal high order of the Bubnov-Galerkin method.

Two-dimensional Shock Interaction problem. For the rectangular mesh case, the initial data and the domain are as defined in Figure 30 (a) where the pressure initial condition P_H stands for a high pressure and P_L a low pressure. The ETG solution for density and energy is shown in Figure 31, and the flux limited Bubnov-Galerkin solution with $\varepsilon = 1/6$ applied to nonlinear wave fields is given in Figure 32. The results were taken at time $t = 95\Delta t$ sec with $\Delta t = (0.25)\ 10^{-2}$, and the improvement over the ETG solution is quite apparent.

For the non-rectangular mesh case, the domain and initial data are defined in Figure 30(b). The numerical results shown in Figure 33 are from the ETG method, while those shown in Figure 34 are from the flux limited Bubnov-Galerkin method with $\varepsilon = 1/6$ applied to the nonlinear wave fields only. Both solutions are taken at time $t = 75\ \Delta t$ sec with $\Delta t = (0.5)10^{-2}$. With initial pressure ratio $P_H/P_L = 10$, which is the same as that of the one-dimensional shock-tube problem, the ETG solution has wide spread $2\Delta x$ wiggles, while the flux limited Bubnov-Galerkin solution behaves monotonically with good shock capturing over about three elements. Also, on both the rectangular and the non-rectangular meshes, the Bubnov-Galerkin with upwind correction does not excessively smear the contact discontinuity, even in the 32 linear element discretization for each side. When the two shocks collide, a sudden rise in temperature occurs and hence, without a proper

damping mechanism, solutions might be contaminated by $2\Delta x$ wiggles or with too much damping, might lose necessary peaks. However, the present flux limited Bubnov-Galerkin method exhibits potential capabilities by overcoming these several difficulties.

Quasi-1D deLaval nozzle problem. The governing equation system in this case has an area-dependent inhomogeneous term in eq.(4.1) of the form

$$C = \left(\frac{d}{dx} \ln A\right) \begin{pmatrix} u\rho \\ um \\ u\,(E+P) \end{pmatrix}$$

The contribution by this term to the LHS matrix eq.(5.28) is,

$$\frac{\partial C_i}{\partial U_j} = \left(\frac{d}{dx} \ln A\right) \begin{bmatrix} 0 & 1 & 0 \\ -u^2 & 2u & 0 \\ u\left((\gamma-1)u^2 - \gamma\rho^{-1}E\right) & \frac{-3(\gamma-1)u^2}{2} + \gamma\rho^{-1}E & \gamma u \end{bmatrix}$$

For a subsonic inflow/outflow boundary, the implicit extrapolation procedure described in Sec (5.3) was employed. The time step Δt is varied according to the ratio of residuals between the previous and the present time as

$$\Delta t^{n+1} = \Delta t^{n} \frac{RHS^{n}}{RHS^{n+1}}$$

such that a steady-state solution can be rapidly achieved.

Two kinds of flow cross-sectional area distribution are chosen to establish a different shock Mach number(M_S). The first is that of Anderson, et al.(1985), where

$$A_1(x) = 1 - 0.8\,x\,(1 - x) \qquad , 0 \le x \le 1$$

By imposing the back pressure $P_b = 0.78$, the analytical solution shock Mach number (M_S) is equal to about 1.3 and is located at x=0.75. The second area distribution is

$$A_2(x) = (x - 0.5)^2 + 0.25 \qquad , 0 \le x \le 1$$

By imposing the back pressure $P_b = 0.70$, the exact solution shock Mach number (M_S) is about 1.8 and is located at x=0.85. In both cases, a mesh containing fifty uniform elements measure are employed. The exact solutions for Mach number are depicted in Figures 35 (a) and (b) for $M_S = 1.3$ and $M_S = 1.8$ respectively.

According to the mathematical theory of hyperbolic partial differential equations, one can have non-unique solutions due to the existence of a sonic region. To the left of the sonic region, one wave propagates to the left, while to the right this wave propagates to the right. Hence, no information can reach the sonic point for this wave and the solution may exhibit a non-physical jump at that point. This is known as the "dog-leg" phenomena, Goodman, et al.(1985). To remove this unphysical jump, a diffusion term must be added explicitly to the neighborhood of the sonic point, where $a_L < 0 < a_R$, in such a way that

$$|a| \le \frac{a^2 + p^2}{4p} \qquad , |a| \le p$$

where $$p = K \max(a_j - a_{j-1}, 0) \ , K > 0$$

This was first proposed by Harten(1983) and was also employed by Liou, et al.(1988). In this study, K was chosen to be unity and this remedy is needed only for the nonlinear fields.

Shown in Figure 36 are the Mach number solution distributions from the Donor-cell and Raymond-Garder methods both with and without sonic point treatment. It may be noticed that the sonic point jump is less pronounced in the Raymond-Garder solution without sonic treatment. Figure 37 shows the Mach number distributions for the Bubnov-Galerkin and the Raymond-Garder methods with upwind correction by $\varepsilon = 1.0$ for all

fields. In this case, the sonic jump can be seen very clearly when not accompanied by the sonic treatment. In Figure 38, the results were produced using the upwind treatment for nonlinear fields only ; the Raymond-Garder solutions are an excellent approximation to the exact solution. Experiments conducted for M_S = 1.8 (see Fig.39,40 and 41) confirm the outcome patterns as in the M_S=1.3 case. Hence, one can conclude that in both transonic and low supersonic flow, damping by upwind differencing may be the major cause of the sonic jump, and its correction can be made via a central differenced diffusion term either locally or globally. Also, the addition of sonic point treatment can improve the solution behavior of any of the tested TWS methods.

Steady oblique shock problems. The supersonic wedge flow and the shock reflection problems are chosen; the problem statements are shown in Figures 42 and 43 respectively. To run these problems, eq.(5.21) is employed as the Taylor series restatement of the conservation laws. For the steady Euler equation system, discontinuities are caused by shocks which are nonlinear waves. When using the Bubnov-Galerkin with upwind correction, the upwind parameter $\varepsilon = 1.0$ is applied to the nonlinear fields only, i.e., fields with wave speed of $u \pm c$.

For the wedge flow problem, the spatial discretization is a 20 x 20 uniform mesh and the initial data are the known exact solution. The steady-state Mach number and flow direction are depicted in Figure 42, where,

for region A, $\rho = 1.0$, $m_1 = 0.984808$, $m_2 = -0.173648$ and $E = 0.947393$

for region B, $\rho = 1.45336$, $m_1 = 1.28557$, $m_2 = 0.0$ and $E = 1.32828$

For the reflection shock problem, the spatial discretization is a 40 x 20 uniform mesh and the initial data used are the known exact solution. The steady-state Mach number and flow direction are depicted in the Figure 43 where

for region A, $\rho = 1.0$, $m_1 = 2.9$, $m_2 = 0.0$ and $E = 5.99$

for region B, $\rho = 1.7$, $m_1 = 4.452868$, $m_2 = -0.86071$ and $E = 9.8702$

for region C, $\rho = 2.687284$, $m_1 = 6.453509$, $m_2 = 0.0$ and $E = 15.0840$

The time step Δt is imposed at each node for a fixed maximum Courant number C_i^{max} such that

$$\Delta t_i \equiv \frac{C_i^{max} h_{\underline{i}}}{|u_{\underline{i}}| + c} \quad , \ \underline{i} \text{ is a directional indicator.}$$

where $h_i \equiv$ element length in the ith-coordinate direction, and

$\Delta t_i \equiv$ time step in the direction of x_i-coordinate.

The temporal contribution to damping is maximized by setting the time integration parameter $\theta = 1$. Hence, to rapidly reach a steady state, $\theta \equiv 1$ and the stability is not affected by time step size. But it was found that the Bubnov-Galerkin with flux limiter encountered a stability problem for $C_i^{max} = 1.0$ for the shock reflection problem. This problem may have been caused by the exact initial data, since the initially steep gradient in the data may not allow such a large time step. For the comparisons shown in Figure 44, the maximum Courant number was limited to 0.5, and the number of time steps taken from the exact initial condition was 250 for both problems. As a surface tangency condition, the one described in Sec. (5.3) is applied for both cases. In the shock reflection problem, the L_2-norms of the residual eq.(5.26) for the Donor-cell method was $(2.56)10^{-2}$ after one time step and $(3.27)10^{-3}$ after 250 time steps. For the flux-limited Bubnov-Galerkin method, residual was $(1.24)10^{-2}$ after one time step and $(1.27)10^{-3}$ after 250 time steps.

For the wedge flow problem, the Donor-cell solution (Fig.44 a) shows a very smeared shock and an oscillation near the tip of the wedge. The flux-limited Bubnov-Galerkin solution does not show the expected sharp and monotone character, Fig. 44 (b). Instead, it shows a severely oscillatory behavior, and both solutions are not acceptable. It seems that ignorance of the orientation of the shock for the flux correction procedure, and the presence of a singularity at the surface leading edge, both contribute significantly to the non-monotone solution character.

For the shock reflection case, the generated solutions (Fig.45) look as expected, and the flux limited Bubnov-Galerkin solution exhibits an improved result over that of the Donor-cell solution. However, it is smoother than that reported by Davis (1984). The usual discretization of the shock reflection problem is 61x21 nodes. Considering the significantly reduced number of nodal points employed in the major flow direction, and the much improved solution over the Donor-cell method, the solution by the present Bubnov-Galerkin method with upwind correction is quite acceptable.

These two test problems show that to capture oblique shocks, the flux-corrected Bubnov-Galerkin TWS method will require additional techniques such as a rotated correction flux difference and/or adaptive grid method to generate acceptable solutions.

CHAPTER 6

SUMMARY AND CONCLUSIONS

A quantization of the Taylor Weak Statement has emerged as a general structure for Computational Fluid Dynamics. It has enabled us to interpret and implement modern finite difference shock capturing schemes, namely flux limiters. The use of flux limiters so far has to be accompanied by some form of compression schemes, that is, the artificial compression method of Harten (1983) or the highly compressive limiter such as the hyper b-function of Roe (1985). However, our results show that, in the one-dimensional shock tube problem, and in the two-dimensional shock interaction problems, the TWS theory seems to be adequate for this type of problem. The principal reason appears to be that our method is based on the spatially high order Galerkin method.

An item of comfort in this study is the general agreement of numerical results with the Fourier modal analyses done on the Taylor Weak Statement, hence the explanation and the prediction of numerical behavior can be possible to some extent. The comparison between the standard and the upwind correction schemes in 1- and 2-dimensional scalar model problems shows a promising future for the new method.

With regard to the sonic jump behavior, and from the experiment on the quasi-one-dimensional Euler equations, we found that the major cause of this problem is the lack of a central difference-type diffusion across the sonic region, and with this type diffusion term, the sonic treatment in Sec. (3.4) can be effective.

In the two-dimensional shock interaction problems, the good feature of the upwind corrected Bubnov-Galerkin method has demonstrated its potential. During the shock interaction, a significant amount of energy is dissipated and hence this type of problem

involves a nonlinear shock interaction. Due to the sudden rise of temperature near the shock interaction, numerical solutions are apt to exhibit wiggles if the method fails to dissipate the temperature rise within a few mesh intervals.

The results shown in the oblique shock cases are smoother than those in the literature. This is probably due to the neglect of a preferred direction. Not to mention the obscurity in the choice of a preferred direction, one fundamental question arises: can a scheme satisfy the conservation of flux around a nodal point when grids are not aligned with the line of discontinuity ? In this regard, we did not pursue the rotated difference scheme. The usual practice in this type of problem is to use an adaptive grid method, as in Lohner, et al. (1986) and Oden, et al. (1986).

Even though there is room for improvement in our present scheme, its extension to a higher dimension appears appropriate. In two space dimensions, LeVeque and Goodman (1985) showed that any TVD scheme in 2D is at most first order accurate. Also, as was stated in Sec (3.3), even in one space dimension, the available argument is that the modified flux is as accurate as the Lax-Wendroff flux up to O (Δx^2), using a local Taylor series expansion in space. Since there are still unresolved problems in two-dimensional cases, the extension of the modal analysis on the TWS to two space dimensions would be a first choice for future work.

The next thing to consider is an approximate factorization solution procedure scheme for high speed flows. In the early 1970's, convergence difficulties were reported for a transonic potential flow problem by Murman and Cole (1971). The main cause has been found in the ill-treatment (central differencing) inside the supersonic dome, and it has been resolved by use of one-sided (upwind) differencing and an iterative line-relaxation solver. Interesting enough, in their report, for other than the relaxation solver, they couldn't obtain a solution for this type of flow. Later it was found in Hafez, et al. (1979)

that the iterative solution procedure actually possesses a damping term in its time-like direction which in our context is the TWS α-term. Since then the time dependent term has been introduced explicitly whether it be a transient or a steady state problem. In this way, approximate factorization via dimensional splitting has emerged as one major stream in CFD due to its efficiency and the ease of parallel processing. Wornom (1984) and Wornom, et al. (1986) reported a new strategy wherein the characteristic wave behavior has been explicitly employed in their implicit Euler solver. Whether the characteristic modelling is a drawback or an advancement, the convergence results shown are noticeable. With those reasons, a revisit to the elliptic solution procedure could be a worthwhile exercise.

The next topic to consider is the use of an adaptive grid method. The scope of this technique is not restricted to the problems presented herein. As the engineering demand grows, the degree of complexity tends to increase. In many cases, this can be overcome by putting more nodes around the difficult regions. Also it would be interesting to consider some relation between the flux limiter idea and the adaptive grid.

Upon completion of these subjects, more realistic problems can be studied such as shock-boundary layer intraction, separation and turbulence. The numerical solution of these problems can only be validated when the theoretical assurance of the basic method is at hand. In this context, I hope this study can be a milestone for future problems.

LIST OF REFERENCES

LIST OF REFERENCES

Anderson, D.A., Tannehill,J.C. and Pletcher,R.H. (1985) Computational Fluid Mechanics and Heat Transfer. Hemisphere Publishing Co., Washington, D.C.

Anderson, W. K., Thomas, J. L. and van Leer, B. (1985) A Comparison of Finite Volume Flux Vector Splittings for the Euler Equations. AIAA-85-0122

Baker, A.J. (1983) Finite Element Computational Fluid Mechanics. Hemisphere Publishing Co., Washington, D.C.

Baker, A.J. (1985) On a Penalty Finite Element Algorithm for high speed flow. Comp. Mtd. Appl. Mech. Eng., Vol. 51, pp.395-420

Baker, A. J. and Soliman, M. O. (1983) A Finite Element Algorithm for Computational Fluid Dynamics. AIAA J., Vol. 21, No. 6, pp.816-827

Baker, A. J. and Kim, J. W. (1986) Analysis on a Taylor Weak Statement for CFD Application. Finite Element Methods for Nonlinear Problems, Springer, Berlin Heidelberg

Baker, A. J. and Kim, J. W. (1987) A Taylor Weak Statement Algorithm for Hyperbolic Conservation Laws. Int. J. Num. Mtd. in Fluid, Vol. 7, pp.489-520

Beam, R. M. and Warming, R. F. (1976) An Implicit Finite-Difference Algorithm for Hyperboloc Systems in Conservation Law Form. J. Comp. Phys., pp.87-110

Boris, J. P. and Book, D. L. (1973) Flux-Corrected Transport. I. SHASTA, a Fluid Transport Algorithm that works. J. Comp. Phys., Vol. 11, pp.38-69

Chakravarthy, S. (1983) Euler Equations - Implicit Schemes and Boundary Conditions. AIAA J., Vol. 21, pp.699-706

Courant, R., Isaacson, E. and Rees, M. (1952) On the solution of nonlinear Hyperbolic differential equations. Comm. Pure. Appl. Math., Vol. 5, pp.243-255

Davis, S. F. (1984) A Rotationally Biased Upwind Difference Scheme for the Euler Equations. J. Comp. Phys., Vol. 56, pp.65-92

Demkowicz, L. and Oden, J. T. (1985) An Adaptive Characteristic Petrov-Galerkin Finite Element Method For Convection-Dominated Linear and Non-Linear Parabolic Problems in One Space variable. TICOM Report, The University of Texas at Austin

Dendy, J. E. (1974) Two methods of Galerkin type Optimum L^2 Rates of Convergence for First order Hyperbolics. SIAM J. Numer. Anal., Vol. 11, pp.637-653

Donea, J. (1984) A Taylor-Galerkin method for convective transport problems. Int. J. Num. Mtd. Eng., Vol. 20, pp.101-120

Godunov, S. K. (1959) A Finite Difference Method for the Numerical calculation of Discontinuous Solutions of the Equations of Fluid Dynamics. (in Russian) Mat. Sb., Vol.47, pp.271-290

Goodman, J.B. and Leveque, R.J. (1984) A Geometric Approach to High Resolution TVD Schemes. ICASE Report No. 84-55

Hafez, M. M., South, J. C. and Murman, E. M. (1979) Artificial Compressibility Methods for Numerical Solution of Transonic Full Potential Equation. AIAA J., Vol. 17, pp.838-844

Harten, A. (1983) High Resolution Schemes for Hyperbolic Conservation Laws. J. Comp. Phys., Vol.49, pp.357-393

Harten, A., Lax, P.D. and van Leer, B. (1983) On Upstream Differencing and Godunov-type Schemes for Hyperbolic Conservation Laws. SIAM Review, Vol.25, pp.35-60

Holt, M. (1984) Numerical Methods in Fluid Dynamics. 2nd Ed. Springer-Verlag Berlin, Heidelberg

Hughes, T. J. R. and Brooks, A. (1979) A Multidimensional Upwind Scheme With no Crosswind Diffusion. AMD Vol. 34, pp.19-35

Hughes, T. J. R. (1984) A Shock-Capturing Finite Element Method. Preprint. Stanford University, Stanford, CA 94305

Hughes, T. J. R. and Mallet, M. (1986) A New Finite Element Formulation For Computational Fluid Dynamics : III. The Generalized Streamline Operator for Multidimensional Advective-Diffusive Systems. Comput. Meth. Appl. Mech. Eng., Vol. 58, pp.305-328

Lax, P. D. (1973) Hyperbolic Systems of Conservation Laws and the Mathematical Theory of Shock Waves. SIAM, Philadelphia, Pennsylvania.

Lax, P. D. and Wendroff, B. (1960) Systems of Conservation Laws. Comm. Pure. Appl. Math.,Vol. 13, pp.217-237

Leonard, B. P. (1979) A Survey of Finite Differences of Opinion on Numerical Muddling of the Incomprehensible Defective Confusion Equation. AMD Vol. 34, pp.1-17

LeVeque, R. J. and Goodman, J. B. (1985) TVD Schemes in One and Two Space Dimensions. Lectures in Applied Mathematics, Vol. 22, pp.51-62

Liou, Meng-Sing and van Leer, B. (1988) Choice of Implicit and Explicit Operator for the Upwind Differencing method. AIAA paper 88-0624.

Lohner, R., Morgan, K. and Zienkiewicz, O.C. (1986) An adaptive finite element procedure for compressible high speed flows.
Comput. Meth. Appl. Mech. Eng., Vol.51, pp.441-466

Lohner, R., Morgan, K. and Zienkiewicz, O.C. (1984) The use of Domain Splitting with an Explicit Hyperbolic Solver.
Comput. Meth. Appl. Mech. Eng., Vol.45, pp.313-329

Morton, K.W. and Parrot, A.K. (1980) Generalized Galerkin Methods for First-Order Hyperbolic Equations. J. Comp. Phys., Vol.36, pp.249-270

Morton, K.W. (1985) Generalised Galerkin Methods for Hyperbolic Problems.
Comput. Meth. Appl. Mech. Eng., Vol.52, pp.847-871

Oden, J. T., Strouboulis, T. and Devloo, Ph. (1986) Adaptive Finite Element Methods For the Analysis of inviscid Compressible flow: I. Fast refinement / unrefinement and Moving mesh methods for unstructured meshes. Comput. Meth. Appl. Mech. Eng., Vol.59, pp.327-362

Osher, S. and Whitlow, Jr. W. (1984) Entropy Condition Satisfying Approximations For The Full Potential Equations of Transonic Flow. NASA Technical Memorandum 85751.

Raymond, W. H. and Garder, A. (1976) Selective Damping in a Galerkin Method for Solving Wave Problems with variable grids. Monthly Weather Review, Vol. 104, pp.1583-1590

Roe, P. L. (1985) Some Contributions to the Modelling of Discontinuous Floes.
Lectures in Applied Mathematics, Vol. 22, pp.163-193

Roe, P. L. (1982) Numerical Modelling of Shockwaves and Other Discontinuities.
Numerical methods in Aeronautical Fluid Dynamics, Ed : P.L.Roe, Academic Press, pp.211-243

Roe, P. L. (1981) Approximate Riemann Solvers, Parameter Vectors, and Difference Schemes. J. Comp. Phys., Vol. 43, pp.357-372

Sod, G. A. (1978) A Survey of Several Finite Difference Methods for Systems of Nonlinear Hyperbolic Conservation Laws. J. Comp. Phys., Vol. 27, pp.1-31

Sweby, P. K. (1984) High Resolution Schemes Using Flux Limiters for Hyperbolic Conservation Laws. SIAM J. Numer. Anal., Vol. 21, pp.995-1011

Thompson, K. W. (1987) Time Dependent Boundary Conditions for Hyperbolic Systems.
J. Comp. Phys., Vol. 68, pp.1-24

van Leer, B. (1979) Towards the Ultimate Conservative Differencing Scheme, V.
A Second-order Sequel to Godnuv's method.
J. Comp. Phys., Vol.32, pp.101-136

van Leer, B. (1974) Towards the Ultimate Conservative Differencing Scheme, II. Monotonicity and Conservation combined in a second order scheme. J. Comp. Phys., Vol.14, pp.361-370

van Leer, B. (1984) On the Relation between the Upwind-Differencing schemes of Godunov, Engquist-Osher and Roe. SIAM J. Sci. Stat. Comput., Vol. 5, pp.1-20

Wahlbin, L. B. (1975) A Dissipative Galerkin method Applied to some Quasi-linear Hyperbolic equations. R.A.I.R.O., Vol. 29, pp.1037-1045

Warming, R. F. and Beam, R. M. (1975) Upwind 2nd order difference schemes and applications in unsteady aerodynamic flows. Proc. AIAA 2nd Comp. Fluid Dynamics Conference, Hartford, CT, pp.17-28

Wornom, S. F. and Hafez, M. M. (1986) Implicit Conservative Schemes for the Euler Equations. AIAA J., Vol. 24, pp.215-223

Wornom, S. F. (1984) A Two-Point Difference Scheme For Computing Steady-State Solution To The Conservative One-dimensional Euler Equations. Computers & Fluids, Vol.12, pp.11-30

Yee, H. C. and Warming, R. F. (1985) Implicit Total Variation Diminishing (TVD) Schemes for Steady-State Calculations. J. Comp. Phys., Vol. 57, pp.327-360

APPENDICES

APPENDIX A

SEMI-DISCRETE FOURIER MODAL ANALYSIS OF THE LINEAR ADVECTION EQUATION IN 1-D

Given the following linear scalar advection equation

$$\frac{\partial u}{\partial t} + \frac{\partial f}{\partial x} = \frac{\partial u}{\partial t} + a\frac{\partial u}{\partial x} = 0 \qquad (A.1)$$

where $a = df / du \equiv$ constant, the semi-discrete form for a spatially uniform discretization (of uniform mesh h) can be written as

$$A_1 \frac{dU_j}{dt} + \frac{a}{h} A_2 U_j = 0 \qquad (A.2)$$

where

$U_j \equiv$ Semi-discrete approximation of u at a node j

$$A_1 = 1 + \sum_{k=1}^{K_1} (p_{-k}\delta_{-k} + p_k \delta_k)$$

$$A_2 = \sum_{k=1}^{K_2} (q_{-k}\delta_{-k} + q_k \delta_k)$$

K_1 = number of discrete interval in A_1

K_2 = number of discrete interval in A_2

p_k , q_k = coefficients corresponding to the kth interval from node j to the right (see Figure A-1).

p_{-k} , q_{-k} = coefficients corresponding to the kth interval from node j to the left (see Figure A-1).

$\delta_{-k} U_j = U_{j-k+1} - U_{j-k}$, k = 1,2, ...

$$\delta_k U_j = U_{j+k} - U_{j+k-1} \quad , k = 1,2, \ldots$$

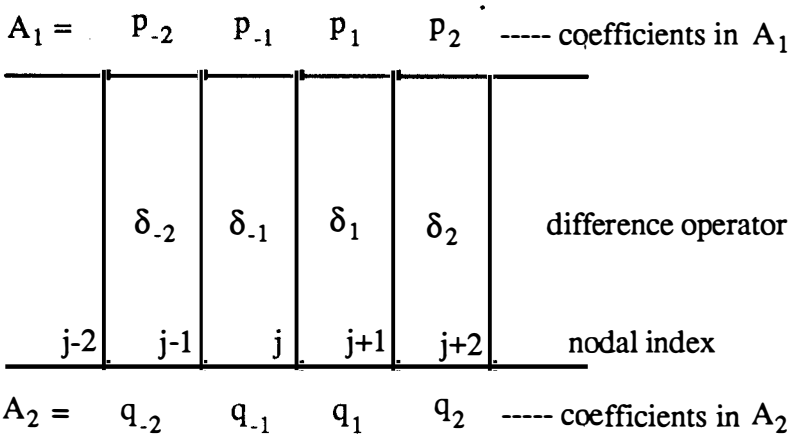

$$A_1 = \ldots + p_{-2}\delta_{-2} + p_{-1}\delta_{-1} + p_1\delta_1 + p_2\delta_2 + \ldots$$

$$A_2 = \ldots + q_{-2}\delta_{-2} + q_{-1}\delta_{-1} + q_1\delta_1 + q_2\delta_2 + \ldots$$

Figure A-1. Coefficients p_k and q_k in A_1 and A_2 of eq. (A.2).

The exact solution for this linear advection equation can be expressed as a superposition of elementary solutions from the Fourier series expansion. The pth Fourier mode of the exact solution, $u_p(x,t)$, is written as

$$u_p(x,t) = \exp[\, i\,(\omega'_p\, t + \omega_p\, x)] \qquad \text{(A.3-1)}$$

where $\omega'_p \equiv$ temporal frequency of pth component of the Fourier series solution

$\omega_p \equiv$ spatial frequency of pth component of the Fourier series solution

$= 2\pi / L_p =$ wave number

$L_p =$ wave length of pth component

$i = \sqrt{-1}$

Substitution of the eq. (A.3-1) into the eq. (A.1) yields the following relation between temporal and spatial frequency.

$$\omega'_p = - a \omega_p$$

Hence, the exact solution for a pth Fourier mode is written as

$$u_p (x,t) = \exp [i \omega_p (x - at)] \qquad (A.3\text{-}2)$$

In the following, we omit subscript p for eq. (A.3-2) for notational simplicity. Then, the discrete solution $U_j (t)$ can be written as

$$U_j (t) = u (jh,t) \qquad (A.4)$$

$$= \exp[i\omega (jh - \Gamma t)]$$

$$= \exp[i\omega (jh - at) + \omega D t + i\omega (a - a^*) t]$$

where $\Gamma = a^* + i D$

$D =$ damping coefficient

$a - a^* =$ wave speed error.

Substitution of $U_j (t)$ into the eq.(A-2), and using the following relations,

$$\delta_{-k} U_j = U_j \{ 1 - \exp (-i \omega h) \} \exp(i \omega h) \exp(-i k \omega h)$$

$$\delta_k U_j = U_j \{ 1 - \exp (-i \omega h) \} \exp(i k \omega h)$$

$$\frac{dU_j}{dt} = - i \omega \Gamma U_j$$

yields the following equation,

$$- i \omega \Gamma \hat{A}_1(\omega) + \frac{a}{h} \hat{A}_2(\omega) = 0 \qquad (A.5)$$

where

$$\hat{A}_1(\omega) = 1 + \sum_{k=1}^{K_1} \left(p_{-k} \exp[-ik(\omega h)] \exp[i(\omega h)] + p_k \exp[ik(\omega h)] \right) \left(1 - \exp[-i(\omega h)] \right)$$

$$\hat{A}_2(\omega) = \sum_{k=1}^{K_2} \left(q_{-k} \exp[-ik(\omega h)] \exp[i(\omega h)] + q_k \exp[ik(\omega h)] \right) \left(1 - \exp[-i(\omega h)] \right)$$

From eq.(A.5), the error due to the spatial discretization can be written as

$$D - i a^* = \frac{-a}{\omega h} \left(\frac{\hat{A}_2}{\hat{A}_1} \right) \tag{A.6}$$

The real part of the RHS of the eq.(A.6) then constitutes the damping coefficient D, while the imaginary part yields the numerical speed a^*. Let

$$\frac{\hat{A}_2}{\hat{A}_1} \equiv \frac{a}{h} \sum_{r=1}^{\infty} M_r (i \omega h)^r \tag{A.7}$$

where

$$M_r = d_r - \sum_{k=1}^{r-1} g_{r-k} M_k$$

$$g_o = 0$$

Then the damping coefficient D and the numerical speed a^* can be written as

$$D = a [M_2 (\omega h) - M_4 (\omega h)^3 + \ldots] \tag{A.8}$$

$$a^* = a [M_1 - M_3 (\omega h)^2 + M_5 (\omega h)^4 - \ldots] \tag{A.9}$$

where

$$\begin{aligned} M_1 &= d_1 = 1 \\ M_2 &= d_2 - g_1 M_1 \\ M_3 &= d_3 - g_2 M_1 - g_1 M_2 \\ M_4 &= d_4 - g_3 M_1 - g_2 M_2 - g_1 M_3 \\ M_5 &= d_5 - g_4 M_1 - g_3 M_2 - g_2 M_3 - g_1 M_4 \end{aligned} \tag{A.10}$$

etc.

and

$$
\begin{aligned}
d_1 &= \Sigma\, q_i \\
d_2 &= (1/2)\,[\,(q_1 - q_{-1}) + 3\,(q_2 - q_{-2}) + \ldots\,] \\
d_3 &= (d_1/6) + (q_2 + q_{-2}) + \ldots \\
d_4 &= (d_2/12) + (1/2)(q_2 - q_{-2}) + \ldots \\
d_5 &= (d_3/20) + (1/5)(q_2 + q_{-2}) + \ldots \\
&\text{etc.}
\end{aligned}
\tag{A.11}
$$

$$
\begin{aligned}
g_1 &= \Sigma\, p_i \\
g_2 &= (1/2)\,[\,(p_1 - p_{-1}) + 3\,(p_2 - p_{-2}) + \ldots\,] \\
g_3 &= (g_1/6) + (p_2 + p_{-2}) + \ldots \\
g_4 &= (g_2/12) + (1/2)(p_2 - p_{-2}) + \ldots \\
g_5 &= (g_3/20) + (1/5)(p_2 + p_{-2}) + \ldots \\
&\text{etc.}
\end{aligned}
\tag{A.12}
$$

where q_i and p_i are coefficients in A_1 and A_2, see Fig. A-1.

As an example of showing how to work with the above formulae, a TWS eq.(3.2) is chosen. From eq.(3.7),

$$A_1 = 1 - \left(\frac{1}{6} + \frac{\alpha}{2} - \gamma\right)\delta_- + \left(\frac{1}{6} - \frac{\alpha}{2} - \gamma\right)\delta_+$$

$$A_2 = \begin{cases} -\mu\,\delta_{-2} + \left(\dfrac{1+2\beta}{2} + 2\mu\right)\delta_- + \left(\dfrac{1-2\beta}{2} - \mu\right)\delta_+ , & a > 0 \\ \left(\dfrac{1+2\beta}{2} + \mu\right)\delta_- + \left(\dfrac{1-2\beta}{2} - 2\mu\right)\delta_+ + \mu\delta_{+2} , & a < 0 \end{cases}$$

Then, with reference to Figure A-1, p_k and q_k, $-2 \le k \le 2$, are determined as

$$p_{-2} = 0 = p_2$$

$$p_{-1} = -(\alpha/2) - (1/6 - \gamma), \text{ and } \quad p_1 = -(\alpha/2) + (1/6 - \gamma)$$

for $a > 0$,

$$q_{-2} = -\mu, \quad q_2 = 0,$$

$$q_{-1} = (1 + 2\beta)/2 + 2\mu, \text{ and } q_1 = (1 - 2\beta)/2 - \mu$$

for $a < 0$,

$$q_{-2} = -\mu, \quad q_2 = 0,$$

$$q_{-1} = (1 + 2\beta)/2 + 2\mu, \text{ and } q_1 = (1 - 2\beta)/2 - \mu$$

From eq. (A.11),

$$d_1 = q_{-1} + q_1 = 1, \quad d_2 = -\beta$$

Then, d_3, d_4 and d_5 are found easily as

$$d_3 = (1/6) - S(a)\,\mu, \quad d_4 = (-\beta/12) + (\mu/2), \text{ and}$$

$$d_5 = 1/120 - S(a)\,\mu/4$$

Also, from eq. (A.12),

$$g_1 = p_{-1} + p_1 = -\alpha \text{ and } g_2 = (p_1 - p_{-1})/2 = 1/6 - \gamma$$

Then,

$$g_3 = -\alpha/6, \quad g_4 = (1/6 - \gamma)/12 \text{ and } g_5 = -\alpha/120$$

Hence, from eq. (A.10) which is a recursion relation for M_i,

$$M_1 = 1$$

$$M_2 = d_2 - g_1 M_1 = \alpha - \beta$$

$$M_3 = d_3 - g_2 M_1 - g_1 M_2 = \gamma - S(a)\mu + \alpha M_2$$

$$M_4 = \alpha/6 - \beta/12 + \mu/2 - (1/6 - \gamma)M_2 + \alpha M_3$$

$$M_5 = -1/180 - S(a)\mu/4 + \gamma/12 + \alpha M_2/6 - (1/6 - \gamma)M_3 + \alpha M_4$$

which are eqs.(3.31-1) thru (3.31-5).

APPENDIX B

FULLY-DISCRETE FOURIER MODAL ANALYSIS

OF THE ADVECTION EQUATION IN 1-D

For integrating eq.(A.2) in time, a variable-implicit(θ), single step method is considered. Then, the fully discrete equation resulting from eq.(A.2) can be written as

$$\left(A_1 + \theta \lambda A_2 \right) \left(U_j^{n+1} - U_j^n \right) = - \lambda A_2 U_j^n \tag{B.1}$$

where $\lambda = a \Delta t / h$ = Courant number and $\theta = 0$ and $0.5 \leq \theta \leq 1.0$ yields stable integration procedures. From eq.(A.4), a single Fourier component of the numerical solution at time $t+\Delta t$ is written as

$$\begin{aligned} U_j(t+\Delta t) &= \exp[i\omega (jh - \Gamma(t+\Delta t))] \\ &= \exp[i\omega (jh - \Gamma t)] \exp[-i\omega \Gamma \Delta t] \\ &= U_j (t) \exp[-i\omega \Gamma \Delta t] \end{aligned} \tag{B.2}$$

where $U_j^{n+1} = U_j(t+\Delta t)$ and $U_j^n = U_j(t)$. If a method is stable, the amplification factor G

$$G = \exp[-i\omega \Gamma \Delta t] \tag{B.3}$$

during a time step Δt must satisfy

$$|G| \leq 1 \tag{B.4}$$

Substituting $U_j^{n+1} = G\, U_j^n$ into eq.(B.1), eq.(B.1) becomes

$$\left(A_1 + \theta \lambda A_2 \right) U_j^n \, (G - 1) = - \lambda A_2 U_j^n \tag{B.5}$$

Since

$$\delta_{-k} U_j = U_j \{ 1 - \exp [-i (\omega h)] \} \exp [i (\omega h)] \exp [- i k (\omega h)]$$

$$\delta_k U_j = U_j \{ 1 - \exp [-i (\omega h)] \} \exp [i k (\omega h)]$$

the amplification factor G is written as

$$G = 1 - \lambda \frac{\hat{A}_2}{\hat{A}_1 + \theta \lambda \hat{A}_2} \tag{B.6}$$

where $\hat{A}_1$ and $\hat{A}_2$ are as defined in the Appendix A, eq.(A.5).

One can evaluate the RHS of eq.(B.6), using an approach similar to that used for the semi-discrete case. Let

$$\frac{\hat{A}_2}{\hat{A}_1 + \theta \lambda \hat{A}_2} = \sum_{r=1}^{\infty} \overline{M}_r (i \omega h)^r \tag{B.7}$$

where

$$\overline{M}_r = d_r - \sum_{k=1}^{r-1} \overline{g}_{r-k} \overline{M}_k, \qquad \overline{g}_o = 0$$

the d_r are as defined in Appendix A, eq.(A.11)

$\overline{g}_i = g_i + \lambda \theta d_i, \qquad i = 1,2,...$

and g_i's are as defined in Appendix A, eq.(A.12)

Then, the amplification factor G can be written as

$$G = 1 - \lambda \sum_{r=1}^{\infty} \overline{M}_r (i \omega h)^r \tag{B.8}$$

where, for M_i as defined in Appendix A, eq.(A.10),

$\overline{M}_1 = M_1 = 1$

$\overline{M}_2 = M_2 - \lambda \theta$

$\overline{M}_3 = M_3 - 2(\lambda \theta) M_2 + (\lambda \theta)^2$

$\overline{M}_4 = M_4 - (\lambda \theta)(2 M_3 + M_2^2) + 3 (\lambda \theta)^2 (M_2^2 + M_3)$

$\overline{M}_5 = M_5 - 2 (\lambda \theta) (M_2 M_3 + M_4) + 3 (\lambda \theta)^2 (M_2^2 + M_3) - 4 (\lambda \theta)^2 + (\lambda \theta)^4$

etc.

To establish the dissipation and dispersion error functional forms for the fully discrete approximation, eq.(B.3) is invoked.

$$\exp[\, -i\omega\, \Gamma \Delta t\,] \;=\; \exp[\, -i\omega\, (a^{*} + iD)\, \Delta t\,] \;=\; G \qquad \text{(B.9)}$$

Then, eq.(B.9) is divided by the analytical amplification to obtain the error in the numerical amplification factor in one time step Δt. Since the analytical amplitude of the pure advection case is $\exp[\, -i\, \omega\, a\, \Delta t\,]$, eq.(B.9) is rewritten as

$$\exp[\, \omega \Delta t\, D + i\omega\, \Delta t\, (a - a^{*})\,] \;=\; G \exp[\, i\omega\, a\, \Delta t\,] \qquad \text{(B.10)}$$

Taking the natural logarithm for both sides of eq.(B.10), one arrives at an expression for the errors as,

$$\omega\, \Delta t\, D + \ln|\omega \Delta t\, (a - a^{*})| + \mathrm{Arg}(\omega \Delta t\, (a - a^{*})) \;=\; \ln |G| + \mathrm{Arg}(G) + \ln |\omega a \Delta t| + \mathrm{Arg}(\omega a \Delta t) \qquad \text{(B.11)}$$

where G is expressed in (B.8). However, eq.(B.11) does not yield a workable formula. Hence, to estimate the dissipation and dispersion errors, the LHS of eq.(B.10) is approximated to the first-order by a Maclaurin series in Δt as

$$\text{LHS of eq.(B.10)} \;\approx\; 1 + \omega\, \Delta t\, D + i\omega\, \Delta t\, (a - a^{*}) \qquad \text{(B.12)}$$

and the RHS of eq.(B.10) is expanded as

$$\text{RHS of eq.(B.10)} \;= \left(1 - \lambda \sum_{r=1}^{\infty} \overline{M}_r\, (i\, \omega\, h)^r \right) \exp[\, i\omega\, a\, \Delta t] \qquad \text{(B.13)}$$

$$= \left(1 - \lambda \sum_{r=1}^{\infty} \overline{M}_r\, (i\, \omega\, h)^r \right) \exp[\, (i\omega h)\, \lambda\,]$$

$$= \left(1 - \lambda \sum_{r=1}^{\infty} \overline{M}_r\, (i\, \omega\, h)^r \right) \sum_{p=0}^{\infty} \frac{(i\omega h)^p\, \lambda^p}{p!}$$

Then, after a lengthy algebra sequence from eqs.(B.12) and (B.13), formulae for the dispersion error $\omega\, \Delta t\, (a - a^{*})$ and the dissipation error $\omega\, \Delta t\, D$ estimates are obtained as follows :

$$\omega \Delta t D = Re \left\{ \lambda \sum_{r=1}^{\infty} \left(\frac{\lambda^{r-1}}{r!} - \sum_{k=1}^{r} \frac{\lambda^{r-k}}{(r-k)!} \overline{M}_k \right) (i \omega h)^r \right\} \tag{B.14}$$

$$\omega \Delta t (a - a^*) = Im \left\{ \lambda \sum_{r=1}^{\infty} \left(\frac{\lambda^{r-1}}{r!} - \sum_{k=1}^{r} \frac{\lambda^{r-k}}{(r-k)!} \overline{M}_k \right) (i \omega h)^r \right\} \tag{B.15}$$

Hence, let

$$\omega \Delta t D = \lambda [b_2 (\omega h)^2 + b_4 (\omega h)^4 + \dots] \tag{B.16}$$

$$\omega \Delta t (a^* - a) = \lambda [b_1 (\omega h) + b_3 (\omega h)^3 + b_5 (\omega h)^5 + \dots] \tag{B.17}$$

where

$$b_1 = 1 - \overline{M}_1 \tag{B.18}$$

$$b_2 = \frac{\lambda}{2} + \overline{M}_2$$

$$b_3 = \frac{\lambda^2}{3} + \lambda \overline{M}_2 + \overline{M}_3$$

$$b_4 = -\left(\frac{\lambda^3}{8} + \frac{\lambda^2}{2} \overline{M}_2 + \lambda \overline{M}_3 + \overline{M}_4 \right)$$

$$b_5 = -\left(\frac{\lambda^4}{30} + \frac{\lambda^3}{6} \overline{M}_2 + \frac{\lambda^2}{2} \overline{M}_3 + \lambda \overline{M}_4 + \overline{M}_5 \right)$$

In terms of λ, θ and M_i's, we have

$$\begin{aligned} \omega \Delta t D = \lambda \Big[& \{ - \lambda (\theta - 1/2) + M_2 \} (\omega h)^2 \\ & + \{ \lambda^3 (\theta - 1/2) \left((\theta - 1/4)^2 + 3/16 \right) \\ & - 3 \lambda^2 \left((\theta - 1/3)^2 + 1/18 \right) M_2 \\ & + \lambda \left(\theta M_2^2 + (2\theta - 1) M_3 \right) - M_4 \} (\omega h)^4 + \dots \Big] \end{aligned} \tag{B.19}$$

$$\omega \Delta t\,(a - a^{*}) = \lambda \Big[\quad (1 - M_1)\,(\omega h) \tag{B.20}$$

$$+ \left\{ \lambda^2 \left((\theta - 1/2)^2 + 1/12 \right) - 2\lambda\,(\theta - 1/2)\,M_2 + M_3 \right\} (\omega h)^3$$

$$- \left\{ \lambda^4 \left(1/30 - \theta/6 + \theta^2/2 - \theta^3 + \theta^4 \right) \right.$$

$$+ \lambda^3 \left(1/6 - \theta + 3\theta^2 - 4\theta^3 \right) M_2$$

$$+ \lambda^2 \left(\theta(3\theta - 1)\,M_2^2 + \left(1/2 - 2\theta + 3\theta^2 \right) M_3 \right)$$

$$+ \lambda \left((1 - 2\theta)\,M_4 - 2\theta\,M_2 M_3 \right)$$

$$\left. + M_5 \right\} (\omega h)^5 + \ldots \Big]$$

Also, it can be found from the finite difference literature, cf., Anderson et.al. (1984), that the coefficients b_i, in eqs.(B.16) and (B.17) correspond to the coefficients of an artificial viscosity equation as

$$\frac{\partial u}{\partial t} + a\frac{\partial u}{\partial x} = a\,\Delta x\,(-b_1)\frac{\partial u}{\partial x} + a\,\Delta x\,(-b_2)\frac{\partial^2 u}{\partial x^2} + a\,\Delta x^2\,(-b_3)\frac{\partial^3 u}{\partial x^3} \tag{B.21}$$

$$+ a\,\Delta x^3\,(-b_4)\frac{\partial^4 u}{\partial x^4} + a\,\Delta x^4\,(-b_5)\frac{\partial^5 u}{\partial x^5} + \ldots$$

APPENDIX C

A PARABOLIC EQUATION IN 1-D

Consider the following time dependent advection-diffusion equation

$$\frac{\partial u}{\partial t} + a\frac{\partial u}{\partial x} = \varepsilon\frac{\partial^2 u}{\partial x^2} \tag{C.1}$$

where a and ε are constants and $\varepsilon > 0$. The exact solution to the above equation can be represented by the Fourier series

$$u(x,t) = \sum_{n=-\infty}^{\infty} A_n \exp[\, i\,\omega_n (x - at)] \exp[-\varepsilon\,\omega_n^2 t] \tag{C.2}$$

Following the same procedure as in Appendix B, the numerical solution $U_j(t+\Delta t)$ at time $t+\Delta t$ is written as

$$U_j(t+\Delta t) = U_j(t)\exp[\, -i\,\omega\,\Gamma\,\Delta t\,] \tag{C.3}$$

or

$$U_j(t+\Delta t) = U_j(t)\,G \tag{C.4}$$

Since the amplification factor G can be found from eq.(B.8), no more difficulties arise than in the pure advection case. Write the amplification factor from eq.(B.9) as

$$\exp[\, -i\omega\,\Gamma\Delta t\,] = \exp[\, -i\omega\,(a^* + iD)\,\Delta t\,] = G \tag{B.9}$$

Also, the analytical amplitude in one time step Δt for the parabolic equation (D.1) is

$$\exp[\, -i\omega\, a\Delta t\,] \exp[\, -\varepsilon\omega^2\,\Delta t]$$

For a single Fourier mode, eq.(B.9) is reduced to

$$\exp[\,\omega\,\Delta t\, D + i\,\omega\,\Delta t\,(a - a^*)\,] = G\exp[\, i\,\omega\, a\,\Delta t]\exp[\,\varepsilon\,\omega^2\,\Delta t] \tag{C.5}$$

Following the same procedure as in Appendix B, the LHS of eq.(C.5) is approximated to first-order by the Maclaurin series in Δt and the RHS is expanded using

the amplification factor G as expressed in eq.(B.8). Hence, one can obtain the dissipation error and the dispersion error estimates as follows :

$$\omega \Delta t\, D = \lambda \left[\left(b_2 - \left(\frac{\varepsilon}{a \Delta x} \right) \right) (\omega h)^2 \right. \tag{C.6}$$

$$\left. + \left(b_4 + \left(\frac{\varepsilon}{a \Delta x} \right) \lambda \left(\frac{\lambda}{2} + \overline{M_2} \right) - \left(\frac{\varepsilon}{a \Delta x} \right)^2 \left(\frac{\lambda}{2} \right) \right) (\omega h)^4 + \ldots \right]$$

$$\omega \Delta t\, (a - a^*) = \lambda \left[\left(b_3 - \left(\frac{\varepsilon}{a \Delta x} \right) \lambda (1 - M_1) \right) (\omega h)^3 + \ldots \right] \tag{C.7}$$

where $M_1 = 1$ and the coefficients b_i are as expressed in eq.(B.18).

APPENDIX D

SOME ASPECTS ON THE BOUNDARY

Since the Euler system is a first order hyperbolic partial differential equation, some aspect on the treatment at the boundary point is considered by resorting to a first order hyperbolic system. In the computation of a wave system, one must define a computational domain. However, a wave cannot be confined in a domain, since some information going out of the domain may be coming back into the domain. Hence, the governing equations that describe interior points are not appropriate at the boundaries. To remove this deficiency, consider the following equation system

$$0 = \frac{\partial U}{\partial t} + \frac{\partial F_i}{\partial x_i} + \vec{H} \qquad (D.1)$$

$$= \frac{\partial U}{\partial t} + A_i \frac{\partial U}{\partial x_i} + \vec{H}$$

Define an equation set at x_1-boundary points (see Fig. D-1) as

$$\frac{\partial U}{\partial t_1} + A_1 \frac{\partial U}{\partial x_1} + H_1 = 0 \qquad (D.2)$$

and at x_2-boundary points (see Fig. D-1) as

$$\frac{\partial U}{\partial t_2} + A_2 \frac{\partial U}{\partial x_2} + H_2 = 0 \qquad (D.3)$$

Then, the eq.(D.1) can be written at an x_1-boundary point as,

$$0 = \frac{\partial U}{\partial t} - \frac{\partial U}{\partial t_1} + A_2 \frac{\partial U}{\partial x_2} + H_2 \qquad (D.4)$$

and at an x_2-boundary point as,

$$0 = \frac{\partial U}{\partial t} + A_1 \frac{\partial U}{\partial x_1} + H_1 - \frac{\partial U}{\partial t_2} \qquad (D.5)$$

Hence, the functional form of $\partial U/\partial t_1$ is required on the x_1-boundary, $\partial U/\partial t_2$ on the x_2-boundary.

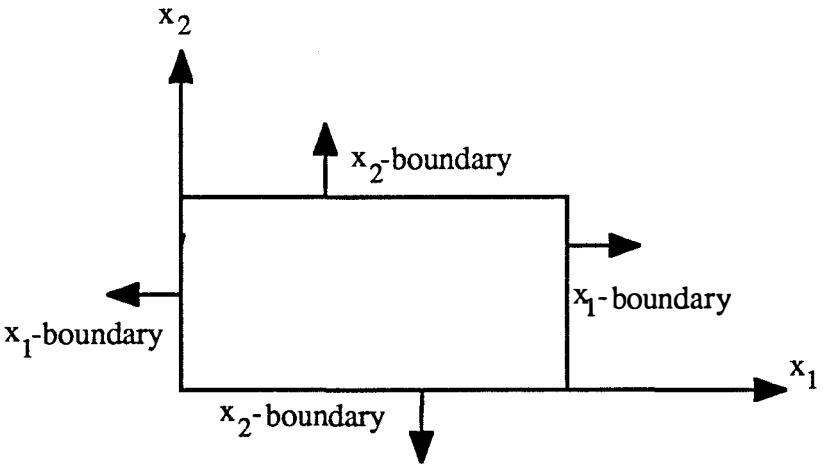

Figure D-1. Definition of x_1-boundary and x_2-boundary.

Consider an x_1-boundary such that

$$0 = \frac{\partial U}{\partial t_1} + A_1 \frac{\partial U}{\partial x_1} + H_1 \qquad \text{(D.6)}$$

Let

$$B_i = B_i(U) \qquad \text{(D.7)}$$

be the boundary condition corresponding to the ith incoming wave. Then, a set of equations for a non-reflecting boundary condition can be written as

$$l_{ij}\frac{\partial u_j}{\partial t_1} + \lambda_i l_{ij}\frac{\partial u_j}{\partial x_1} + l_{ij}h_j = 0 \qquad \text{(D.8)}$$

where l_{ij} is a component of left eigenvector matrix, λ_i is outgoing, i is a free index, j is summed and

$$\frac{\partial B_i}{\partial t_1} = 0 \quad \text{for } \lambda_i \text{ incoming.} \qquad \text{(D.9)}$$

In terms of the original variables, eqs.(D.8) and (D.9) can be combined into the convenient form

$$L_1^{(t)}\frac{\partial U}{\partial t_1} + L_1^{(s)}A_1\frac{\partial U}{\partial x_1} + L_1^{(s)}H_1 = 0 \qquad \text{(D.10)}$$

where

$$\text{the row of } L_1^{(t)} = \begin{cases} l_{ij} & \text{for outgoing wave} \\ \dfrac{\partial B_i}{\partial U} & \text{for incoming wave} \end{cases}$$

$$\text{the row of } L_1^{(s)} = \begin{cases} l_{ij} & \text{for outgoing wave} \\ 0 & \text{for incoming wave} \end{cases}$$

Hence, the new equation for $\partial U/\partial t_1$ can be determined as

$$\frac{\partial U}{\partial t_1} = -\left[L_1^{(t)}\right]^{-1} L_1^{(s)}\left(\frac{\partial F_1}{\partial x_1} + H_1\right) \qquad \text{(D.11)}$$

Then, at x_1-boundary points a proper set of equations can be written as

$$\frac{\partial U}{\partial t} + \left[L_1^{(t)}\right]^{-1} L_1^{(s)}\left(\frac{\partial F_1}{\partial x_1} + H_1\right) + \frac{\partial F_2}{\partial x_2} + H_2 = 0 \qquad \text{(D.12)}$$

Similarly, at x_2-boundary points,

$$\frac{\partial U}{\partial t} + \frac{\partial F_1}{\partial x_1} + H_1 + \left[L_2^{(t)}\right]^{-1} L_2^{(s)}\left(\frac{\partial F_2}{\partial x_2} + H_2\right) = 0 \qquad \text{(D.13)}$$

APPENDIX E

FIGURES

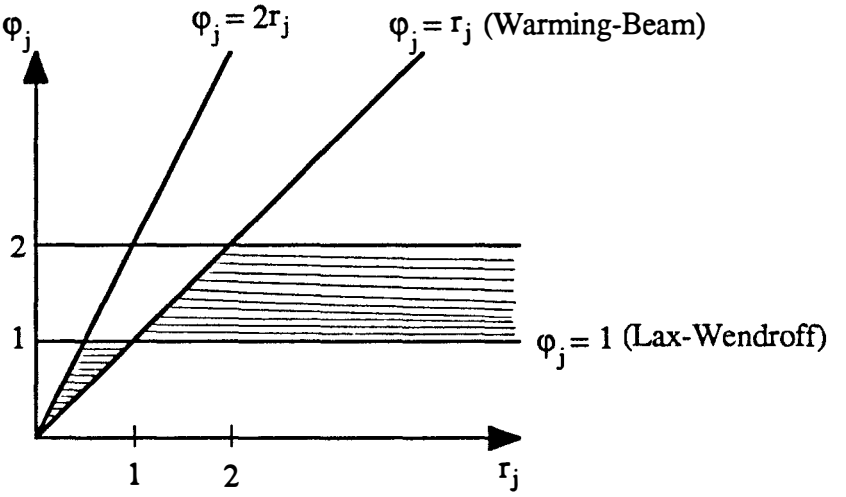

Figure 1. Region of TVD (shaded area) selected by Sweby (1984).

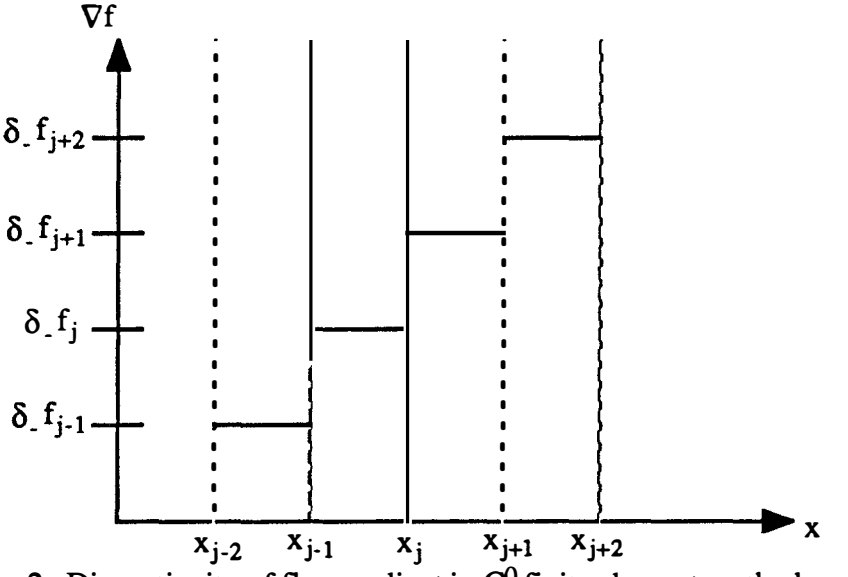

Figure 2. Discontinuity of flux gradient in C^0 finite element method.

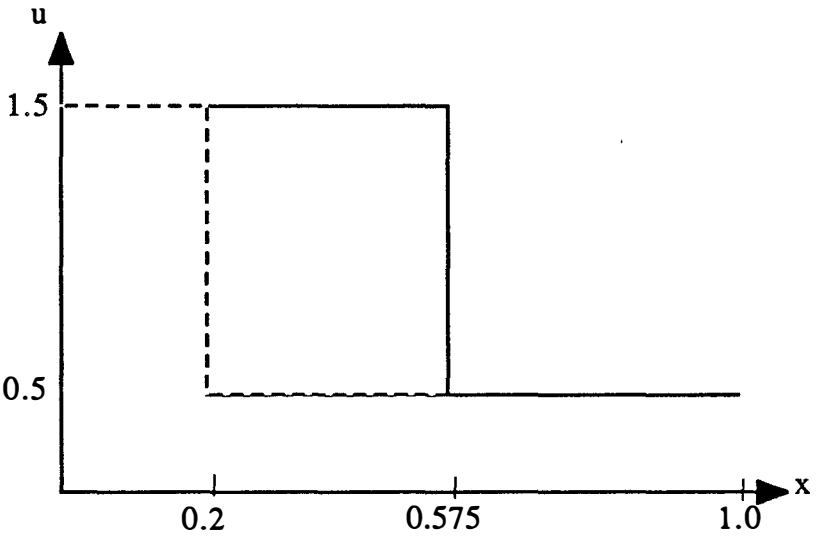

Figure 3. Initial data (dashed line) and exact solution (solid line) at $t - t_0 = 0.375$ sec for linear step problem.

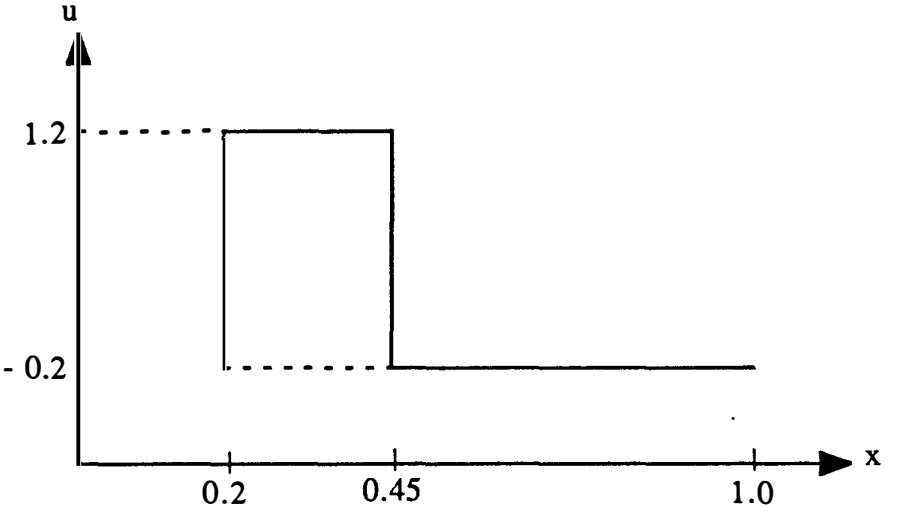

Figure 4. Initial data (dashed line) and exact solution (solid line) at $t - t_0 = 0.5$ sec for nonlinear Burgers step problem.

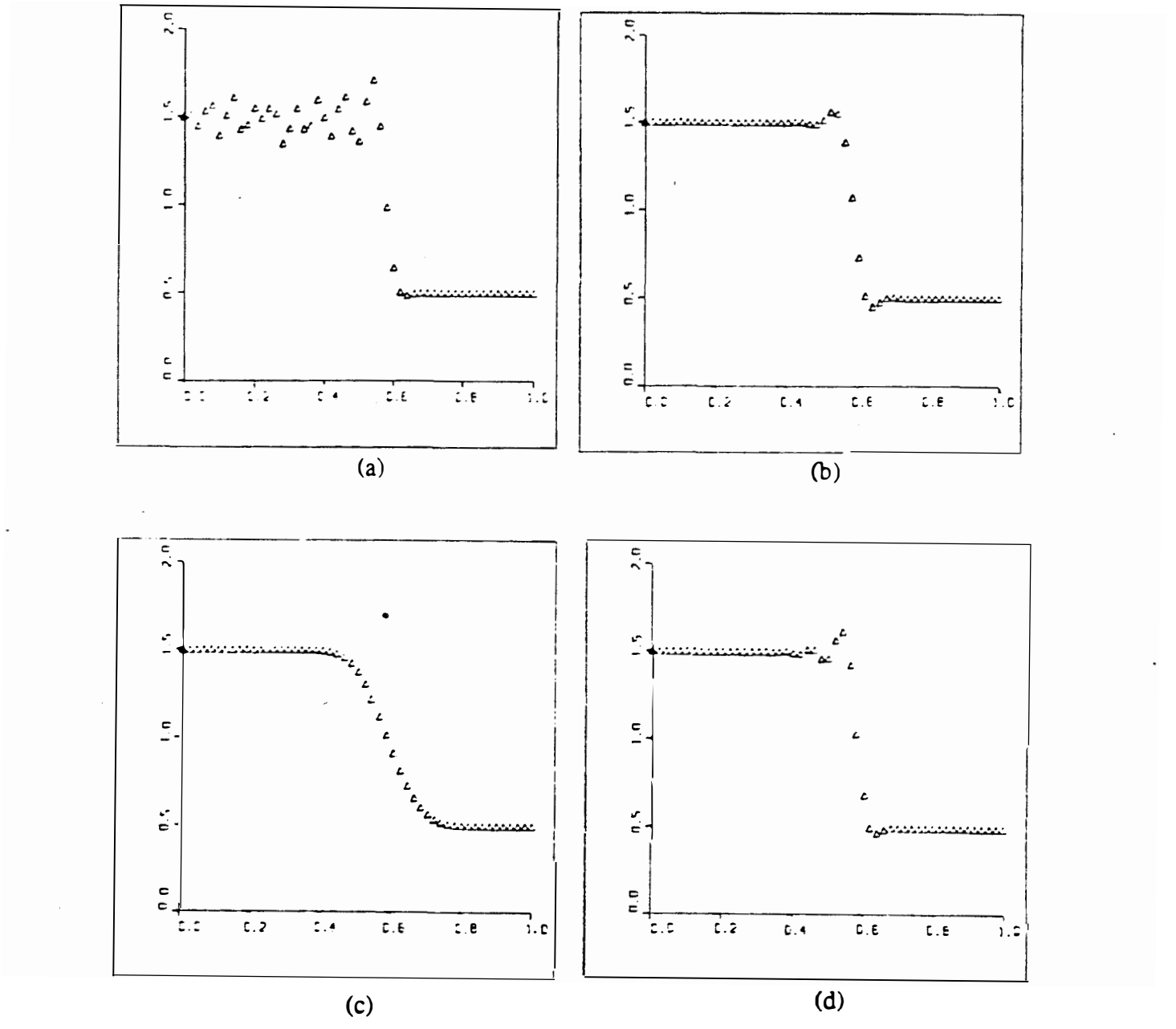

Figure 5. TWS Nodal Solutions for Linear Step problem.

(a) Galerkin, $\alpha = 0 = \beta = \gamma = \mu$, $\theta = 0.5$

(b) Raymond-Garder, $\alpha = (15)^{-1/2} = \beta$, $\theta = 0.5$

(c) Donor-cell, $\alpha = 0 = \mu$, $\beta = 1/2$ and $\gamma = 1/6$, $\theta = 0.0$

(d) diss. Galerkin, $\alpha = \beta = 0.1$ and $\gamma = 0 = \mu$, $\theta = 0.5$

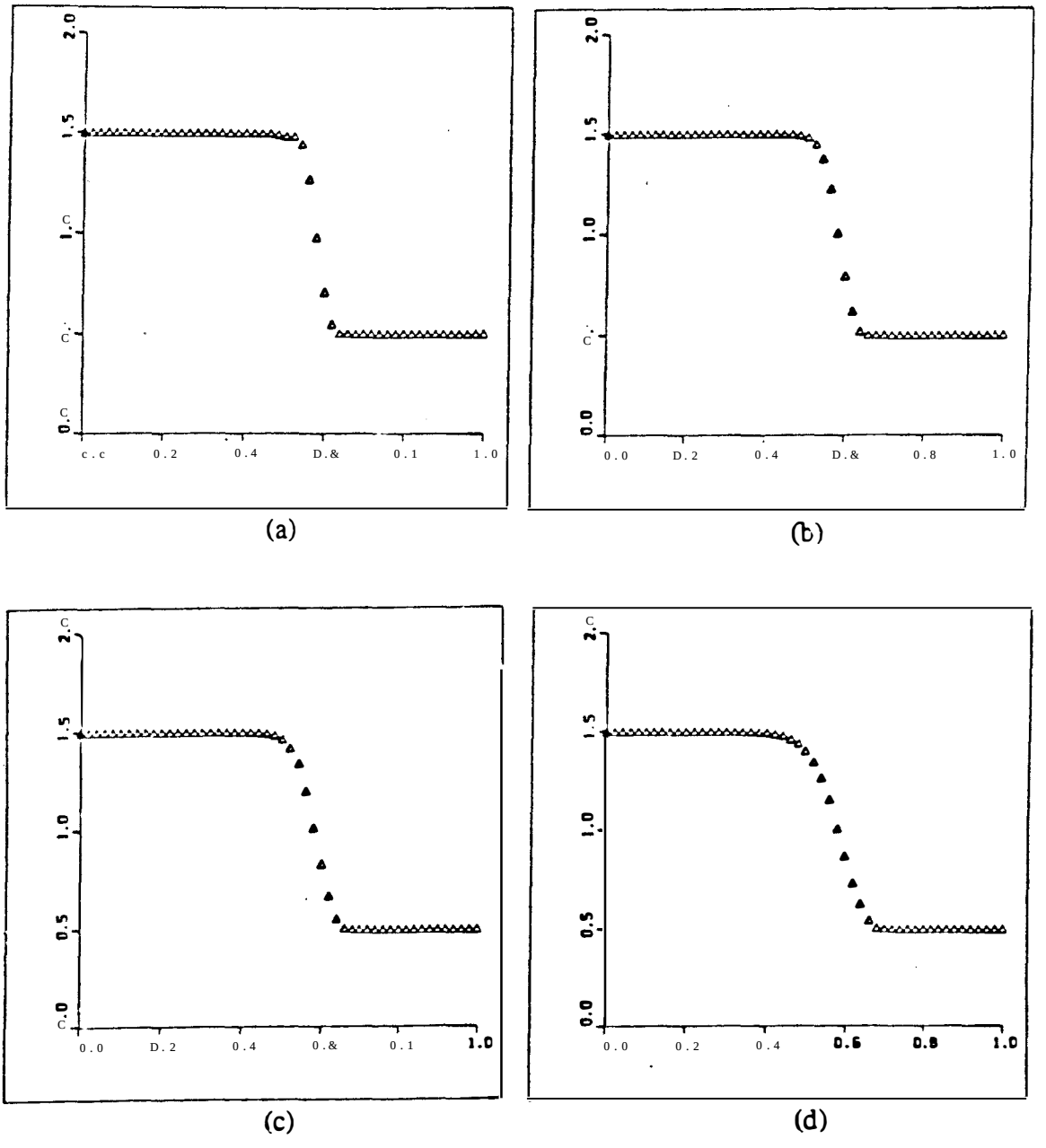

Figure 6. TWS Nodal Solutions for Linear Step problem using Flux-limited Galerkin ($\alpha = 0 = \beta$).

(a) $\varepsilon = 0.1$ (b) $\varepsilon = 0.3$ (c) $\varepsilon = 0.5$ (d) $\varepsilon = 1.0$

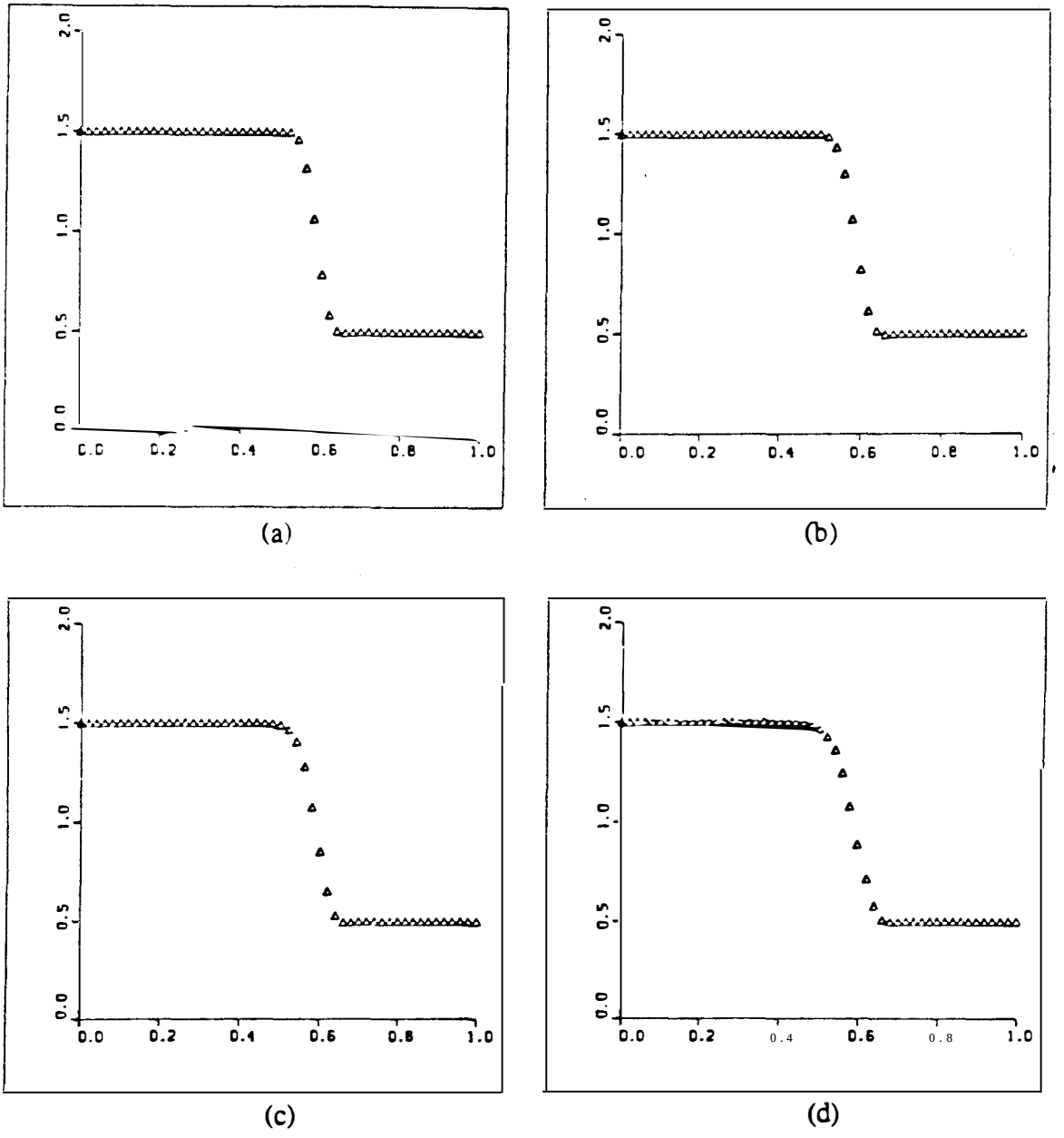

Figure 7. TWS Nodal Solutions for Linear Step problem using
Flux-limited Raymond-Garder ($\alpha = (15)^{-1/2} = \beta$), $\theta = 0.5$.
(a) $\varepsilon = 0.1$ (b) $\varepsilon = 0.3$ (c) $\varepsilon = 0.5$ (d) $\varepsilon = 1.0$

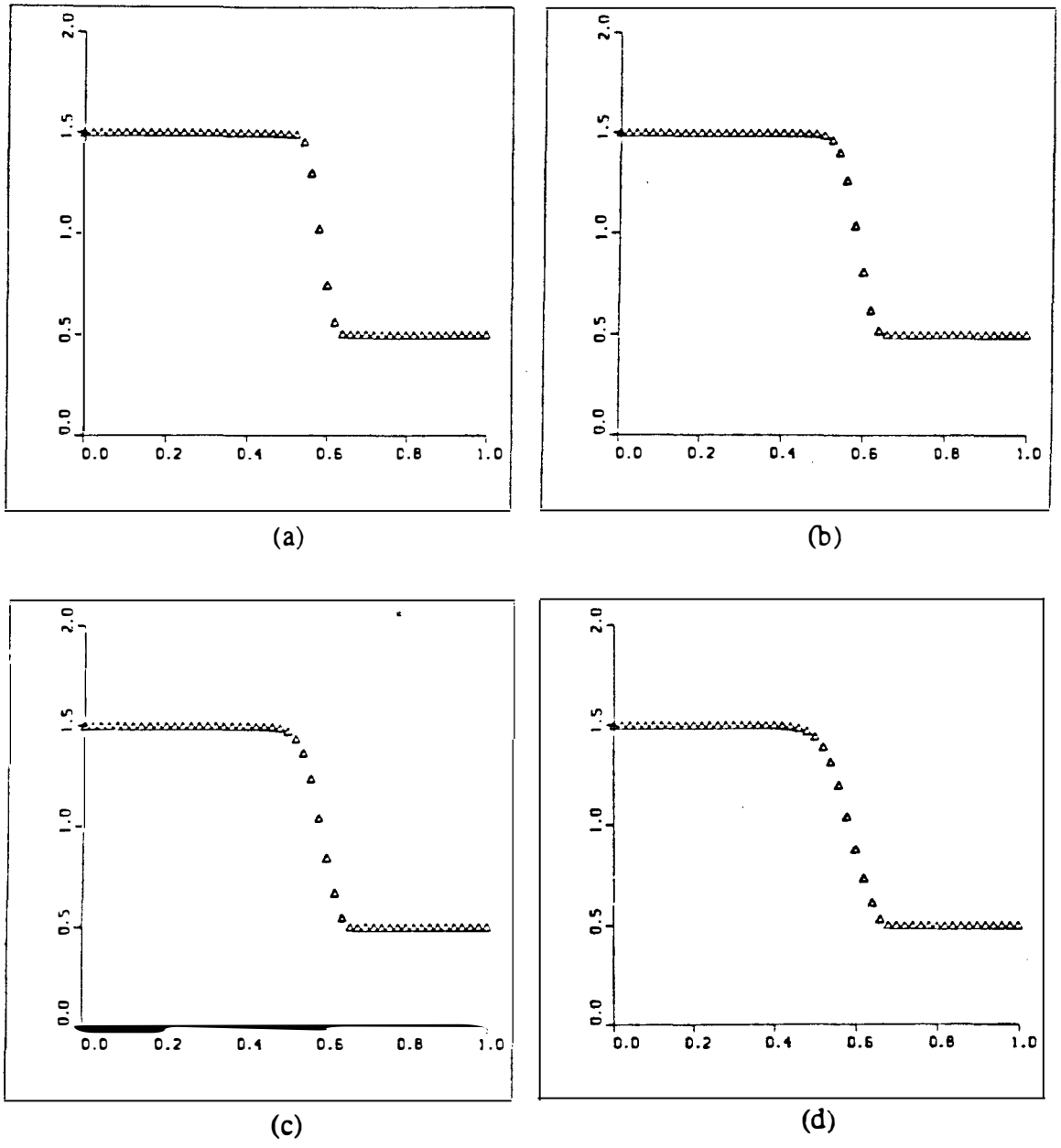

Figure 8. TWS Nodal Solutions for Linear Step problem using
Flux-limited dissipative Galerkin ($\alpha = 0.1 = \beta$), $\theta = 0.5$.
(a) $\varepsilon = 0.1$ (b) $\varepsilon = 0.3$ (c) $\varepsilon = 0.5$ (d) $\varepsilon = 1.0$

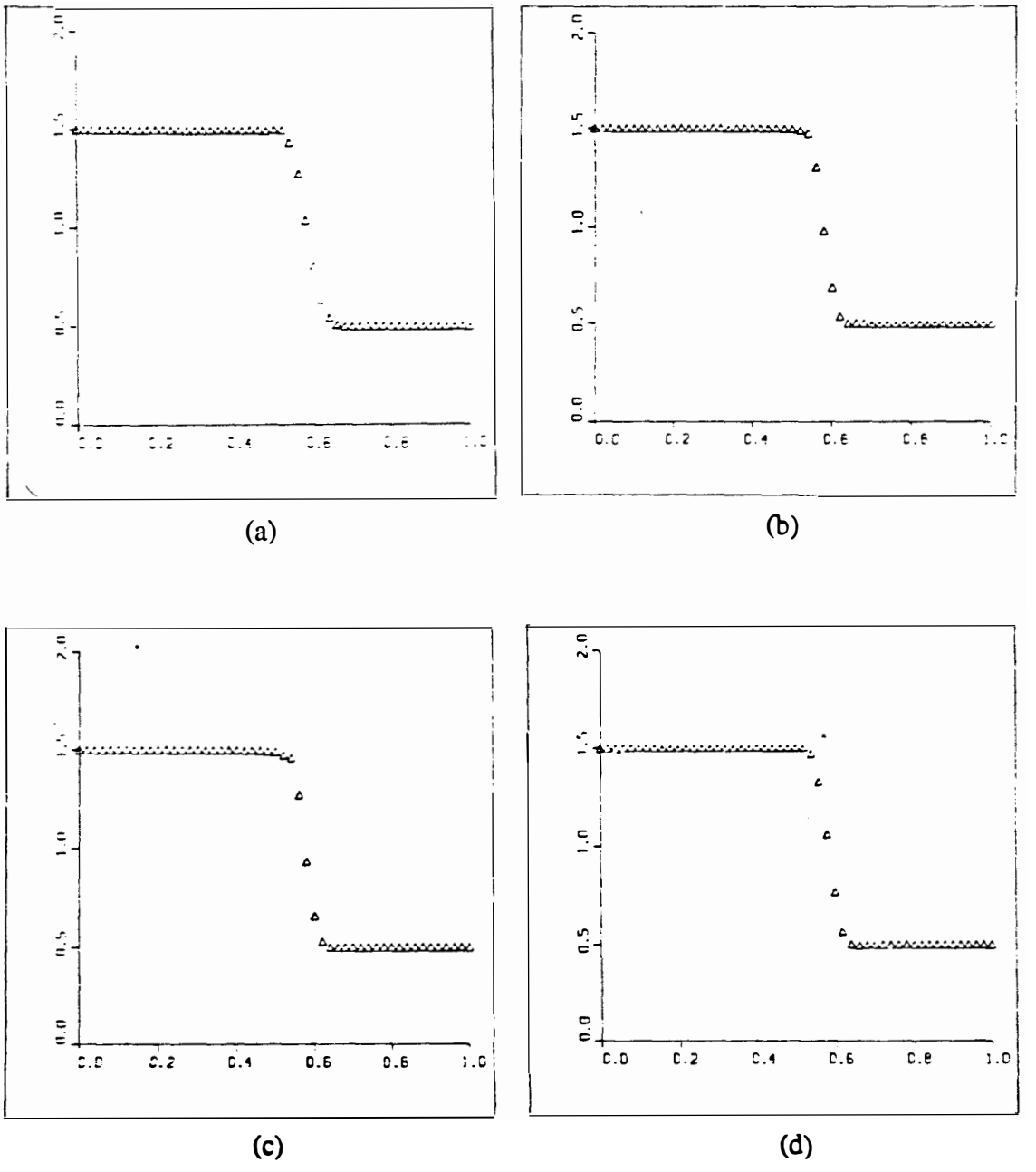

Figure 9. TWS Nodal Solutions for Linear Step problem.

(a) first-order dissipative Galerkin ($\underline{\alpha} = 0.0, \underline{\beta} = 0.125$), $\varepsilon = 0.0$, $\theta = 0.5$

(b) dissipative Galerkin ($\underline{\alpha} = 0.1 = \underline{\beta}$), $\varepsilon = 0.01$, $\theta=0.5$

(c) Bubnov-Galerkin ($\underline{\alpha} = 0.0 = \underline{\beta}$), $\varepsilon = 0.01$, $\theta=0.5$

(d) Raymond-Garder ($\underline{\alpha} = (15)^{-1/2} = \underline{\beta}$), $\varepsilon = 0.01$, $\theta=0.5$

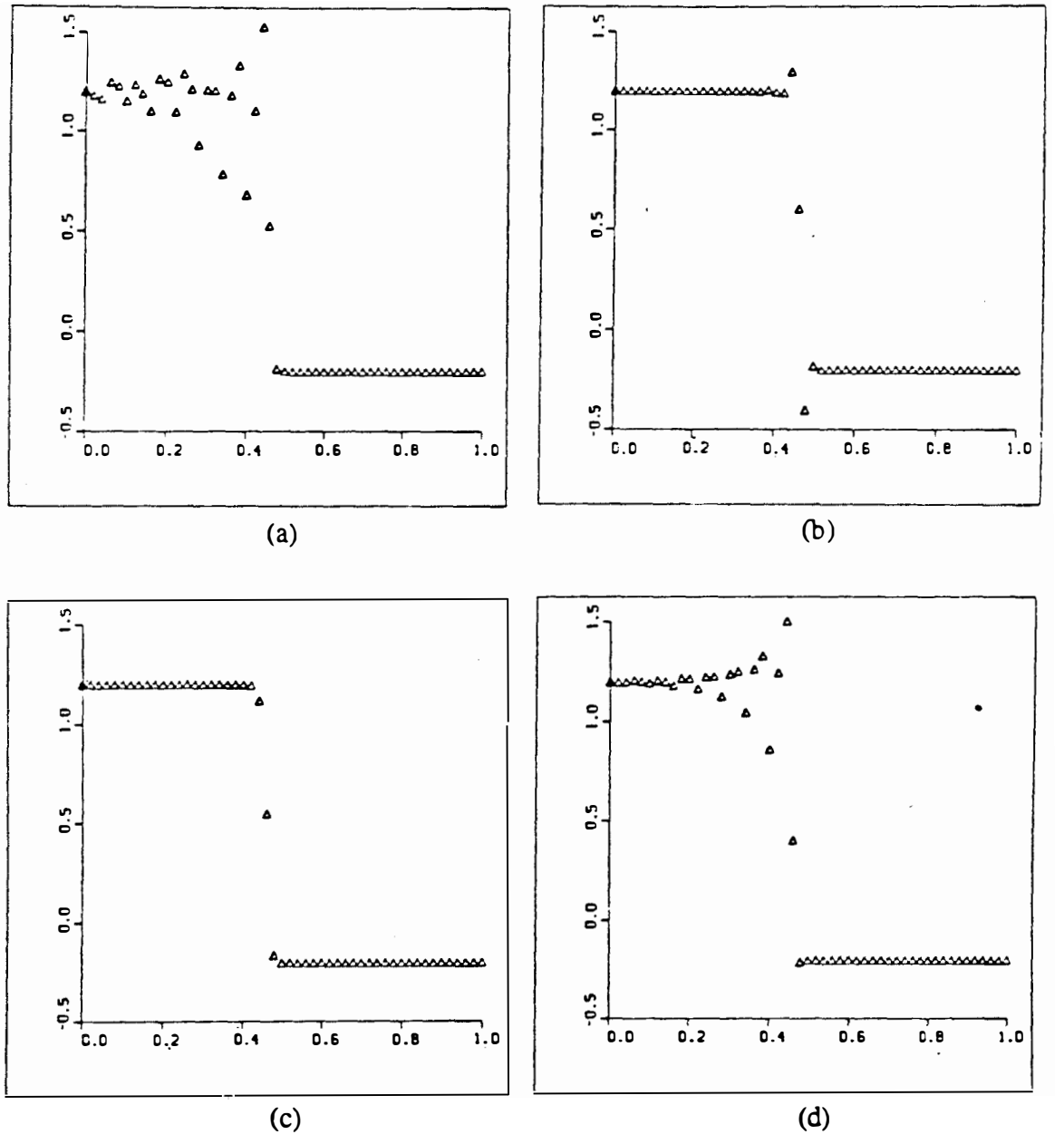

Figure 10. TWS Nodal Solutions for Burgers Step problem.

(a) Bubnov-Galerkin (θ=1.0)

(b) Raymond-Garder($\alpha = (15)^{-1/2} = \beta$, $\theta = 0.5$)

(c) Donor-cell ($\theta = 0.0$) (d) Diss. Galerkin ($\alpha = 0.1 = \beta$, $\theta = 0.5$)

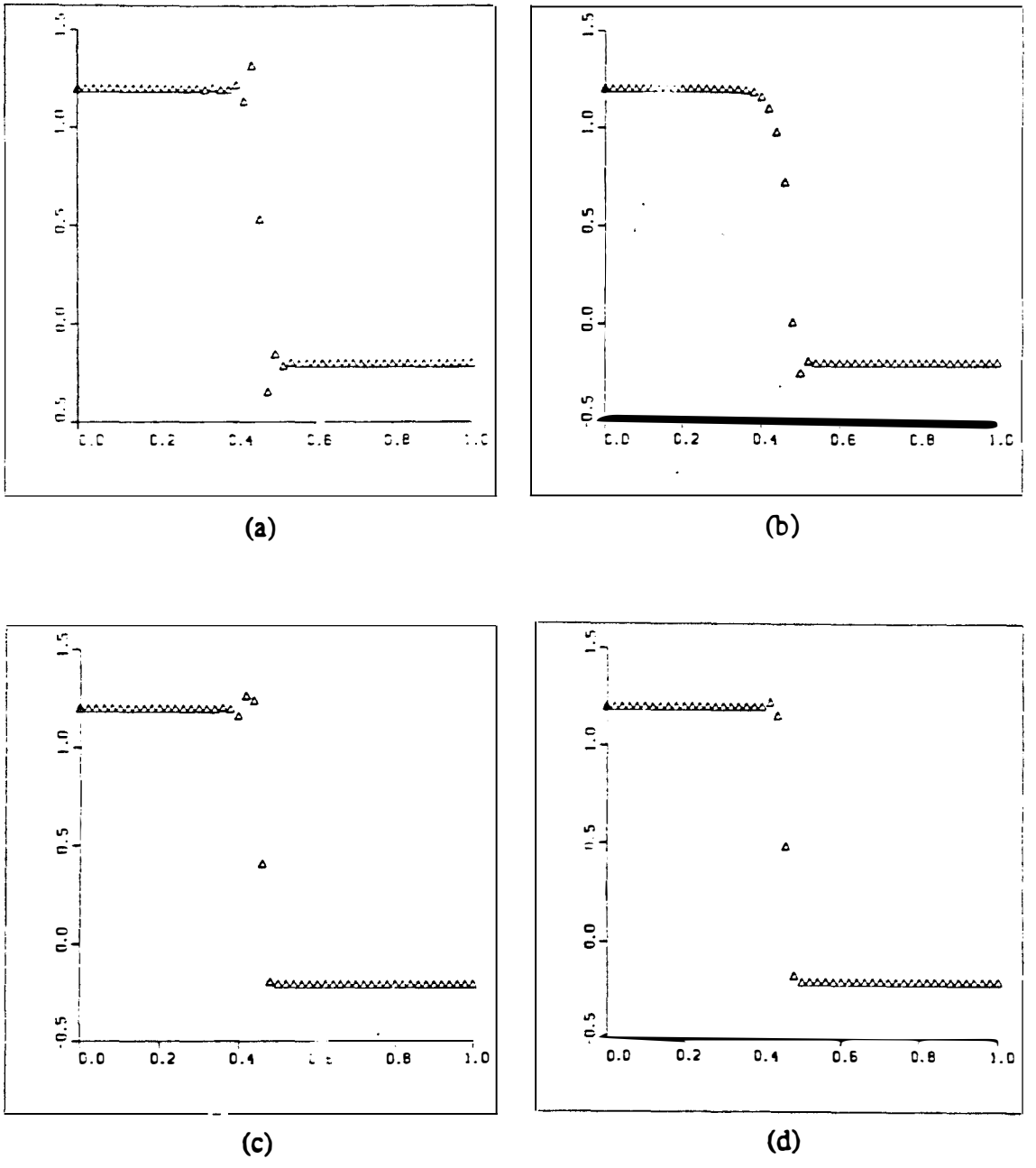

Figure 11. TWS Nodal Solutions for Burgers Step problem using first-order dissipative Galerkin algorithm with $\varepsilon = 0.0$.

(a) $\underline{\alpha} = 0$, $\underline{\beta} = 0.25$, $\theta = 0.5$ (b) $\underline{\alpha} = 0$, $\underline{\beta} = 0.75$, $\theta = 0.5$

(c) $\underline{\alpha} = 0$, $\underline{\beta} = 0.25$, $\underline{\gamma} = 1/6$ (lumped mass matrix), $\theta = 0.5$

(d) $\underline{\alpha} = 0$, $\underline{\beta} = 0.375$, $\underline{\gamma} = 1/6$ (lumped mass matrix), $\theta = 0.5$

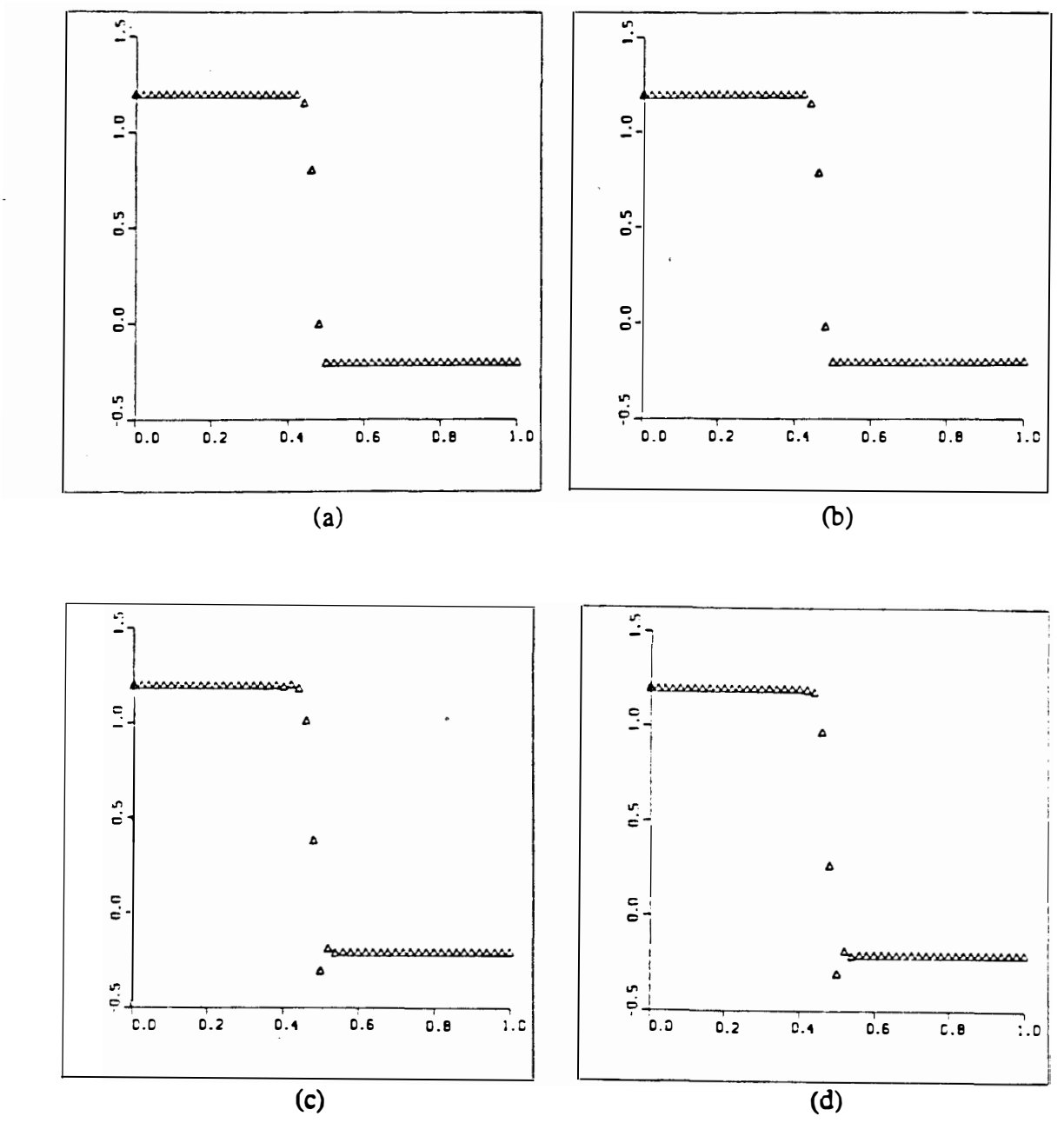

Figure 12. TWS Nodal Solutions for Burgers Step using Bubnov-Galerkin ($\alpha = 0 = \beta$, $\theta = 0.5$).

(a) $\gamma = 1/6$ (lumped mass matrix), $\varepsilon = 0.25$

(b) $\gamma = 1/6$ (lumped mass matrix), $\varepsilon = 0.50$

(c) $\gamma = 0.0$ (consistent mass matrix), $\varepsilon = 0.25$

(d) $\gamma = 0.0$ (consistent mass matrix), $\varepsilon = 0.50$

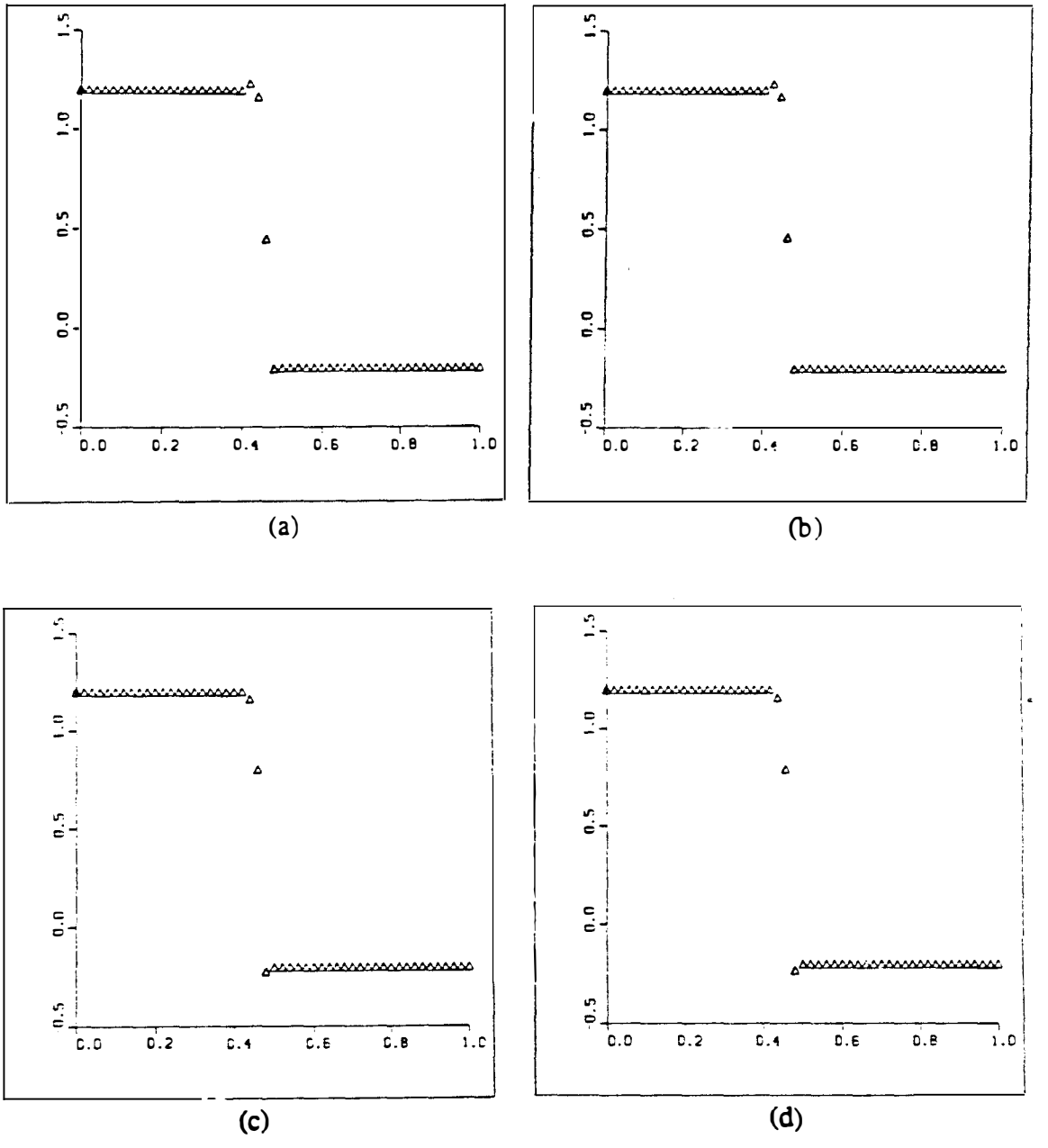

Figure 13. TWS Nodal Solutions for Burgers Step using Raymond-Garder ($\alpha = (15)^{-1/2} = \beta$, $\theta = 0.5$).

(a) $\gamma = 1/6$ (lumped mass matrix), $\varepsilon = 0.25$

(b) $\gamma = 1/6$ (lumped mass matrix), $\varepsilon = 0.50$

(c) $\gamma = 0.0$ (consistent mass matrix), $\varepsilon = 0.25$

(d) $\gamma = 0.0$ (consistent mass matrix), $\varepsilon = 0.50$

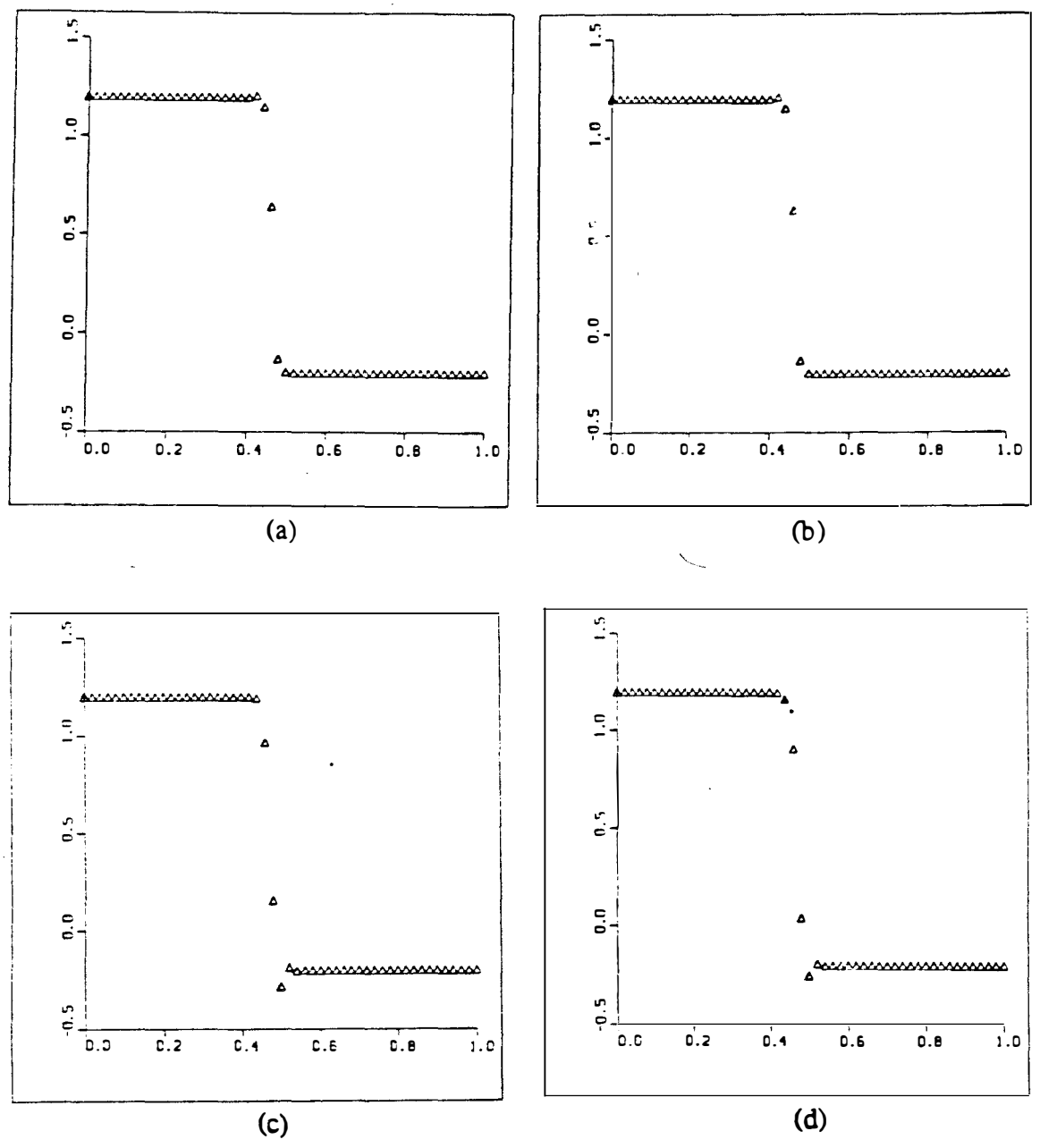

Figure 14. TWS Nodal Solutions for Burgers Step using Dissipative Galerkin ($\alpha = 0.1 = \beta$, $\theta = 0.5$).

(a) $\gamma = 1/6$ (lumped mass matrix), $\varepsilon = 0.25$

(b) $\gamma = 1/6$ (lumped mass matrix), $\varepsilon = 0.50$

(c) $\gamma = 0.0$ (consistent mass matrix), $\varepsilon = 0.25$

(d) $\gamma = 0.0$ (consistent mass matrix), $\varepsilon = 0.50$

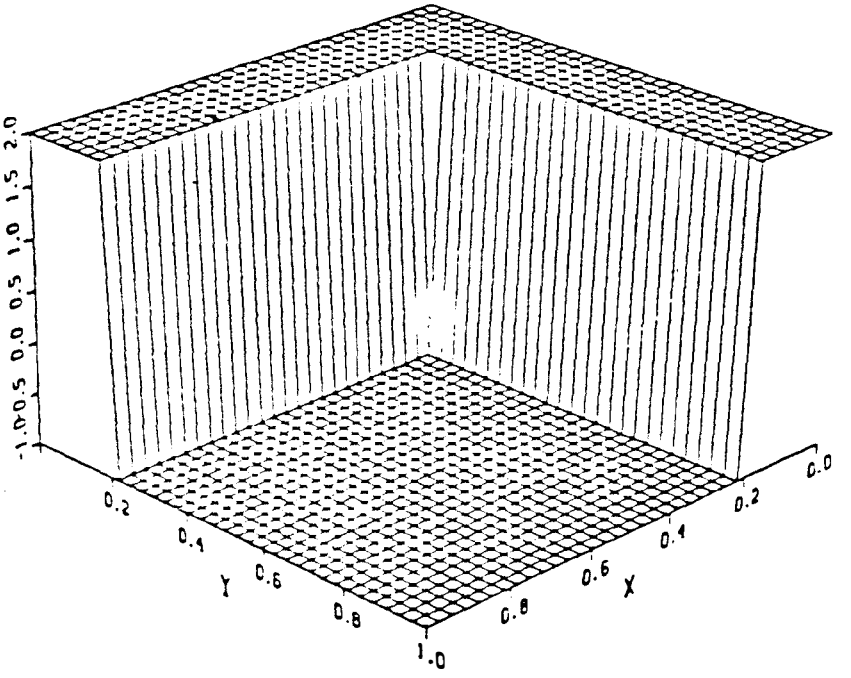

Figure 15. Initial data for discontinuity aligned with grid.

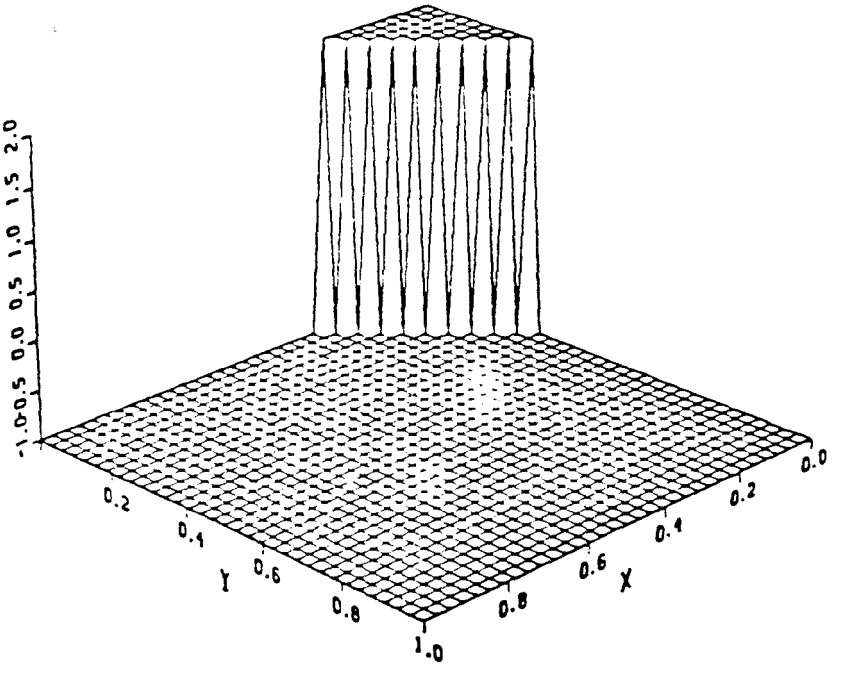

Figure 16. Initial data for the discontinuity skewed to the grid by 45 degrees.

(a)

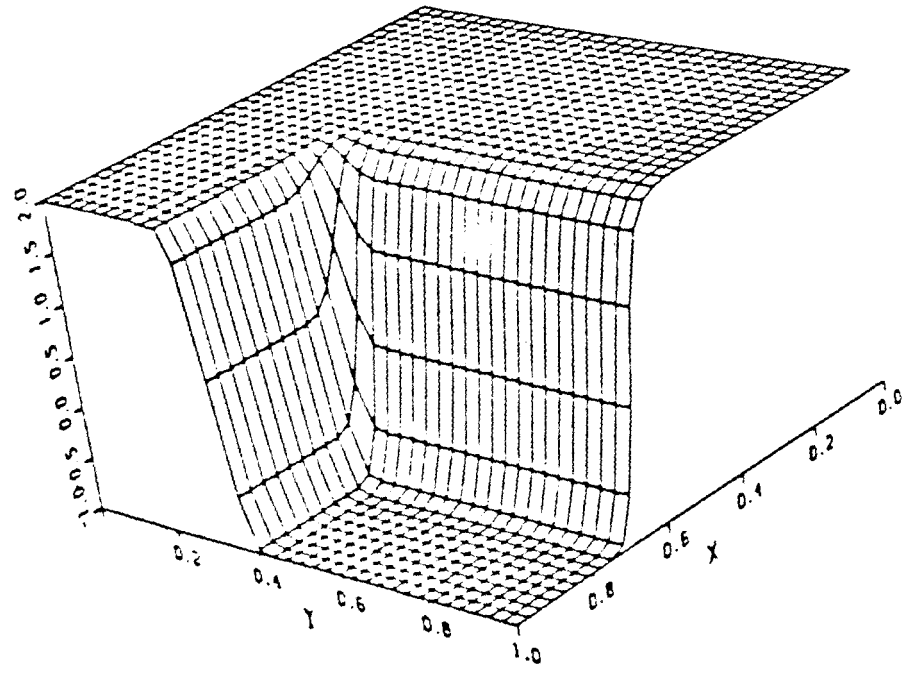

(b)

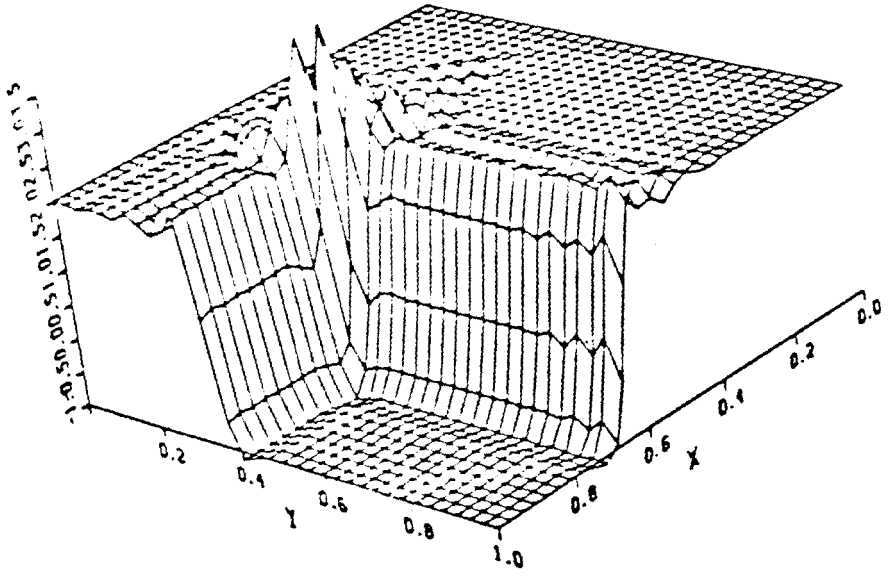

Figure 17. TWS Field Solutions for Two-dimensional Linear case
(discontinuity aligned with grid), $C_x = 0.096$, $C_y = 0.032$.
(a) Bubnov-Galerkin, $\varepsilon = 1/6$ ($\theta = 0.5$) (b) Raymond-Garder ($\theta = 0.5$)

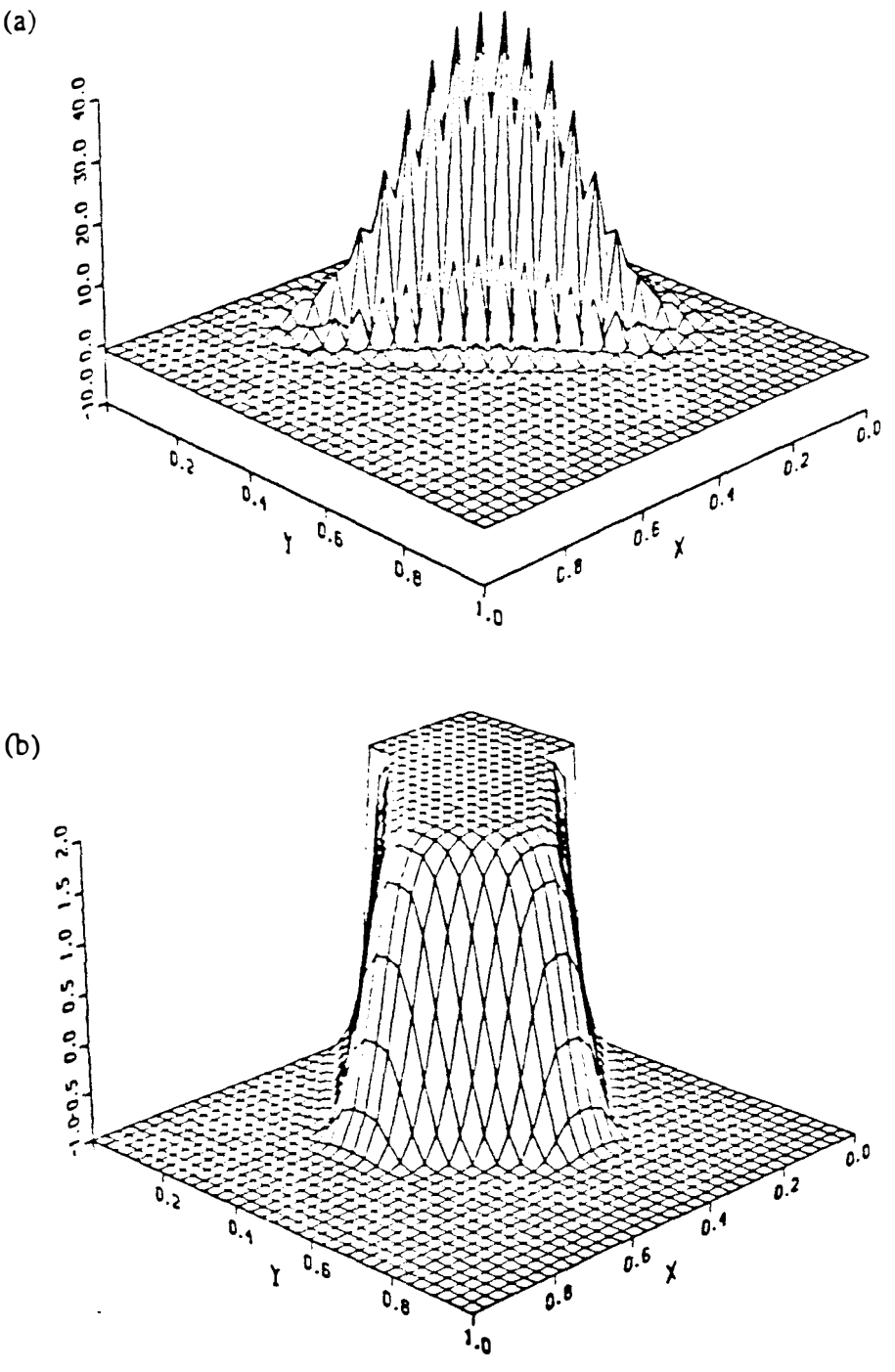

Figure 18. TWS Field Solutions for Two-dimensional Linear case (45 degrees skewed with grid), $C_x = 0.064 = C_y$.

(a) Raymond-Garder ($\theta = 0.5$) (b) Bubnov-Galerkin, $\varepsilon = 1/6$ ($\theta = 0.5$)

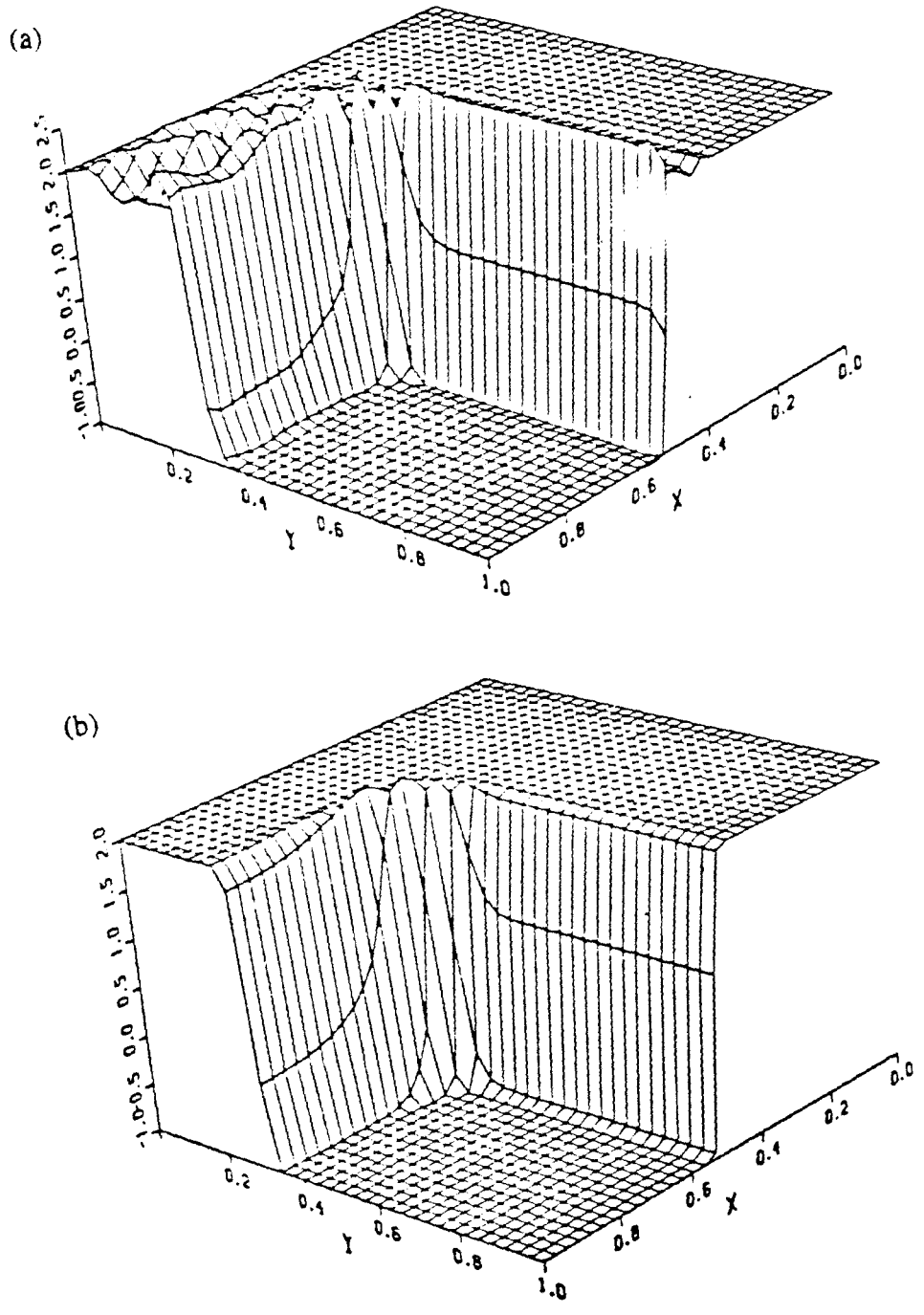

Figure 19. TWS Field Solutions for Two-dimensional Burgers case (discontinuity aligned with grid).
(a) Raymond-Garder ($\theta = 0.5$) (b) Bubnov-Galerkin, $\varepsilon = 1.0$ ($\theta = 0.5$)

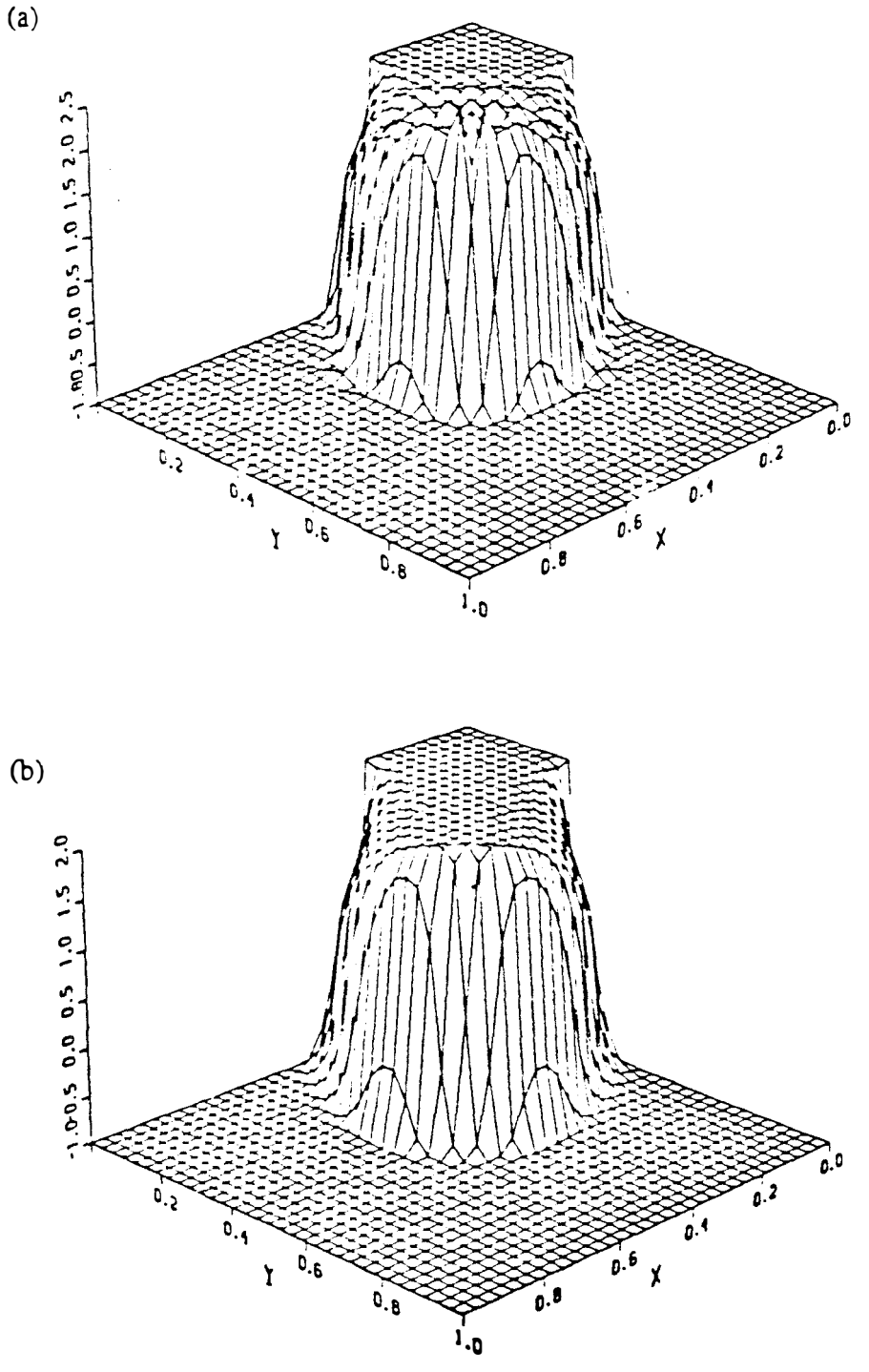

Figure 20. TWS Field Solutions for Two-dimensional Burgers case (45 degree skewed with grid).
(a) Raymond-Garder ($\theta = 0.5$) (b) Galerkin, $\varepsilon = 1.0$ ($\theta = 0.5$)

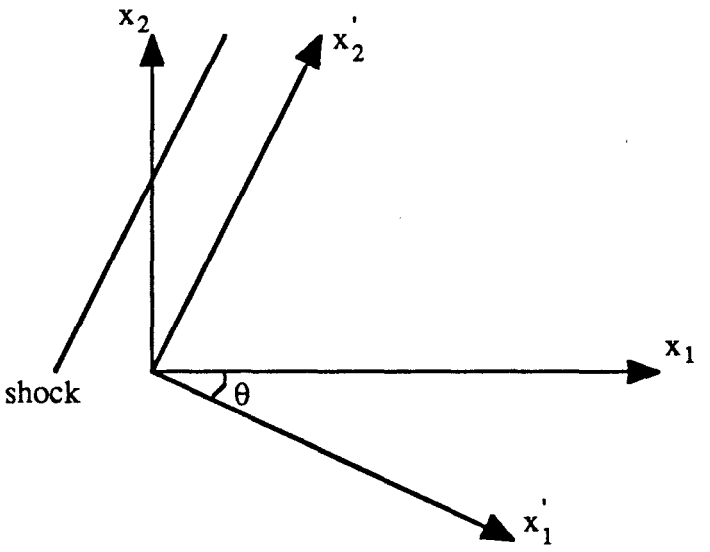

Figure 21. Local coordinate axes rotated by angle θ.

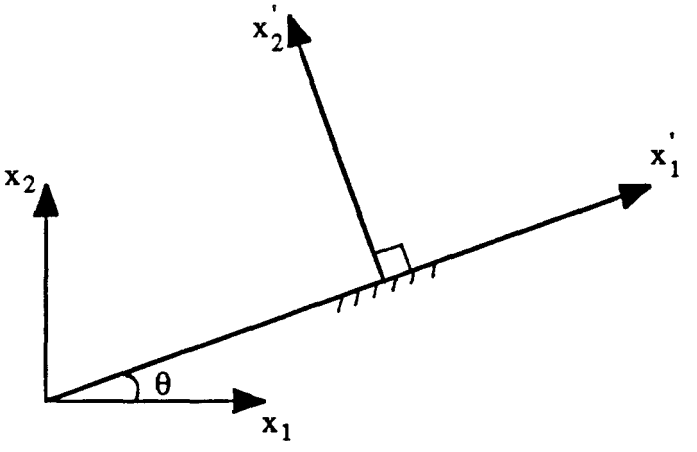

Figure 22. Tangential (x_1') and Normal (x_2') axes at a surface.

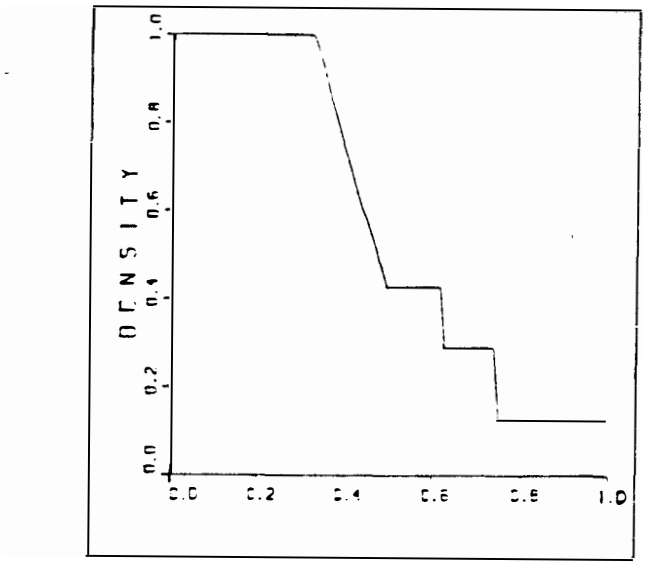

(a)

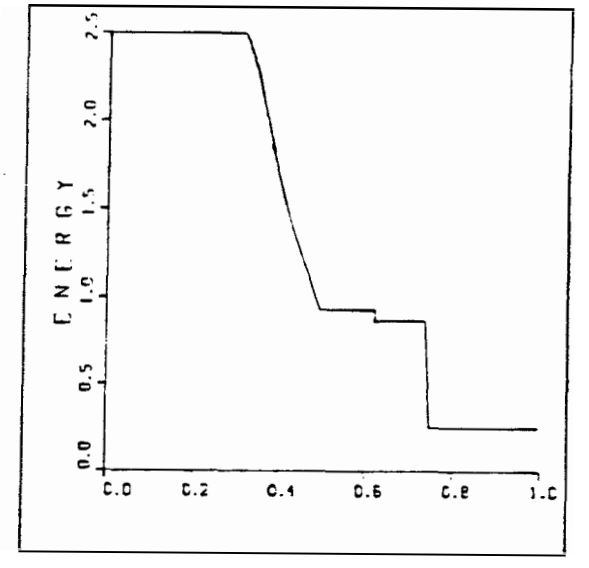

(b)

Figure 23. Exact solution for One-dimensional Riemann shock tube problem.
(a) Density (b) Energy

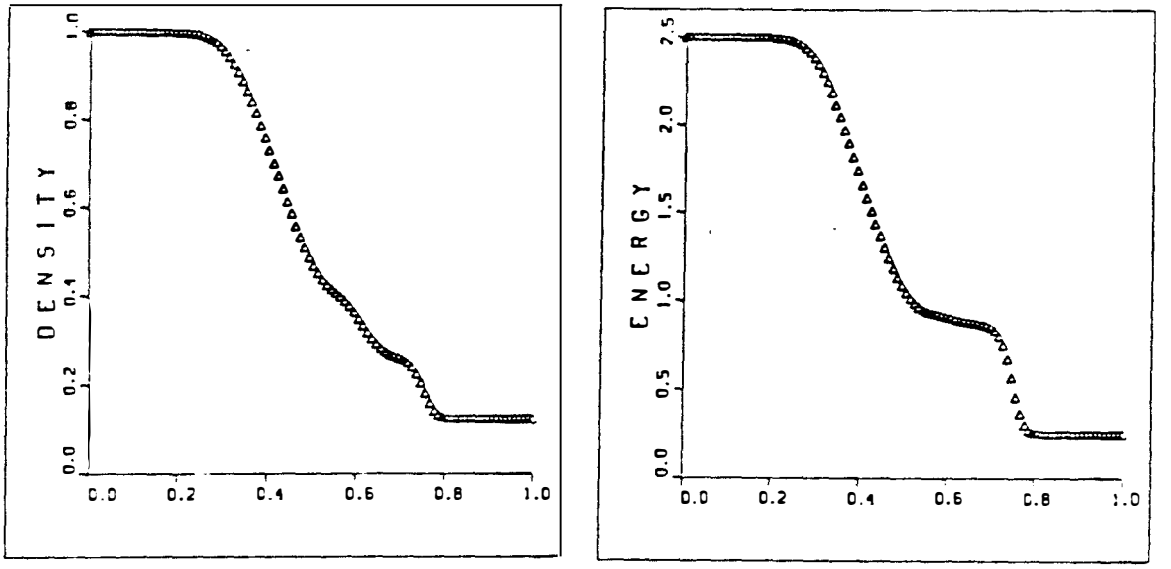

(a) (b)

Figure 24. Riemann shock tube solution by Donor-cell ($\theta = 0.0$).
(a) Density (b) Energy

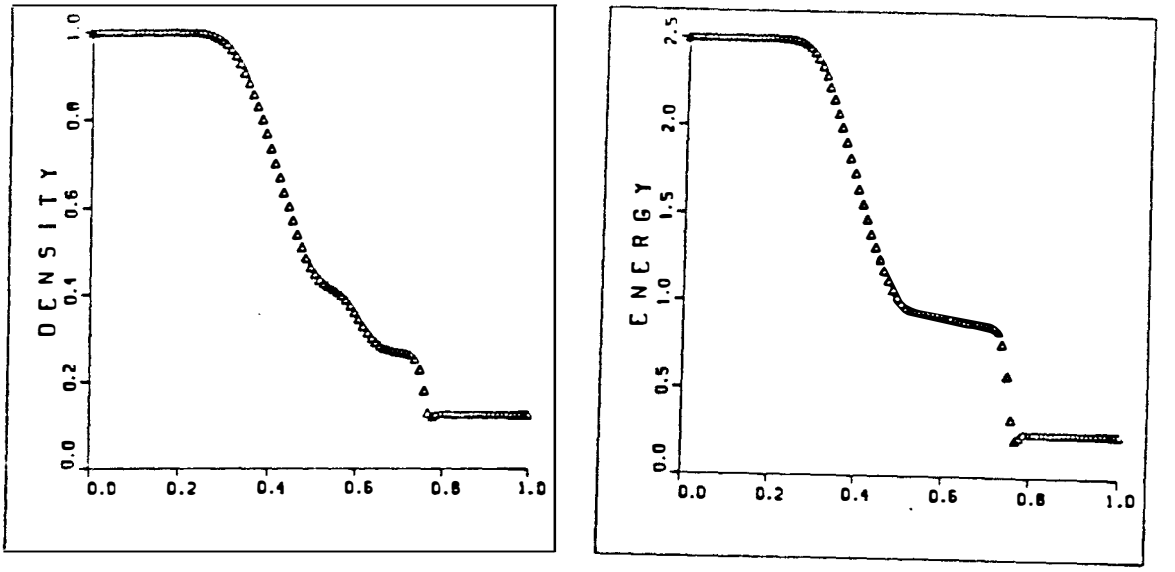

(a) (b)

Figure 25. Riemann shock tube solution by Raymond-Garder ($\theta = 0.5$).
(a) Density (b) Energy

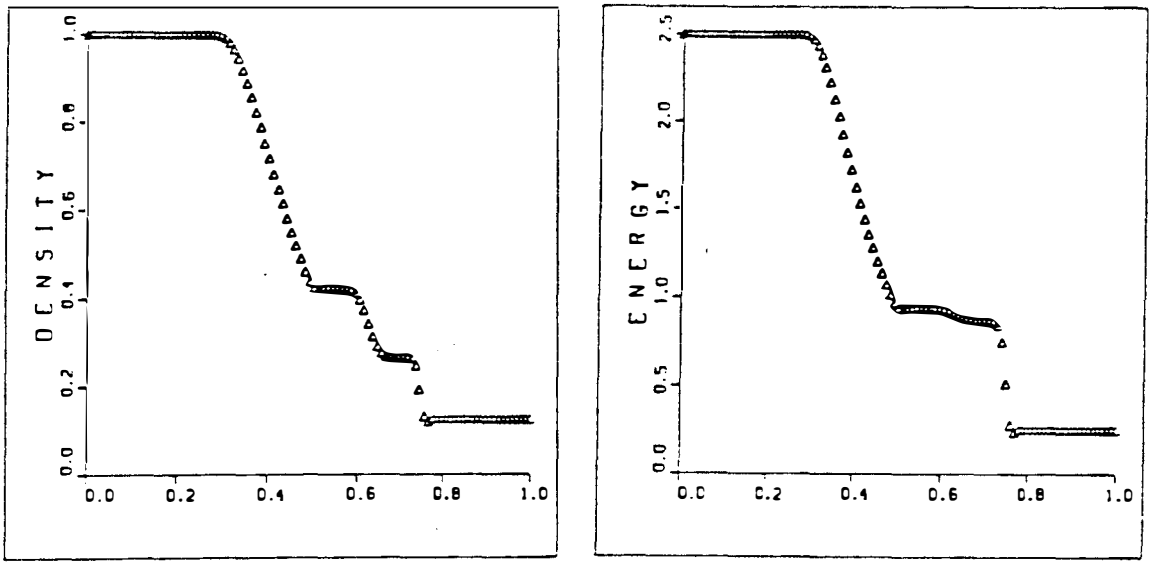

(a) (b)

Figure 26. Riemann shock tube solution by Euler Taylor-Galerkin.
(a) Density (b) Energy

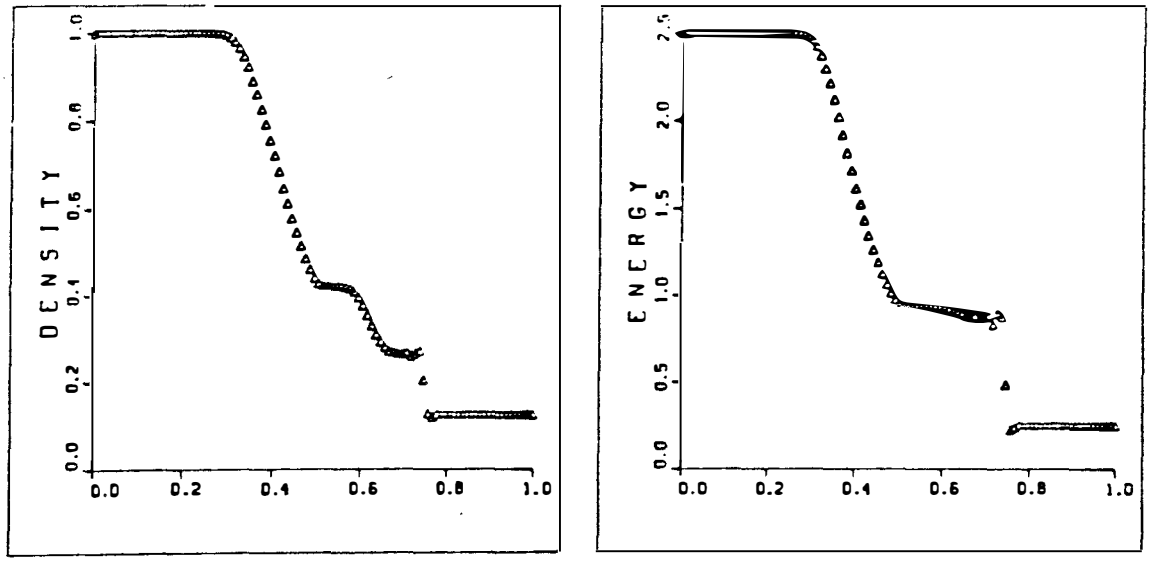

(a) (b)

Figure 27. Riemann shock tube solution by dissipative Galerkin ($\alpha = 0.1 = \beta$).
(a) Density (b) Energy

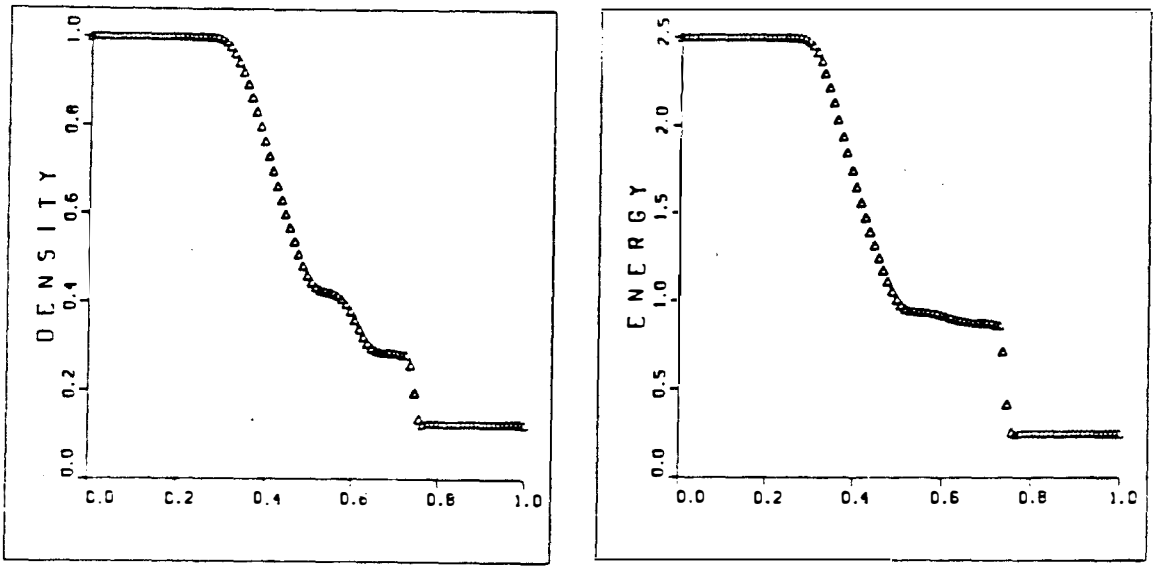

(a) (b)

Figure 28. Riemann shock tube solution by diss. Galerkin ($\alpha = \beta = 0.1$) with $\varepsilon = 0.1$ for non-linear fields only. (a) Density (b) Energy

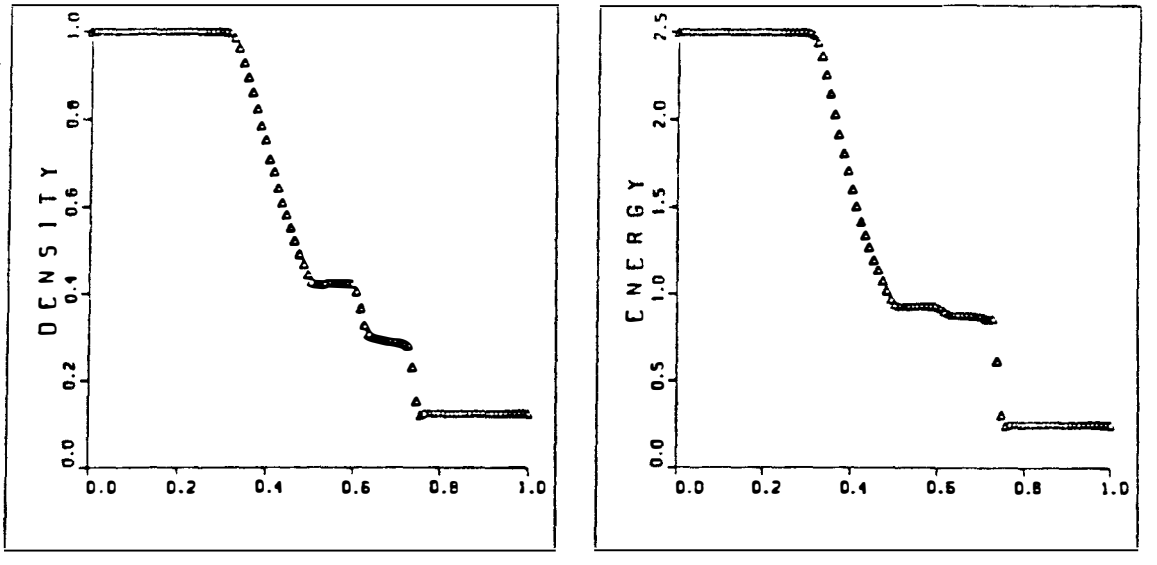

(a) (b)

Figure 29. Riemann shock tube solution by Bubnov-Galerkin with $\varepsilon = 0.1$ for non-linear fields only. (a) Density (b) Energy

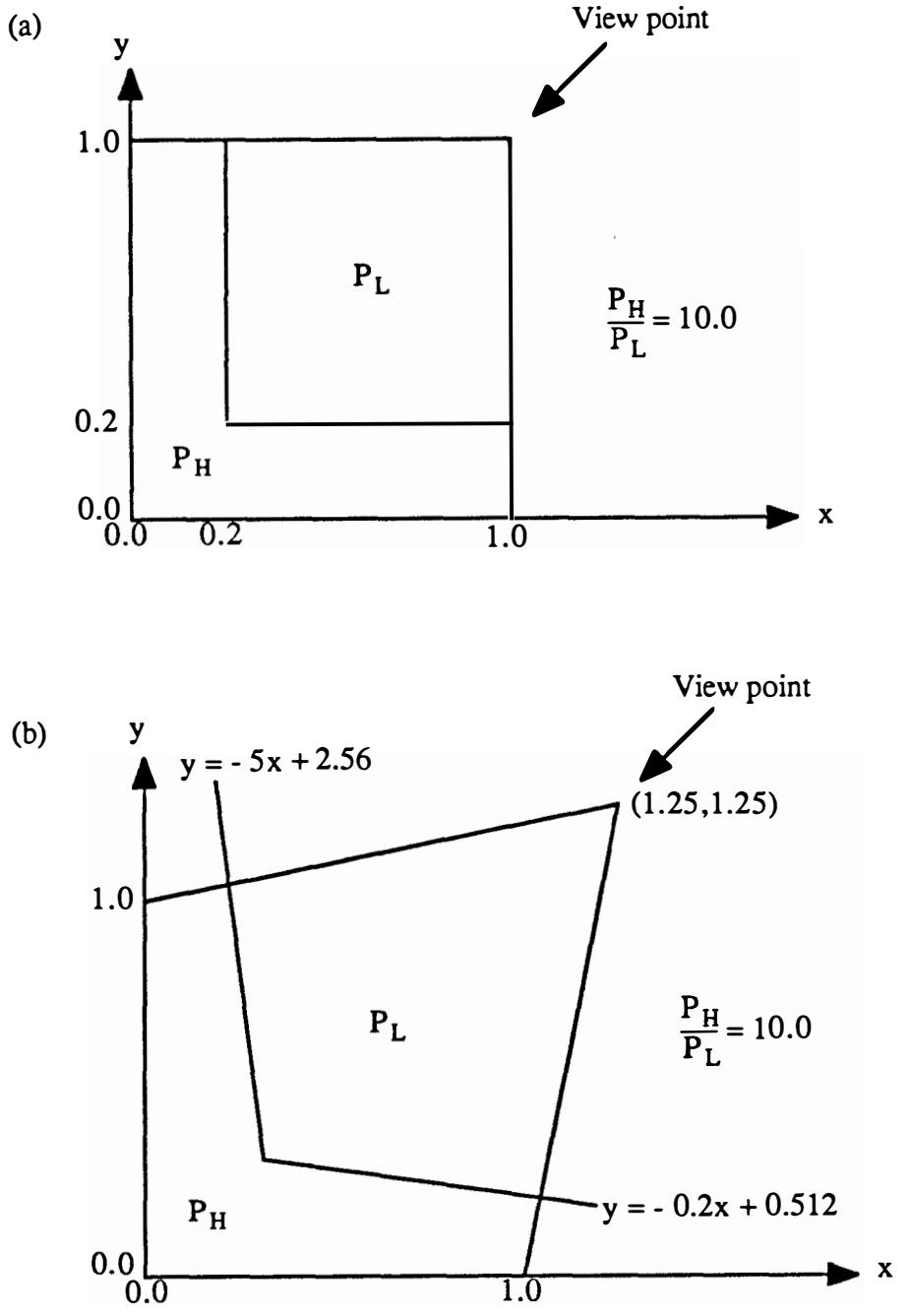

Figure 30. Domain and initial data for two-dimensional shock interaction problem.
(a) Initial discontinuities are aligned with grid lines.
(b) Initial discontinuities are not aligned with grid lines.

(a)

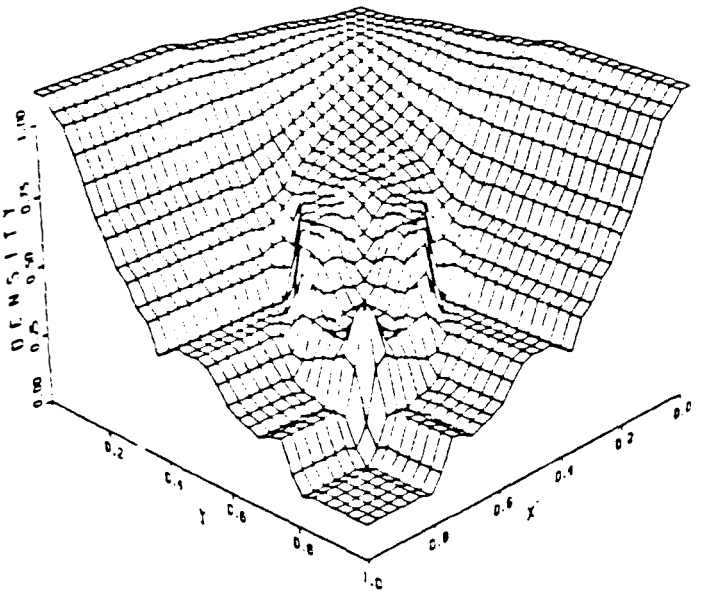

(b)

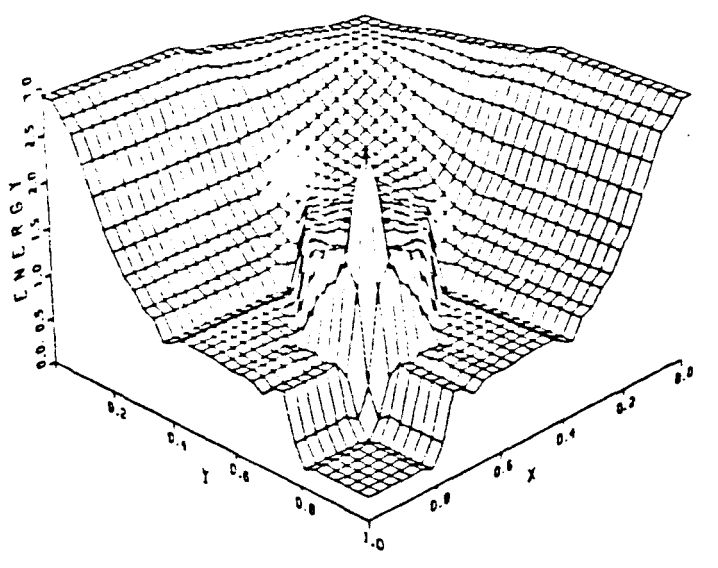

Figure 31. ETG solution for two-dimensional shock interaction problem on a rectangular grid. (a) Density (b) Energy

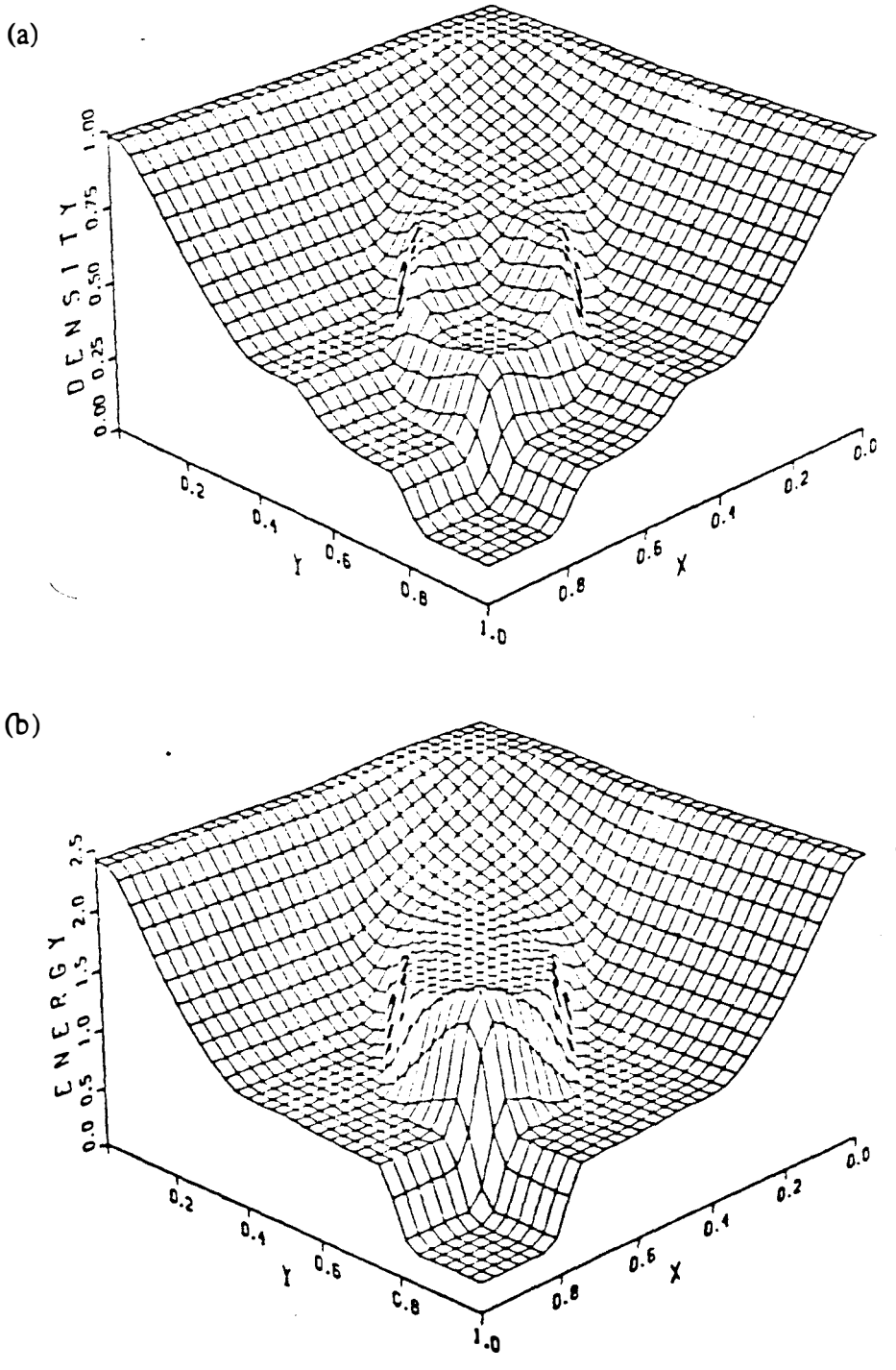

Figure 32. Bubnov-Galerkin solution for two-dimensional shock interaction problem on a rectangular grid with $\varepsilon = 1/6$ for non-linear field only.
(a) Density (b) Energy

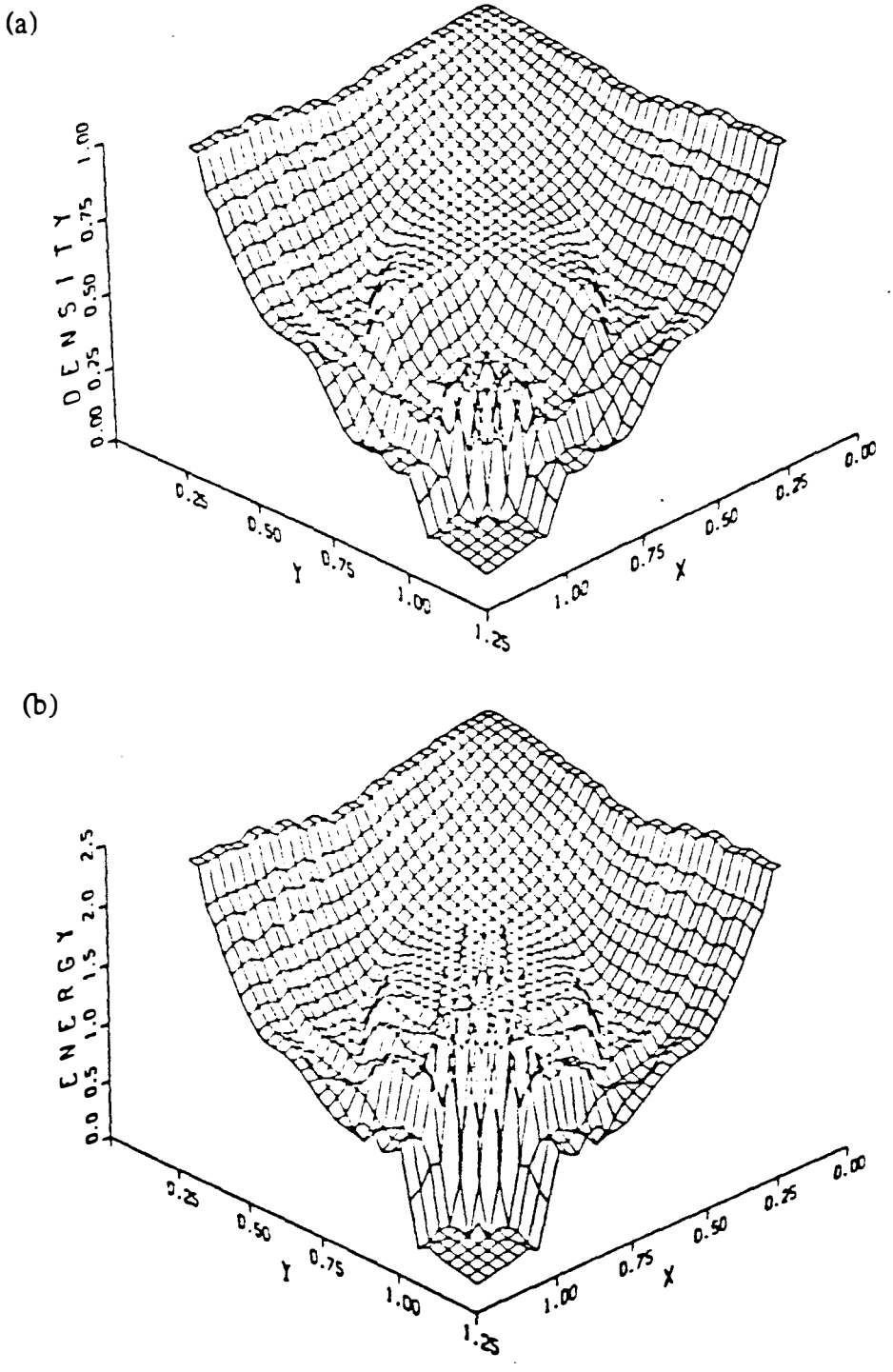

Figure 33. ETG solution for two-dimensional shock interaction problem on a nonrectangular grid. (a) Density (b) Energy

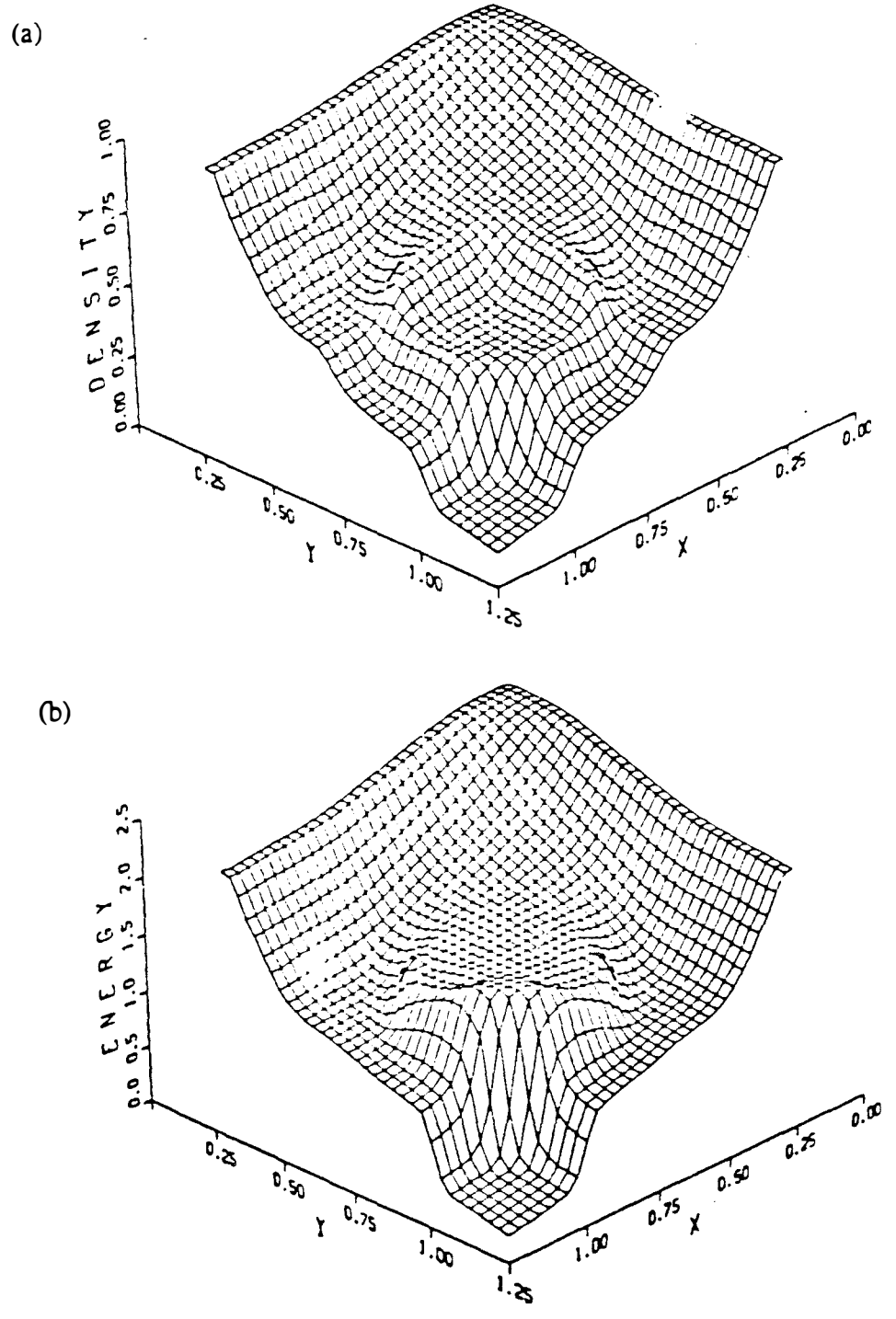

Figure 34. Bubnov-Galerkin solution for two-dimensional shock interaction problem on a nonrectangular grid with $\varepsilon = 1/6$ for non-linear field only.
(a) Density (b) Energy

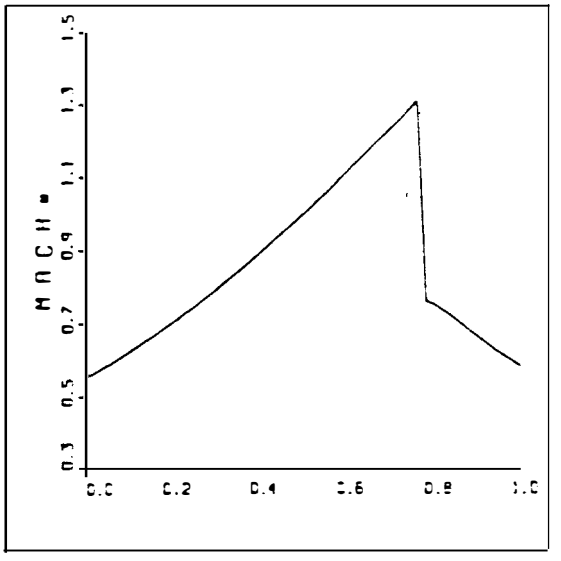

(a)

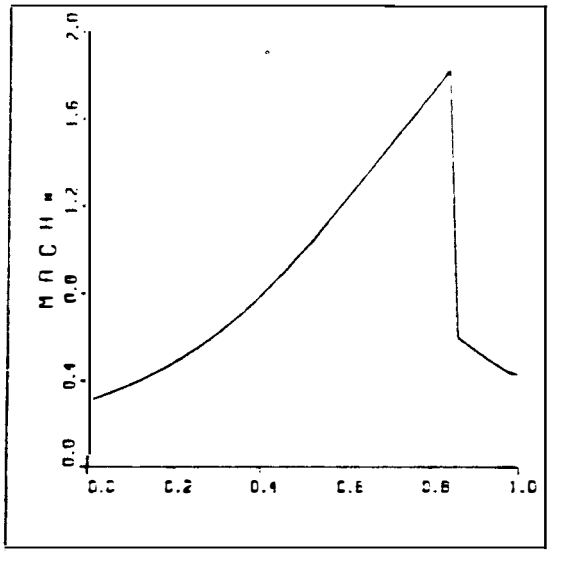

(b)

Figure 35. Exact solution for Mach number for Quasi One-dimensional deLaval nozzle problem.
(a) M_S (shock mach number) = 1.3 (b) M_S = 1.8

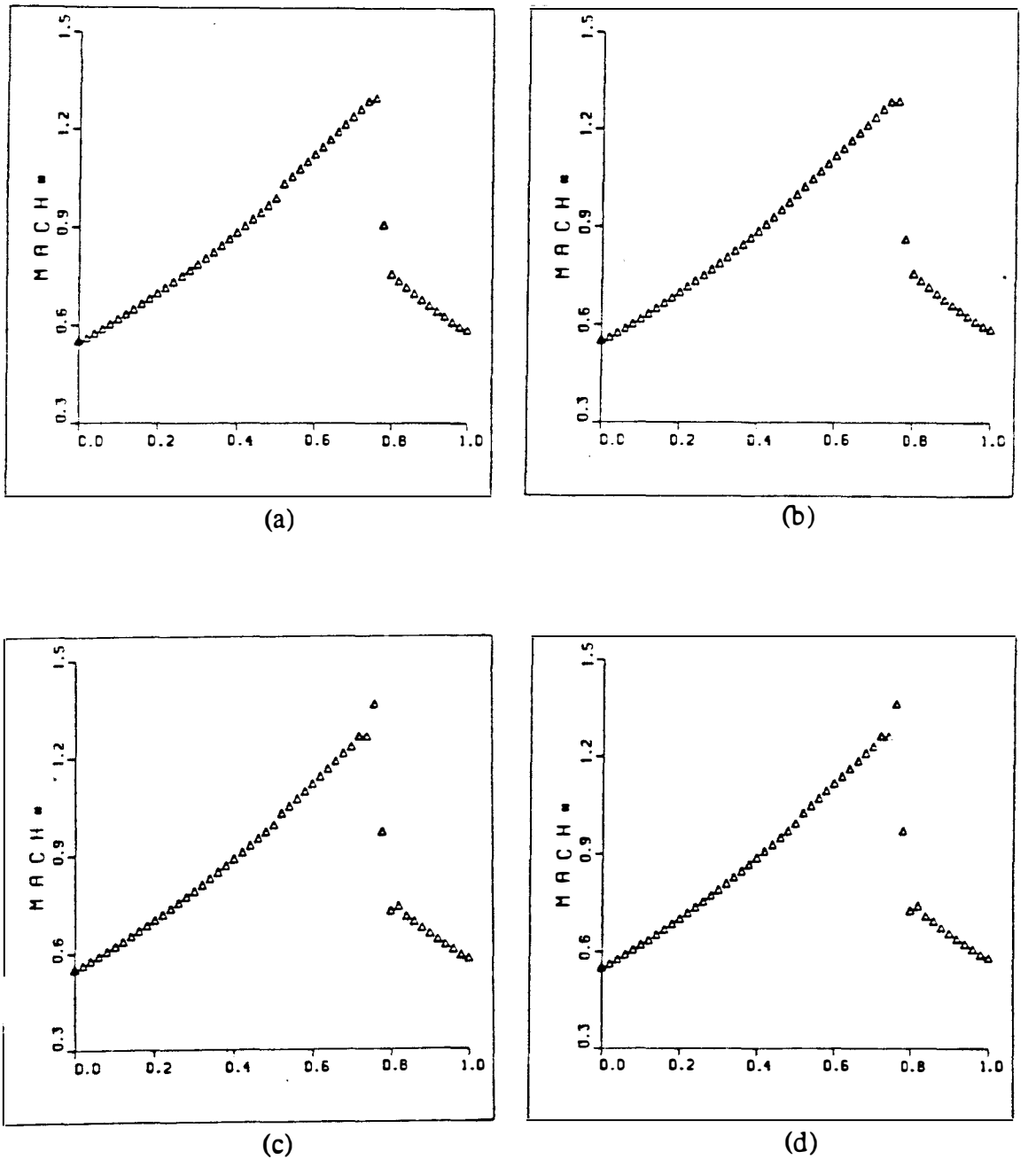

Figure 36. Mach number for Q1D deLaval nozzle problem by Donor-cell and Raymond-Garder methods for $M_S = 1.3$.
(a) Donor-cell without sonic treatment
(b) Donor-cell with sonic treatment
(c) Raymond-Garder without sonic treatment
(d) Raymond-Garder with sonic treatment

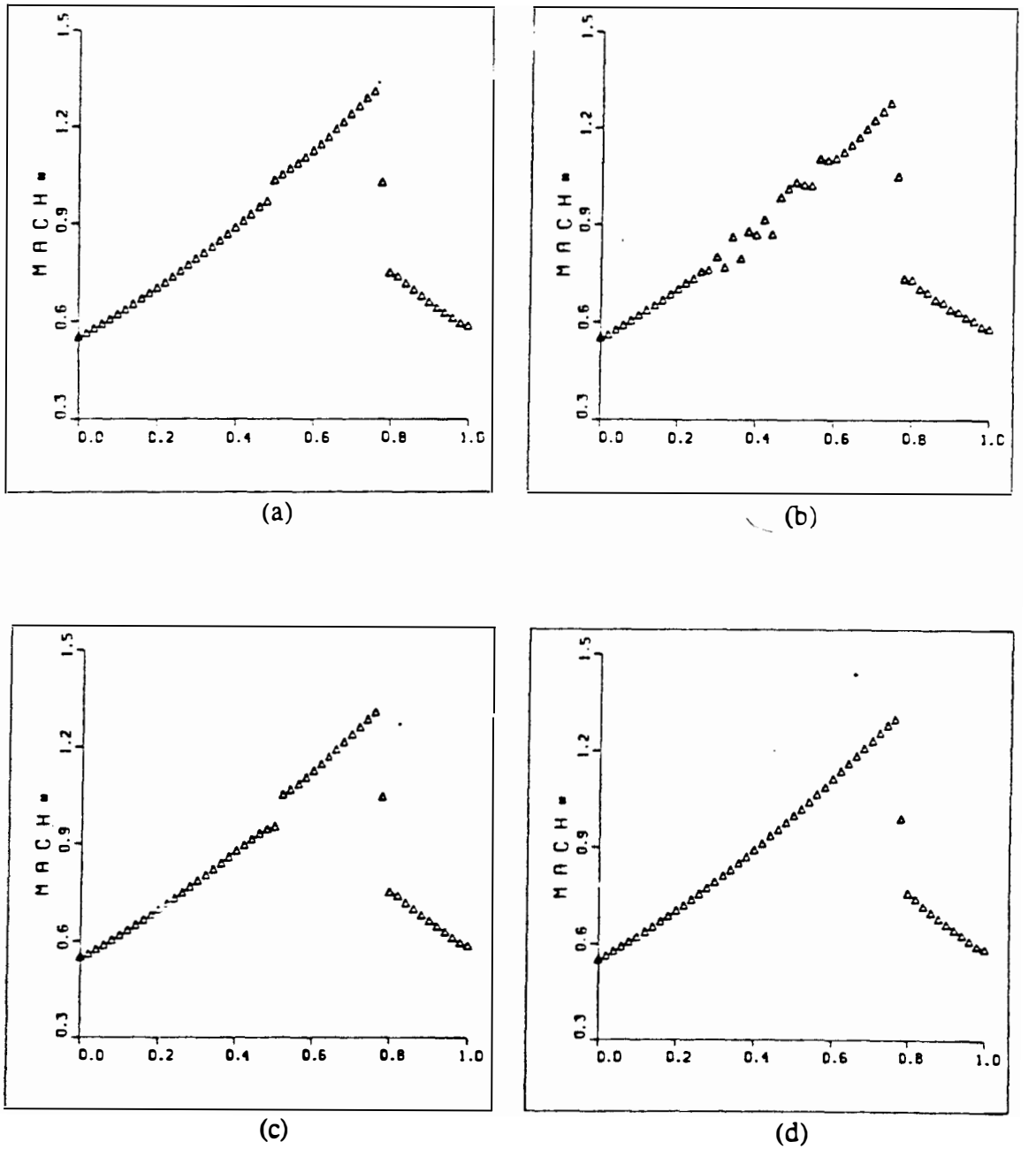

Figure 37. Mach number for Q1D deLaval nozzle problem by Bubnov-Galerkin and Raymond-Garder methods with $\varepsilon = 1.0$ for all field ($M_S = 1.3$).
(a) Bubnov-Galerkin without sonic treatment
(b) Bubnov-Galerkin with sonic treatment
(c) Raymond-Garder without sonic treatment
(d) Raymond-Garder with sonic treatment

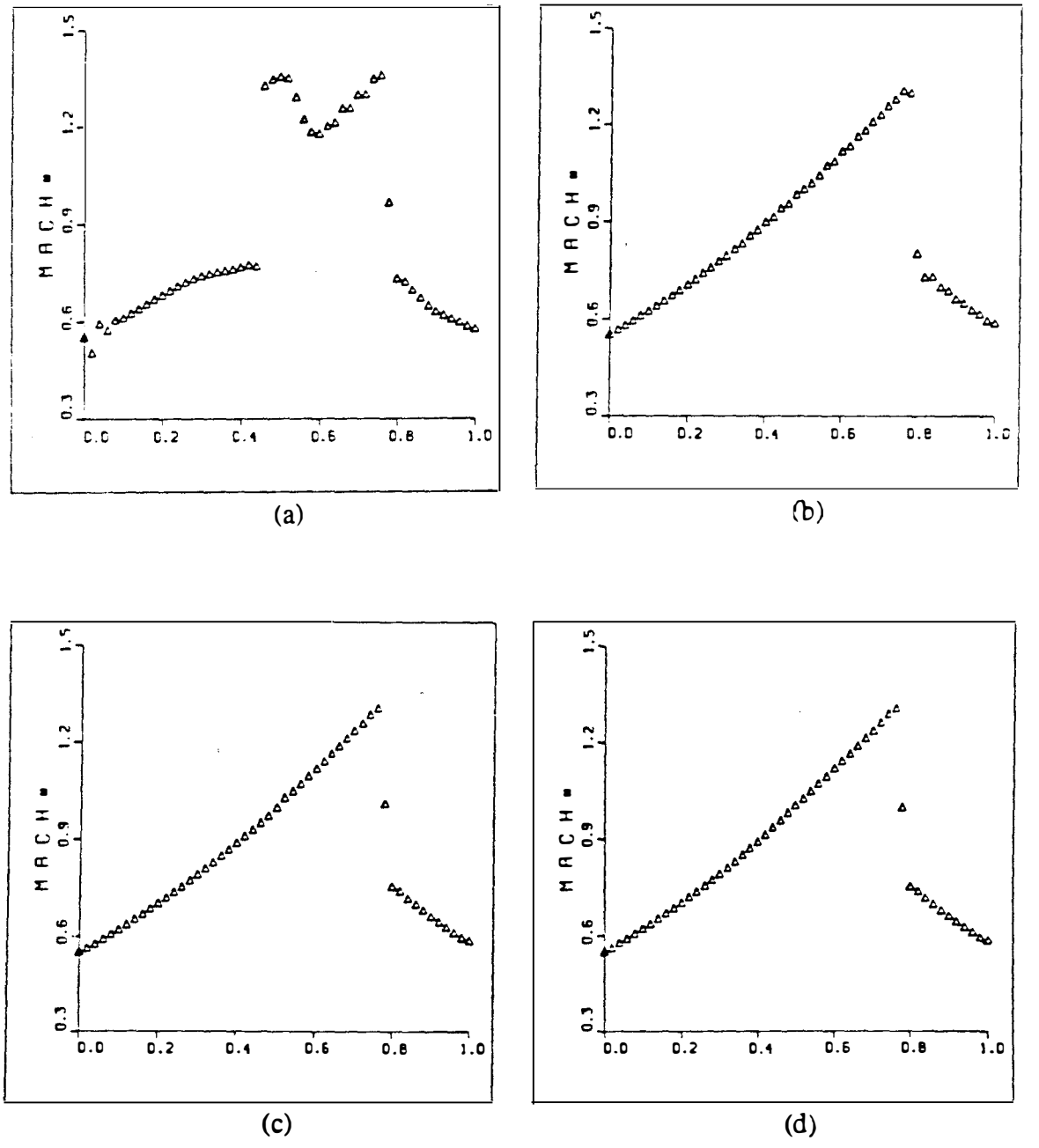

Figure 38. Mach number for Q1D deLaval nozzle problem by Bubnov-Galerkin and Raymond-Garder methods with $\varepsilon = 1.0$ for non-linear field only ($M_S = 1.3$).
(a) Bubnov-Galerkin without sonic treatment
(b) Bubnov-Galerkin with sonic treatment
(c) Raymond-Garder without sonic treatment
(d) Raymond-Garder with sonic treatment

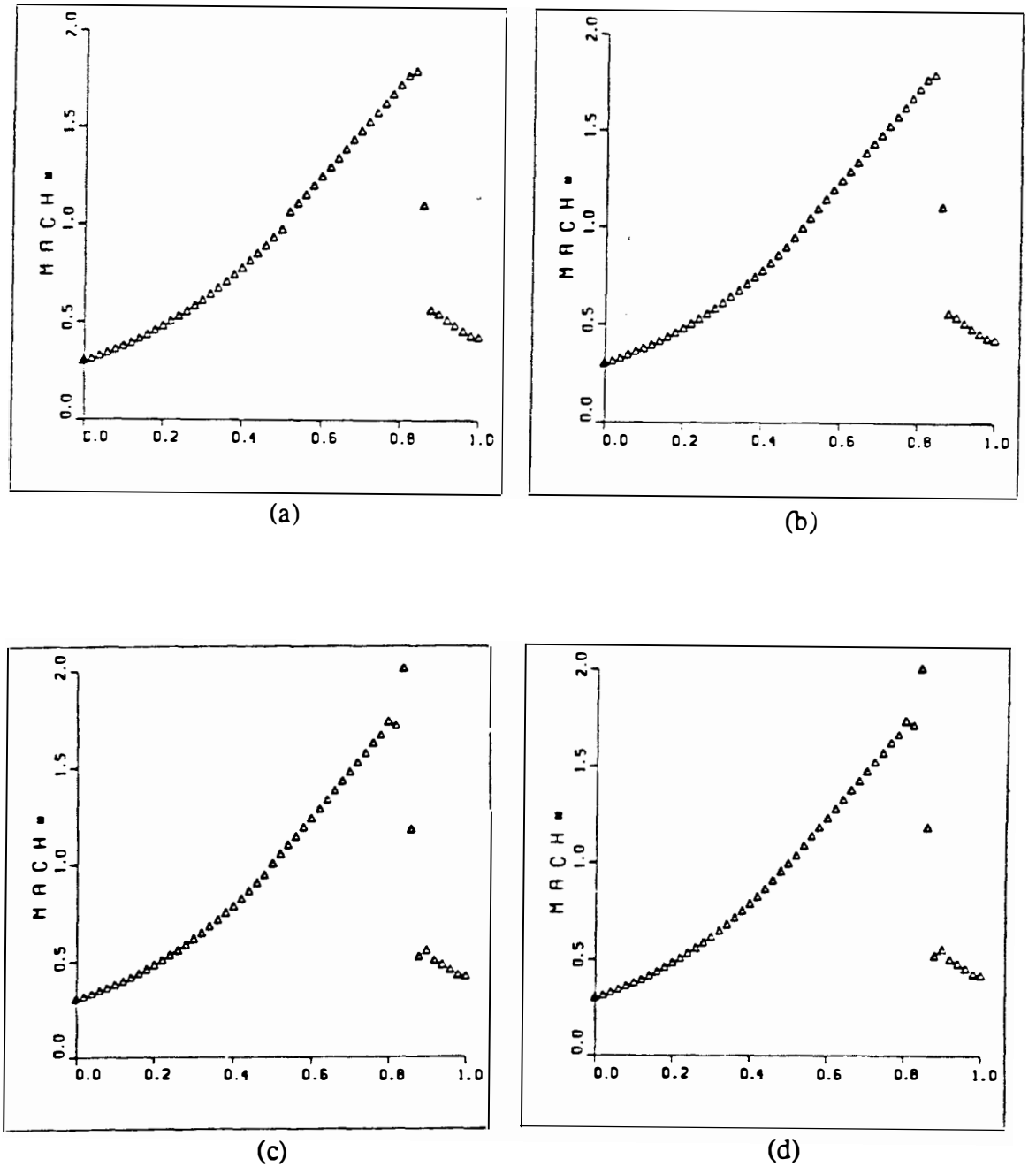

Figure 39. Mach number for Q1D deLaval nozzle problem by Donor-cell and Raymond-Garder methods for $M_S = 1.8$.
(a) Donor-cell without sonic treatment
(b) Donor-cell with sonic treatment
(c) Raymond-Garder without sonic treatment
(d) Raymond-Garder with sonic treatment

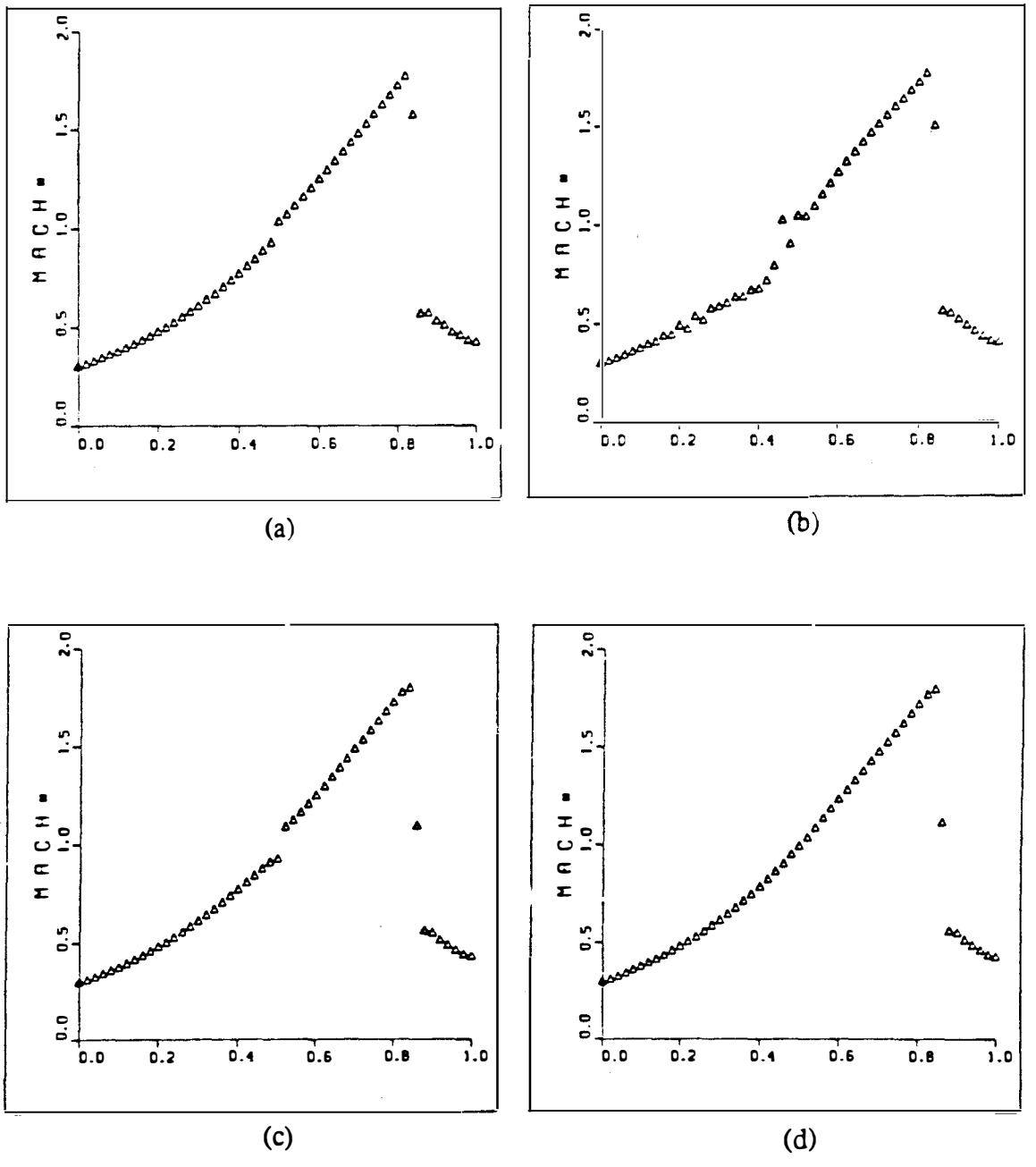

Figure 40. Mach number for Q1D deLaval nozzle problem by Bubnov-Galerkin and Raymond-Garder methods with $\varepsilon = 1.0$ for all field ($M_S = 1.8$).
(a) Bubnov-Galerkin without sonic treatment
(b) Bubnov-Galerkin with sonic treatment
(c) Raymond-Garder without sonic treatment
(d) Raymond-Garder with sonic treatment

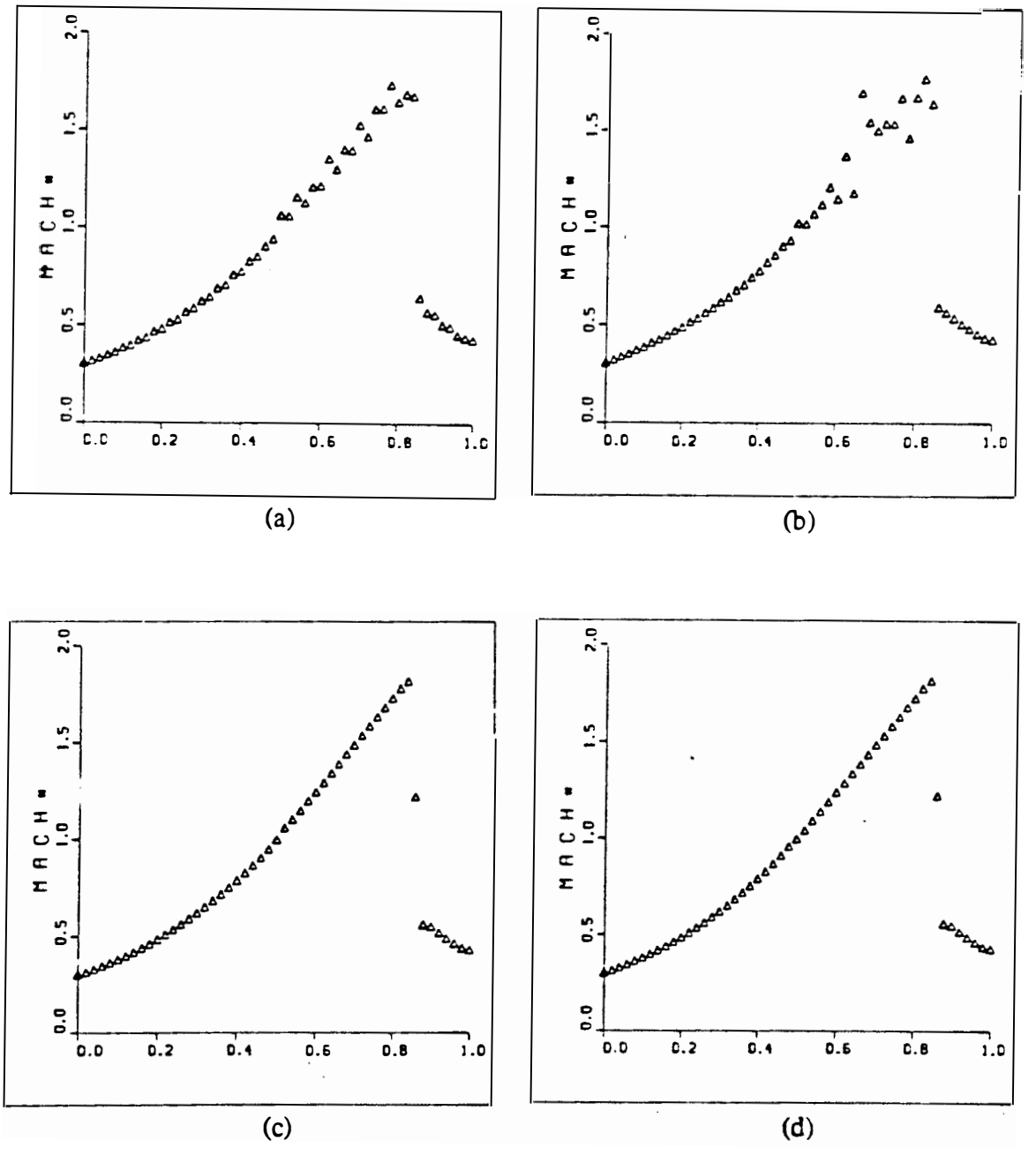

Figure 41. Mach number for Q1D deLaval nozzle problem by Bubnov-Galerkin and Raymond-Garder methods with $\varepsilon = 1.0$ for non-linear field only ($M_S = 1.8$).
(a) Bubnov-Galerkin without sonic treatment
(b) Bubnov-Galerkin with sonic treatment
(c) Raymond-Garder without sonic treatment
(d) Raymond-Garder with sonic treatment

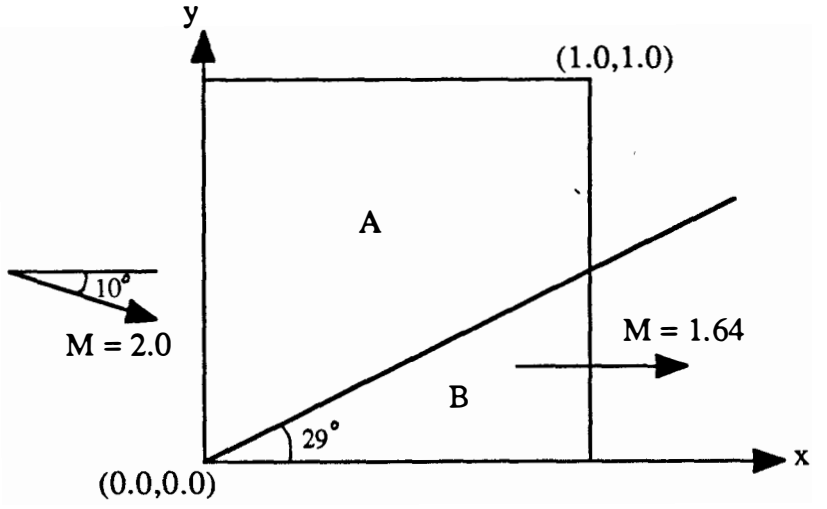

Figure 42. Wedge flow problem statement.

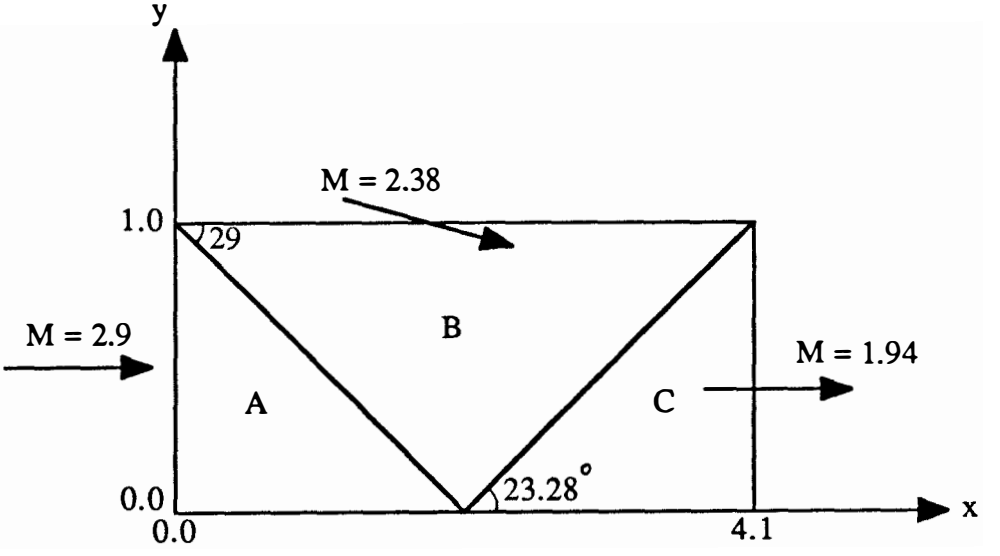

Figure 43. Shock reflection problem statement.

(a)

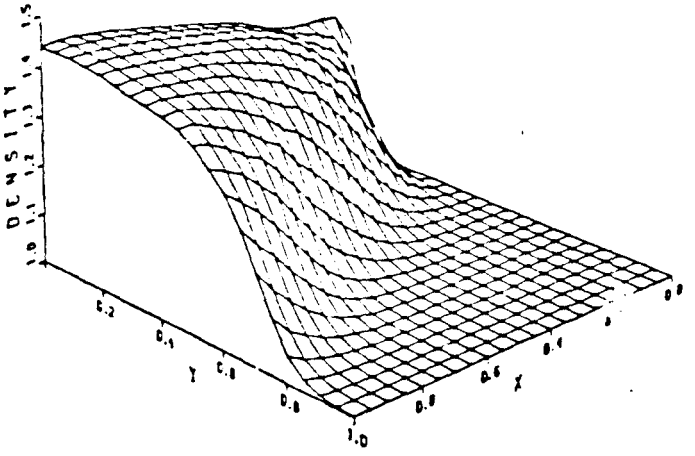

(b)

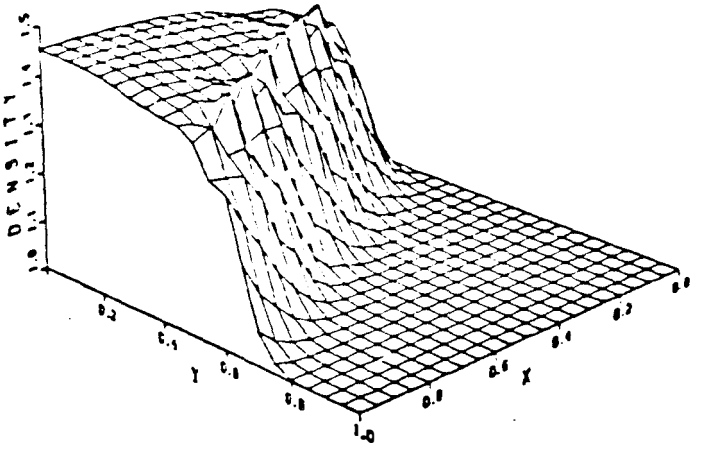

Figure 44. Density solution for Wedge flow problem.
(a) Donor-cell (b) Bubnov-Galerkin ($\varepsilon = 1.0$)

(a)

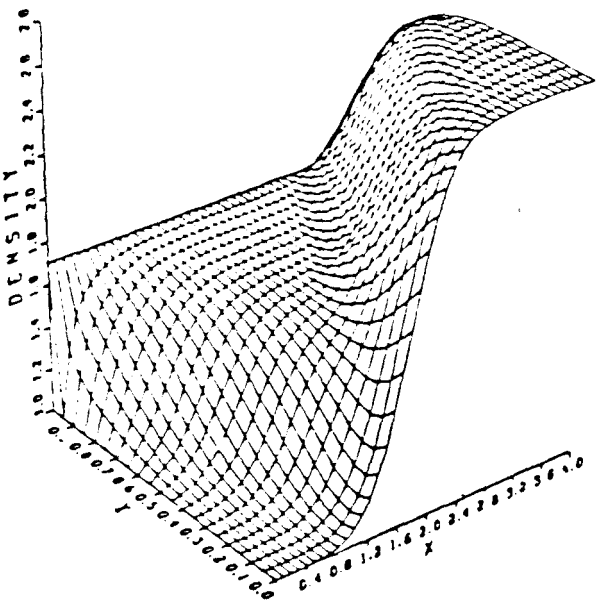

(b)

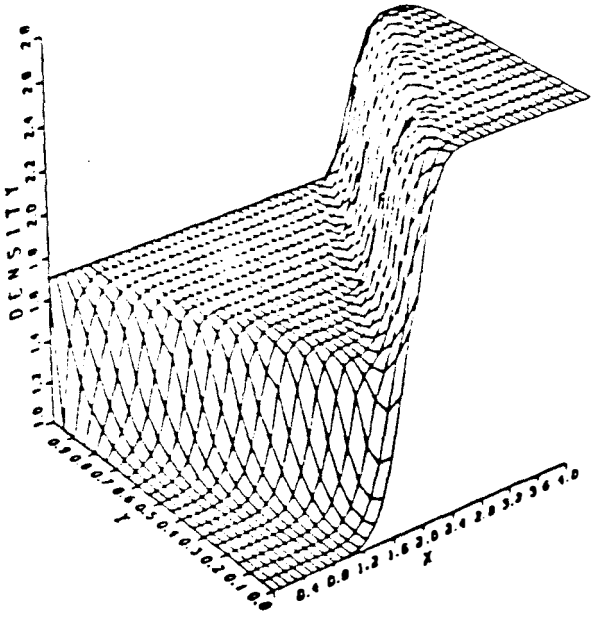

Figure 45. Density solution for Shock reflection problem.
(a) Donor-cell (b) Bubnov-Galerkin ($\varepsilon = 1.0$)

VITA

Jin Whan Kim was born in Busan, Korea on January 14, 1950. He attended ToSung elementary school for 6 years, KyungNam Junior High school for 3 years and KyungNam Senior High school for 3 years. He entered Engineering college of Seoul National University in March, 1968 and graduated from that school in August 1973 with a Bachelor of Science Degree in Electrical Engineering. He started a professional career in October 1973 in a small computing company named Korea Information and Computing Company located in Seoul, Korea.

In March 1977, he started graduate work at the University of Tennessee in Knoxville and received a Master of Science Degree in Industrial Engineering in December 1979. For a further education, he remained as a graduate student in the department of Engineering Science and Mechanics and he is expected to receive a Ph.D degree in Engineering Science in December 1988. He is now being employed at a computational company named COMCO in Austin, Texas and pursues his professional career in the field of Computational Fluid Dynamics.

He married to a native high school teacher in Busan, Korea on August 31, 1980 and presently has one 5 year old son.